TITLE OF DOCTORAL DISSERTATION

by

MELISSA SANCHEZ HERRERA

A Dissertation submitted to the

Graduate School-Newark

Rutgers, The State University of New Jersey

In partial fulfillment of the requirements

Of the degree of

Doctor of Biology

Graduate Program in

written under the direction of

Dr. Jessica L. Ware

and approved by

_____

_____

_____

_____

_____

Newark, New Jersey

October 2016

Copyright page:

ABSTRACT OF THE DISSERTATION

WHY SO MANY COLORS? EXPLORING THE ROLE OF COLOR POLYMORPHISM IN THE ENIGMATIC NEOTROPICAL *POLYTHORE* SELYS DAMSELFLIES.

Dissertation Director:

Dr. Jessica L. Ware

The Neotropics is a center of global diversity for many groups of organisms, including the dragonflies and damselflies (Odonata). While the number of biodiversity surveys and new species descriptions for neotropical odonates is increasing, diversity in this region is still under-explored, and very few studies have looked at the genetic and morphological diversity within taxa. Here, I will present an overview of the evolutionary history, species diversity and morphological diversity of the Neotropical damselfly genus *Polythore*. Species in *Polythore* are stunningly colorful; their wings display varying shades of orange, black and white in complex patterns. Despite this color diversity, they lack variation in classical reproductive traits (e.g. male genitalia) commonly used for species description. The genus comprises 21 described morphospecies distributed along the eastern slopes of the Andes cordillera and the Amazon basin, from Colombia to northern Bolivia; they dwell in small, fast flowing streams with highly oxygenated waters. I used novel morphological methods (geometric morphometrics, chromaticity analysis, and Gabor wavelet transformation) to analyze the complexity of the wing color patterns present in this genus. I explored species and population relationships through phylogenetic reconstructions and species delimitation analyses incorporating mitochondrial (COI, ND1, 16S) and nuclear (18S, 28S, PMRT) sequences. I was able to quantify the color

polymorphism and detect that wing color is not due to common descendent, i.e. not just result of phylogenetic history. I have discovered that the presence of four new cryptic species, which are new to science, are inflating the estimates species diversity within this genus. Furthermore, my phylogenetic reconstruction for the family Polythoridae suggests that *Polythore* has one common ancestor, however, other genera will need to be taxonomically revised. Finally, the divergence time calibration analyses indicate that important geological events like the Andes Cordillera uplift may have had an impact on the diversification of these Neotropical damselflies.

Acknowledgement and Dedication

Para mis padres, por su apoyo incondicional a través de estos años.

Thanks to all my mentors and students who have made this journey such an amazing experience.

Always dream BIG!

Table of Contents

List of Tables

CHAPTER ONE

CHAPTER TWO

CHAPTER 3

List of Illustrations

CHAPTER 1

CHAPTER 2

Introduction

Color is a complex physical phenomenon, produced either by selective absorption or reflection of white light wavelengths. Within living organisms, organic molecules such as pigments (i.e. carotenoids, chlorophylls) have features that help them reduce the energy needed to excite their electrons and thus provide them with color (Farrant, 1997). However, this may also trigger other chemical reactions, and depending on the chemical environment the perceived colors may vary (Farrant, 1997). Within the animal kingdom, color production can be generated by pigments, structures or a combination of both. Pigments are produced by chemical reactions within the tissues, while structural colorations rely on microscopic features at the surface of the organisms that can affect the path the wavelengths changing their perception (Farrant, 1997).

Dragonflies and damselflies (Odonata) are very conspicuous among insects. Despite their colorful bodies, displaying red, blue, yellow and greens, they also show coloration in their wings (Corbet 1999). Wing colorations in insects are generated through a variety of mechanisms, including pigments, Tyndall scattering and optical interference (Corbet 1999, Fitzstephens & Getty, 2000, Vukusic 2003). In damselflies (Zygoptera) pigmentation is the mechanism responsible for producing intense coloration in their wings (Chapman 1998). A high number of species within the family Calopterygoidea possess wing colorations mainly generated by the sequestration of either melanin (black and blue) or carotenoid (red and orange) pigments; moreover, a waxy pruinosity on the wings may also generate a white and/or ultraviolet colors (Hooper et al., 1999). Within this superfamily, the intensity, uniformity and spatial extent in males have been used as a

proxy of mate quality and male fitness (i.e. mating success; Gether 1996, Siva-Jothy 2000, Joop et al. 2006, Cordoba-Aguilar 2002). These remarkable traits together make these damselflies outstanding models to study the evolution of sexually selected traits (Cordoba-Aguilar 2008).

In most odonates, wing coloration is mostly simple; inter-species differences are usually based on the color employed or the relative size of the color patch. For example, in the temperate genus *Calopteryx*, simple changes in the color pattern allow relatively effective conspecific recognition during mating among the species; even though their genetic structures are not significantly different and if they are sympatric (Svensson et al 2006, Svensson & Friberg 2007, Tykkynen et al. 2008, Wellenreuther et al 2010a, Wellenreuther et al 2010b, Lorenzo-Carballa et al. 2014). Damselflies from the genus *Polythore* are an enigmatic among all odonates, because they display complex bands or other geometric shapes of at least two combinations of the following colors, black, white, orange, yellows and whites. Their vibrant coloration has been the primary trait used for their species description (Bick and Bick 1985, 1986, Garrison et al. 2010). There is, in fact, a surprising lack of variability in classical reproductive traits use in odonate species descriptions in the family Polythoridae, such as male cerci, which functions as the "lock and key" mechanisms to ensure reproductive isolation and maintain the species integrity (Garrison et al. 2010). *Polythore* comprises 21 described morphospecies based in the wing color pattern, mainly distributed along the small streams in healthy forests in the Northern Eastern slope of the Andes South America. To understand why selection favors such elaborate color patterns in these damselflies, a quantitative assessment of these

complex wings is necessary. In the first chapter of my dissertation, I quantify the inter- and intraspecies color polymorphism of five morphospecies using three novel methodologies: geometric morphometrics, chromaticity, and Gabor wavelets. Additionally, I recover phylogenetic relationships among these morphospecies based on color, pattern and shape coefficients, and compare them with the genetic background (i.e. barcode Cytochrome Oxidase gene) for all the five morphospecies. The current species concepts of *Polythore* are based on wing color patterns, and this may have inflated or lowered estimates species diversity. My second chapter, I use multilocus Coalescent-based species delimitation analyses of seventeen populations across the geographic range of *Polythore* to establish the most probable species tree and the real number of independent lineages among thirteen of the described morphospecies. How are the *Polythore* damselflies related to other members of the family Polythoridae? Are they sharing only one common ancestor? In my third chapter, I reconstruct the phylogenetic relationships of the family Polythoridae and using a time-calibrated analyses I explore the influence of significant geological events including the Andes Cordillera uplift in the diversification of these Neotropical damselflies.

Chapter One: Mixed Signals? Morphological and Molecular Evidence Suggest a Color Polymorphism in some Neotropical *Polythore* Damselflies

Sánchez Herrera, Melissa[1¶], Kuhn, William.R.[1¶], Lorenzo-Carballa, Maria Olalla [2,3¶], Harding, Kathleen M.[2], Ankrom, Nikole[4], Sherratt, Thomas N.[5], Hoffmann, Joachim [6], Van Gossum, Hans[7], Ware, Jessica L.[1], Cordero-Rivera, Adolfo[2] & Beatty, Christopher D.[2,4¶*]

[1]Department of Biological Sciences, Rutgers University, Newark, New Jersey, United States of America
[2]Grupo de Ecoloxía Evolutiva e da Conservación, Departamento de Ecoloxía e Bioloxía Animal, Universidade de Vigo, Galiza, Spain
[3]Department of Evolution, Ecology and Behaviour, Institute of Integrative Biology, University of Liverpool, Liverpool, United Kingdom
[4]Department of Biology, Santa Clara University, Santa Clara, California, United States of America
[5]Department of Biology, Carleton University, Ottawa, Ontario, Canada
[6]ALAUDA–Arbeitsgemeinschaft für landschaftsökologische Untersuchungen und Datenanalysen, Hamburg, Germany
[7]Evolutionary Ecology Group, University of Antwerp, Antwerp, Belgium

Sánchez Herrera M, Kuhn WR, Lorenzo-Carballa MO, Harding KM, Ankrom N, et al. (2015) Mixed Signals? Morphological and Molecular Evidence Suggest a Color Polymorphism in Some Neotropical Polythore Damselflies. PLoS ONE 10(4): e0125074. doi: 10.1371/journal.pone.0125074

Abstract

The study of color polymorphisms (CP) has provided profound insights into the maintenance of genetic variation in natural populations. We here offer the first evidence for an elaborate wing polymorphism in the Neotropical damselfly genus *Polythore*, which consists of 21 described species, distributed along the eastern slopes of the Andes in South America. These damselflies display highly complex wing colors and patterning, incorporating black, white, yellow, and orange in multiple wing bands. Wing colors, along with some components of the male genitalia, have been the primary characters used in species description; few other morphological traits vary within the group, and so there are few useful diagnostic characters. Previous research has indicated the possibility of a cryptic species existing in *P. procera* in Colombia, despite there being no significant differences in wing color and pattern between the populations of the two putative species. Here we analyze the complexity and diversity of wing color patterns of individuals from five described *Polythore* species in the Central Amazon Basin of Peru using a novel suite of morphological analyses to quantify wing color and pattern: geometric morphometrics, chromaticity analysis, and Gabor wavelet transformation. We then test whether these color patterns are good predictors of species by recovering the phylogenetic relationships among the 5 species using the barcode gene (COI). Our results suggest that, while highly distinct and discrete wing patterns exist in *Polythore*, these "wingforms" do not represent monophyletic clades in the recovered topology. The wingforms identified as *P. victoria* and *P. ornata* are both involved in a polymorphism with *P. neopicta*; also, cryptic speciation may have taking place among individuals with the *P. victoria* wingform. Only *P. aurora* and *P. spateri* represent monophyletic species with a single wingform in our

molecular phylogeny. We discuss the implications of this polymorphism, and the potential evolutionary mechanisms that could maintain it.

Key Words. Color polymorphism; Geometric morphometrics; Chromaticity; Gabor wavelet transformation; Systematics; Population genetics; Odonata; Zygoptera; Calopterygoidea; Polythoridae

Introduction

A polymorphism occurs when genetic diversity produces discrete variation in a phenotypic trait among individuals within a species. Ford (1957) defined polymorphism as "the presence of two or more discontinuous forms of a species in such proportions that the rarest of them cannot be maintained merely by recurrent mutation". Studies of the evolution of color polymorphism (CP, hereafter) in a number of model systems (*Biston betularia* moths (Lees and Creed 1975), *Cepaea* snails (Cain and Sheppard 1954; Davison and Clarke 2000), 'Happy Face' spiders (Franks and Oxford 2009), and side-blotched lizards (Sinervo and Lively 1996; Svensson and Sinervo 2004) have been highly productive, increasing our understanding of the selective forces that maintain these polymorphisms. Recent research has shown that there are several mechanisms that contribute to the maintenance of CPs in natural populations, and that also contribute to the speciation process (Gray and McKinnon 2007); in many systems polymorphisms are maintained by natural selection in the form of predation, but sexual selection in the form of mate choice is also common. Despite this research, our knowledge of how genetic diversity is maintained in nature and its relation with CP is still poorly understood. The exploration of novel polymorphic systems can add new insights and fill some of these gaps. We here present our initial findings on wing color diversity in the Neotropical damselfly genus *Polythore* (Zygoptera: Calopterygoidea: Polythoridae), which appears to maintain an elaborate polymorphism in wing color.

Dragonflies and damselflies (Insecta: Odonata) are amongst the most conspicuous of insects, often due to their wing coloration (Corbet 1999). These colors are generated by a variety of mechanisms, such as pigments, Tyndall scattering, and optical

interference (Corbet 1999; Fitzstephens and Getty 2000; Vukusic and Sambles 2003). Some of the most intense wing color employed by damselflies (Zygoptera) is produced through wing pigmentation. A number of species, mainly in the superfamily Calopterygoidea, possess wing coloration generated by sequestration of either carotenoid (red and orange) pigments or melanin (black); waxy pruinosity on the wings may also generate white and/or ultraviolet colors (Chapman 1998; Hooper et al. 1999). The intensity, uniformity and spatial extent of wing coloration in males typically indicates mate quality and impacts male fitness (i.e. mating success; Grether 1996a, 1996b, 1997; Siva–Jothy 2000; Córdoba-Aguilar 2002; Joop et al. 2006). These damselflies thus present an extremely productive model system for the study of the evolution of sexually selected traits (Córdoba-Aguilar 2008).

In most odonate species, wing color patterns are fairly simple; interspecific differences are usually based on the single color employed and/or the relative size and shape of the color patch. Among species in the genus *Calopteryx*, for example, small differences in simple wing patterns appear to allow for effective conspecific recognition during mating; while mating structures are not significantly differentiated between species, hybridization events appear to be relatively rare, even in places where different species live syntopically (Svensson et al. 2006; Svensson and Friberg 2007; Tynkkynen et al. 2008a, 2008b, Wellenreuther et al. 2010a, 2010b; Lorenzo-Carballa et al. 2014).

The genus *Polythore* currently contains 21 described species, distributed primarily along the eastern slopes of the Andes in South America (Bick and Bick 1985; Garrison et al. 2010). *Polythore* typically dwell in small stream environments within healthy rainforests; larvae live in the streams and adults generally remain close to their stream habitat (Bick

and Bick 1985; Sánchez-Herrera and Realpe 2010). In most calopyterygid species, either red/orange pigments or black pigments are used, but not both (Chapman 1998; Hooper et al. 1999; Contreras-Garduño et al. 2007). *Polythore*, however, is the rare exception: many "wingforms" use at least two colors to generate combinations of black, white, yellow, and orange, displayed in bands and other geometric patterns that differ dramatically between described species (Fig. 1). Their vibrant wing color pattern is the primary trait used to describe the species in this genus (Bick and Bick 1985, 1986). There is, in fact, a surprising lack of variability in other morphological traits: structures such as the male cerci, which function as a "lock and key" mechanism during copula in many other species (Robertson and Paterson 1982) show little or no variation in *Polythore*, even over wide geographic distances. Why selection has brought about such elaborate wing patterning in *Polythore* is thus of interest, and a key first step to addressing this question would be the quantitative assessment of these patterns. Recent work by Sánchez Herrera et al. compared the variability in wing patterns of *P. procera* from Colombia, and analyzed genetic diversity in several populations; morphological characters (including wing color patterning and the structure of male accessory genitalia) were not significantly different among populations, but genetic diversity among certain populations was quite high, suggesting the presence of at least one cryptic species (Sánchez Herrera et al. 2010).

Here we quantify the wing color patterns of individuals from five *Polythore* species (*P. aurora, P. neopicta, P. ornata, P. spaeteri,* and *P. victoria*). The first of these species has a relatively wide distribution in the Amazon Basin in Peru, Ecuador and Brazil; the remaining species have limited distributions in the Amazon Basin of Central Peru on the

eastern slopes of the Andes. As the wing patterns of these species are very elaborate, quantification is not a simple task. We here utilized three methodologies: geometric morphometrics, chromaticity analysis, and Gabor Wavelet Transformation (GWT). These methods allow us to measure differences in wing color pattern, and to determine which components of the wing pattern contribute to those differences. To begin exploring phylogenetic relationships, we also sequence the mitochondrial barcode gene Cytochrome oxidase I (COI) to assess species definitions and population genetic diversity. Finally, we use the results of our morphometric analysis in a novel approach, to generate a morphological dataset for phylogenetic analysis, and directly compare the resulting tree with our molecular phylogeny. The use of wing color and pattern to describe species is based on one hypothesis about the congruence between morphological and genetic diversity in these damselflies. First, coloration may have been selected through sexual selection to indicate mate quality or mate identity. If this were the case, we would predict that there would be high congruence between wing color diversity and phylogenetic patterns. If, however, speciation is currently taking place or there is introgression between individuals with different wing forms, we would not expect congruence in morphological and molecular data.

We found that, while wing pattern diversity is high, distinct and discrete wingforms exist. However, these distinct wingforms do not match clearly with individual species as determined through preliminary phylogenetic analysis: significant differences exist in the genetic diversity of individuals with the same wingforms, while in other cases, there are no differences in wingforms between individuals that are different genetically. We

consider the implications of these results regarding the true diversity within this genus, and the potential explanations for why this diversity may have evolved.

Methods

Taxon Sampling

A total of 94 specimens were collected from localities in regions of the lower and central Amazon basin of Peru in July and September of 2008 (Fig. 2A, Table A in S1 File). Specimens were collected with permission from the Instituto Nacional de Recursos Naturales (INRENA) of Peru (Authorization #62-2008-INRENA-IFFS-DCB and #016 C/C-2008-INRENA-IANP). All *Polythore* specimens used for these analyses were collected on private lands with permission from the landowners. No protected species were sampled. After collection, specimens were either placed in individual glassine envelopes that were stored in airtight dry containers, or in vials with absolute ethanol. Both dried and ethanol-preserved specimens of males and females were used for wing coloration and DNA analysis.

Color Polymorphism Quantification

In order to measure morphological differences in the wings among *Polythore* species and among males and females within those species, and to facilitate quantitative comparison of morphological and molecular evidence, we analyzed images of wings using three different methods. First, shape analysis (geometric morphometrics) was used to compare the shape and relative position of bands in the wings (see "Landmarking analysis" below). Second, differences in the color of different parts of the wings were captured using a novel method for color analysis (see "Chromaticity analysis" below). Finally, wing patterning (the arrangement of light and dark patches in the wings) was compared

using a technique that is common in the field of computer vision (see "Gabor wavelet transformation (GWT) analysis" below). These approaches allowed us to numerically describe three different, but interconnected aspects of wing morphology (shape, color, and patterning) in the highly polymorphic *Polythore*.

Imaging

Four males of *P. aurora*, 21 males and 5 females of *P. neopicta*, 17 males and 6 females of *P. ornata*, 11 males of *P. spaeteri*, and 16 males of *P. victoria* were digitized for morphological analysis. The left forewing and hindwing of each specimen was excised and scanned using a HP Deskjet F2180 scanner/printer (Hewlett-Packard Co., Palo Alto, CA, USA) in color (RGB) at a resolution of 600 dpi. The wings were placed so that the ventral side of the wing was scanned (the side of the wing most often in view at rest and most commonly in view from the ground during flight). Images were saved as JPEG files.

Computation

Images were processed and analyzed (except where indicated) using custom scripts written in *Mathematica* (v10; Wolfram Research 2010). These scripts are available for download as a *Mathematica* notebook (Supplementary File S2).

Landmarking analysis

To compare relative position and shape of wing banding patterns, allowing for comparison among individuals, landmarks (LMs, hereafter; i.e. Cartesian coordinates) were placed on the wing scans. A standard set of 50 LMs (Fig. 3A) was placed on each digitized fore- and hindwing using tpsDig (v2.05; Rohlf 2005); all landmarking was performed by a single technician to ensure consistent LM placement.

Two subsets of landmarks were applied to each wing. LMs 1–14 designated the position of junctions of six major longitudinal veins in the wing, reflecting underlying wing structure (Fig. 3A, red dots). LMs 15–50 were positioned to designate the outlines of color bands on the surface of the wing (Fig. 3A, blue dots). A number of different bands exist in the wings of *Polythore* species; to account for all possible banding patterns we designed a "default wing" (Fig. 3) with six total bands (numbered I–VI) as a template for placement of LMs, such that there were sufficient LMs to capture the full range of wing patterning for all species under study. See Fig. A in S1 File for examples of wing scans and their respective landmarks.

LMs were placed exactly where the band intercepted with six reference veins (the anterior edge, RA, RP3, IRP1, MP, and the posterior edge, using venation terminology from Riek & Kukalová-Peck (Riek and Kukalová-Peck 1984)), so that there were six LMs per band. In some cases, a specimen lacked one or more bands and/or had bands that did not extend all the way to the anteroposterior or proximodistal edges of the wing. In order to account for this, LMs were "collapsed" to other LMs using a standardized protocol as described below.

The default wing was divided into two parts between bands III and IV (Fig. 3B). If the specimen lacked any of the bands I–III, the points for that band were collapsed to the next existing band to the right (distally), or to the outermost point (LM 7) if the specimen lacked band I. Likewise, if the specimen lacked any of the bands IV–VI, the LMs for those bands were collapsed to the next existing band to the left (apically). If band VI was absent, its LMs were collapsed equally between LMs 1 and 14, with the upper three LMs being collapsed to LM 1 and the lower three being collapsed to LM 14. When a band did

not extend all the way to the anterior or posterior edge of the wing, it was collapsed medially to the point where the next closest reference vein intersected the band (Fig. 3C).

To remove the effects of scale and rotation, LMs for the full set of fore- and hindwings were Procrustes superimposed (Zelditch et al. 2004), separately, and recombined into one dataset for analysis. Procrustes superimposition was done using the Geometric Morphometrics package for *Mathematica* (v11.1; Polly 2014). The landmarking procedure described here resulted in 200 coefficients per specimen (50 two-dimensional Cartesian coordinates per fore- and hindwing).

Image squaring

As preprocessing for the remaining morphological analyses, wing scans were standardized for comparison, using an automated script. Images were converted into a 512-px square with a black background, in which the wings were masked, rotated so that their upper margins (costa vein) were horizontal, and then rescaled to a length of 512 px, and where the fore- and hindwings are placed at the top of the upper- and lower halves of the square, respectively (Fig. B in S1 File). The square shape was chosen because it is required for the Gabor wavelet transformation (GWT), while the 512-px dimensions of the square were chosen as a compromise between image detail and computation required for image analysis. Manual masking was required for one *P. victoria* male (pv18), for which scan the automatic preprocessing script failed. Supplementary File S2 provides a more detailed explanation of the image processing procedure, along with the script.

Chromaticity analysis

To compare wing coloration across specimens, square RGB images were separated into their component image channels (red, green, and blue), where each channel is an array of pixel values ranging from 0 (black) to 1 (white). Pixel values were transformed into chromaticity coordinates (CCs), which removes the possible effect of non-standardized lighting between images (luminance) and the correlation between red, green, and blue channels (Gillespie et al. 1987; Woebbecke et al. 1995; Sonnentag et al. 2012). CCs (*r*, *g*, and *b*) are calculated with a simple transformation $r = R/(R + G + B)$, $g = G/(R + G + B)$, and $b = B/(R + G + B)$, where *R*, *G*, and *B* are the pixel values for the red, green, and blue channel, respectively (Sonnentag et al. 2012).

Instead of comparing every transformed pixel value among the images of every specimen, which would be computationally taxing and potentially uninformative, the square images were broken into successively smaller sub-images: the first comprising the entire image, the next two comprising each wing, separately, then the proximal, middle, and distal thirds of each wing, and finally the upper and lower halves of each of those wing thirds (see Fig. C in S1 File for visual explanation). This image-sampling procedure is somewhat similar to that of the GWT (see below; Russell et al. 2007). The mean pixel values for *r*, *g*, and *b* were then calculated for each sub-image. This process yielded 63 chromaticity coefficients per image (21 sub-images × 3 CCs per sub-image).

Gabor wavelet transformation (GWT) analysis

A Gabor wavelet is a type of scalable, rotatable, two-dimensional wave form, which can be used to distill the complex features of an image into relatively few coefficients that describe the gross patterning of light and dark regions in the image (e.g. wing veins,

edges, and color patches). Gabor wavelet transforms (GWTs), where a set of Gabor wavelets are convolved over images to encode them, have many applications for image processing, including optical character recognition, fingerprint and iris recognition, and image compression (Daugman 1988; Weldon et al. 1996) since Gabor wavelets behave similarly to cells of the visual cortex in mammals (Daugman 1980).

In this study, GWTs were used to transform each of the square images into a list of coefficients, describing the patterning of its wings. Each RGB image was first converted to grayscale, then the two components of the wavelet (real and imaginary) were applied using four scales (512, 256, 128, and 64 px in diameter; see Fig. D in S1 File for wavelet arrangement) and three rotations (0°, 120°, 240°), giving 510 coefficients per image. The script for this analysis was adapted from code provided by G.J. Russell.

Comparative analysis of wing morphology

Wingform morphology was compared using the landmarking, chromaticity and GWT datasets individually, as well as a combined set of all three. Each dataset was transformed using Discriminant Analysis of Principal Components (DAPC)(Jombart et al. 2010). This two-step analysis comprised (1) finding the first 50 principal component axes (PCs, in *Mathematica*), and (2) finding the Linear Discriminants (LDs) of those PCs in PAST (Hammer et al. 2001). To determine which coefficients from the untransformed dataset contributed most to each DAPC axis (i.e. the separation between wingforms), the contributions of each coefficient were calculated (similarly to (Jombart et al. 2010)) as DAPC contribution vectors = |(loading vectors for 1st 50 PCs) · (LD loading vectors)|. Values in each contribution vector were converted to proportions of the sum of values in

that vector, so that each value in a contribution vector gave the relative contribution of the corresponding dataset coefficient to that DAPC axis (i.e. for a given contribution vector, coefficients with the highest values contributed the most to the separation of wingforms along the corresponding DAPC axis). For the seven wingforms analyzed in this paper, the DAPC process produced 6 (7 groups - 1) DAPC axes, and therefore, 6 DAPC contribution vectors. Additionally, Mahalanobis distances (Szeliski 2010) were calculated between wingform centroids, using all 6 DAPC axes, to compare how well each analysis separated wingforms.

Phylogenetic Reconstruction

DNA amplification and sequencing

Genomic DNA was extracted from thoracic muscle using either a CTAB protocol (modified from Doyle and Doyle 1987) or the NucleoSpin Tissue kit (Macherey-Nagel, Düren, Germany), following the manufacturer's instructions, except that we incubated the sample at 50 °C for 24 h and used 50 µL to elute the DNA.

Nucleotide variation was assessed in one mitochondrial gene (Cytochrome oxidase I, COI), using the universal primers CJ-2195 and TL2-N-3014 (Simon et al. 1994). PCR was carried out in 20 µL volume reactions containing 1 to 2 µL of DNA, 1X Buffer, 2 mM $MgCl_2$, 0.8 mM dNTPs, 0.5 mM of each primer, and 0.03 U/µL of KapaTaq DNA polymerase. PCR conditions were 94 ^{o}C for 60 s (two cycles), followed by 94 ^{o}C for 45 s, 48 ^{o}C for 45 s and 72 ^{o}C for 60 s, and 29 cycles at 94 ^{o}C for 45 s, 52 ^{o}C for 45 s and 72 ^{o}C for 1 min and 30 s. PCR products were purified using the NucleoSpin Gel and PCR purification kit (Macherey-Nagel, Düren, Germany). Sanger Sequencing reactions were performed bidirectionally at MACROGEN Inc. laboratories (Seoul, Korea). Forward and

reverse sequence strands were assembled and edited using SeqManII v5.03 (DNAstar, Inc., Madison, WI, USA) and consensus sequences were aligned using Clustal W (Thompson et al. 1994), as implemented in MEGA v. 5.1 (Tamura et al. 2011).

Molecular phylogenetics

In order to increase our overall sample size and improve the resolution of our phylogenetic analyses, we included the individuals used for wing morphometric analysis as well as sequences from an additional 31 individuals from the following species: *P. procera* (19 individuals), *P. spaeteri* (6 individuals), *P. gigantea* (5 individuals) and the confamilial *Euthore fasciata* which was used as outgroup (one individual). The sequences associated with these additional individuals were downloaded from GenBank (see Table A in S1 File for accession numbers for all sequence data). Phylogenetic reconstructions were performed using maximum likelihood (ML) and Bayesian inference (BI) criteria. ML analysis was implemented in Garli (v2.0; (Zwickl 2006)). The best nucleotide substitution model for our data was HKY+G, as selected by Mega (v5.2; (Tamura et al. 2011)). Bootstrap supports for each branch were obtained after running 5000 pseudo-replicates of the best estimated topology; the consensus tree was summarized using SumTrees (v3.3; (Sukumaran and Holder 2008)). The BI analysis was performed in MrBayes (v3.2; (Ronquist et al. 2012)), where two independent runs were conducted. Four different heated MCMC chains were used; we ran 10 million generations, sampling a topology every 100 cycles, using default priors for all parameters, and using the GTR+I+G substitution model previously selected by jModeltest 2 (Guindon and Gascuel 2003; Darriba et al. 2012). Convergence in the posterior probabilities for the two runs was assessed by examining the average standard deviation of split frequencies, and using

Tracer v1.6 (Rambaut et al. 2014). Burn-in samples (1 million generations) were discarded and the remaining samples were combined to produce a 50% majority-rule consensus tree, with bipartition frequencies equal to posterior probability values. Both topologies (i.e. ML and BI) were visualized using FigTree (v1.4.1; (Rambaut 2014)). We estimated the evolutionary net divergence between the obtained clades and the standard error using Mega (Tamura et al. 2011).

Morphological phylogenetics

For comparison with the molecular topologies, we also performed a morphological phylogenetic reconstruction using parsimony. Coefficients from the landmarking, chromaticity, and GWT analyses were combined into one-character matrix of continuous characters. Characters that contained only zeros were removed from the matrix, then each character was standardized so that its standard deviation and mean were 1 and 0, respectively, rescaled so that its values were between 0 and 1, and rounded to three decimal places for analysis. Only male Peruvian specimens were used for this analysis to allow for identification of relationships between individuals from this single region, and to allow for a single wingform (that of the male) to be potentially associated with the molecular species identification. Phylogenetic reconstructions were performed on these morphological data using TNT (v1.1; Goloboff et al. 2008). Trees were reconstructed using the 'traditional search algorithm' in TNT with 1000 replicates of Wagner trees set as the starting trees and subtree-pruning-regrafting (SPR) as the swapping algorithm. Consistency and retention indices were calculated for the best topology. Bootstrapping was also performed in TNT using the same conditions as above with 500 replicates.

Resultant topologies were exported as Nexus files, processed in Mesquite v2.75 (Maddison and Maddison 2011), and visualized in FigTree (Rambaut 2014).

Population genetics analysis

In order to assess the intraspecific genetic variation that the traditional phylogenetic tree analyses lack the power to solve (Posada and Crandall 2001), we applied a network representation of the haplotype relationships, including unsampled haplotype variants. Thus we calculated a Minimum Spanning Network (MSN) in the population genetic suite Arlequin (v3.5, (Excoffier and Lischer 2010)), and visualized it using HapStar (Teacher and Griffiths 2011). To establish the genetic diversity of the geographical populations sampled, polymorphism statistics (i.e. number of haplotypes (h), haplotype diversity (Hd), genetic diversity (π), and genetic diversity per segregating sites (θ (S)) were estimated for each geographical population where the total number of individuals was > 10 (e.g. Pozuzo, Pampa Hermosa, and Panguana) with DnaSP (v5.10; (Librado and Rozas 2009)). Neutral evolution was tested with the Tajima D test (Tajima 1989) in Arlequin, assuming the well-accepted premise that mtDNA does not recombine. To determine the degree of population structure between all the geographical populations, pairwise F_{ST} values were calculated in Arlequin and 95% statistical significance for each test was obtained by 10,000 randomizations.

Species delimitation

To test if the morphospecies described using color patterns are consistent with our phylogenetic hypothesis; we ran a single-marker model for species delimitation called a Poisson Tree Processes (PTP). This model relies on the number of substitutions of a tree topology, assuming that the number of substitutions among species will be higher than

the number of substitutions within the species(Zhang et al. 2013). The ML phylogram was used to calculate the probabilities that support species boundaries detected by the model. PTP was run via the web interface sponsored by the Exelixis Lab (Alexis Stamatakis: http://sco.h-its.org/exelixis/web/software/PTP/index.html).

Results

Color Polymorphism Quantification

In total, the wings of 79 *Polythore* specimens from the five species collected from Peru were analyzed with the three color polymorphism (CP) quantification methods (landmarking, chromaticity, and GWT). These included both males and females of *P. neopicta* and *P. ornata*, and males only for *P. aurora*, *P. spaeteri*, and *P. victoria*—seven wingforms in total. Upon visual comparison, patterning varied markedly both within and among wingforms (Fig. 1). *P. aurora* males appeared to be the most variable, while *P. neopicta* males and *P. ornata* females appeared to be the least variable.

Landmarking analysis

Wings in all scans were landmarked; examples of specimens with landmarks are shown in Fig. A in S1 File. Mean shapes for the wingforms are shown in Fig. 4. In all wingforms, at least one band was collapsed to the proximal or distal end of the wing, while all six bands were collapsed in the forewing of *P. ornata* females and hindwing of *P. spaeteri* males (see Fig. 1).

Comparison of morphological analyses

DAPC and Mahalanobis distances (MDs) were used to determine which morphological analysis produced the best separation between wingforms. Plots comparing the first two DAPC axes (i.e. the first two dimensions of the 6-dimensional discriminant space) are

shown in Fig. 5A–C and Fig. F.A in S1 File for the landmarking, chromaticity, GWT, and combined analyses, respectively. From these DAPC plots, the combined analyses and landmarking analysis appeared to give the most separation, while the chromaticity analysis appears to give the least separation. Interestingly, different wingforms group together depending upon the method used. For instance, *P. victoria* males grouped with *P. neopicta* males in the chromaticity, GWT, and combined analyses, but grouped with *P. ornata* males in the landmarking analysis. Similarly, *P. ornata* female and *P. spaeteri* males were very similar according to the landmarking and combined analyses, but very different according to chromaticity and GWT. *P. aurora* males were consistently separated from all other groups. Despite these apparent differences, however, the MD for pairs of wingforms (measured in standard deviations), calculated from all six DAPC axes, showed similar degrees of separation between most wingforms (Table 1). Mean MDs were as follows: landmarking, 4.32, combined, 4.31, GWT, 4.27, and chromaticity, 3.67. MD values consistently exceeded an arbitrary threshold of 3.0 for all wingform pairs except for *P. neopicta* male—*P. ornata* male and *P. neopicta* male—*P. victoria* male, which consistently showed lower MDs, and *P. ornata* male—*P. victoria* male and *P. spaeteri* male—*P. victoria* male, which had lower MDs from the chromaticity analysis. *P. aurora* males showed the highest degree is separation from all other wingforms along with *P. neopicta* female—*P. ornata* female.

The axes of the DAPC plots shown in Fig. 5A–C and Fig. F.A in S1 File each comprise a linear combination of the original coefficients that were analyzed. We can determine the relative contribution of each of the original coefficients to each DAPC axis (i.e. which coefficients contributed the most to an axis, and thus best discriminated between

wingforms). Relative contributions for the first and second DAPC axes for each analysis are shown in Figs. E and F.B in S1 File; the five highest-contributing coefficients are highlighted in red. Each of the coefficients corresponds to a particular location on the wings of our specimens, which can be mapped back onto the wings to determine which wing parts are most informative for wingform discrimination. In Fig. 5D–F and Fig. F.C in S1 File, the parts of the wings corresponding to the highest-contributing coefficients for each analysis have been highlighted on an example specimen, where blue and red shapes represent the highest contributors to the first and second DAPC axes, respectively. In the figure, landmarks are represented as small circles; chromaticity sub-images are represented as boxes around the appropriate portion of the square image, and letters "r", "g", or "b" tell which chromaticity channel the sub-image corresponds to; and Gabor wavelets are represented as circles over the piece of the image to which they were applied, each with an arrow denoting the direction of wavelet rotation. The top coefficients for the combined analysis all correspond to Gabor wavelets. Notice that there is some overlap between coefficients that contribute the most to the first and second DAPC axis (represented as overlapping red and blue shapes). Overall, the medial section, and to a lesser extent the distal section, of the fore- and hindwings contributed the most to discrimination between the different wingforms. This particularly corresponds with wing bands IV and V (Fig. 2A). The top contributing coefficients in the landmark analysis were *y*-components–the *y*-axis here corresponds to the proximodistal axis of the wings–of landmarks 33–38 in the forewing and 27–28 in the hindwing (Fig. 5D); while in the chromaticity analysis, the most important features were all in the red and blue chromatic channels of the image, not in the green channel (Fig. 5E).

Phylogenetic Reconstructions

Molecular phylogenetics

The phylogenetic topologies recovered for both criteria, ML and BI, were consistent (Fig. 2B). *P.aurora* forms a well-supported monophyletic lineage, and seems to be the sister clade to all of the other taxa, although neither of the analyses estimates a support value for this branch. The highly supported *P. gigantea* clade is sister to all the other taxa, followed by two highly supported reciprocal monophyletic clades: *P. procera* from Colombia and a clade that contains all of the individuals collected in the Central Amazon Basin of Peru (i.e. *P. ornata, P. spaeteri, P. neopicta* and *P. victoria,* Fig. 2B). Within this Amazon Basin clade, a distinctive clade of the species, *P. ornata/P. spaeteri* encompasses two reciprocal monophyletic clades (Net divergence =1.27%, SE= 0.004), while another equal clade composed of *P. neopicta* and *P. victoria* shows no distinction between these species, with their distinct wingforms (Net divergence = 0.052%, SE=0.0028). Interestingly, *P. neopicta* shows a paraphyletic position across the Amazon Basin clade; some individuals sampled in Oxapampa are closely related to *P. ornata,* while other individuals sampled in Pozuzo localities and the Perené River Road region are close to, and in some cases even indistinguishable from, *P. victoria* (Fig. 2A).

Morphological phylogenetics

For our phylogenetic analyses that include morphological traits (767 characters), we limited our dataset to males (68), such that each species would be represented by a single wingform. We obtained only one most parsimonious tree with a tree length of 4500.780 steps. The overall topology has a consistency index of 0.170, suggesting these traits are highly homoplasic. The retention index was 0.519, showing that, despite the homoplasic

nature, the synapomorphic characters are informative. We recovered *P. aurora* as sister to all other species, however only two individuals of this species clustered as a monophyletic clade (Fig. G in S1 File). The remaining species were recovered as monophyletic, although *P. ornata* and *P. victoria* had low bootstrap branch supports (9 and 5%, respectively), and two individuals of *P. ornata* were recovered within *P. victoria*.

Population Genetic Analyses

Overall, among the species and populations of *Polythore* included in this analysis we observed a total of 28 COI haplotypes. Of the two species sampled from Colombia, *P. procera* shows a higher number of haplotypes (h=8) in comparison with *P. gigantea* (h=3). Forty-one missing or unsampled haplotypes are estimated between *P. procera* and *P. spaeteri* from Panguana in Peru. The haplotype network suggests *P. spaeteri* (h=8) as the source haplotypes from which all the remaining Peruvian *Polythore* haplotypes are derived (Fig. 6). Eight unsampled haplotypes associate *P. ornata* from Pampa Hermosa, and *P. neopicta* from Oxapampa to *P. spaeteri*; while 12 unsampled haplotypes bridge *P. spaeteri* to *P. neopicta* and *P. victoria* from localities near Pozuzo and the Perené River Road. Finally, *P. neopicta* from the Perené River Road and *P. aurora* from Iquitos are joined by more than 100 missing haplotypes between them (Fig. 6).

Genetic polymorphism statistics for the Peruvian populations with more than 10 individuals are shown in Table 2. The Panguana population (*P. spaeteri*) shows high haplotype and genetic diversity in comparison with Pampa Hermosa (*P. ornata*) and Pozuzo populations (*P. victoria –P. neopicta*). Pampa Hermosa (*P. ornata*) on the other hand shows a lack of genetic diversity, with only one haplotype representing the entire

population. Tajima's neutrality tests were all negative and non-significant (Table 2), which suggest that the COI sequence is not subject to selection and is evolving neutrally.

The calculated fixation index values for population structure (F_{ST}) show that the Panguana population (*P. spaeteri*) exhibited high and significant population structure (e.g. $F_{ST} > 0.88$) compared to all the other sampled geographic populations (Fig. 6 and Table B in S1 File). The Pampa Hermosa population (*P. ornata*) showed high and significant population structure except with the Oxapampa population (*P. neopicta*) where the F_{ST} value is 0, suggesting possible gene flow or a shared ancestral polymorphism between these two populations. Among the six localities sampled near to Pozuzo (*P. victoria* - *P. neopicta*), we observed a degree of significant population structure across some of these populations (Fig. 6 and Table B in S1 File). Pozuzo 1, 2 and 3 show high structure as compared to Pozuzo 4 and 6, suggesting restricted gene flow among these populations. The lack of structure among Pozuzo 1, 2 and 3 and Pozuzo 4, 5 and 6 suggests possible recent gene flow between these two sets of geographical populations. Interestingly the F_{ST} value of the Perené River Road population with Pozuzo 1, 2 and 3 is ~ 0, suggesting gene flow or a shared ancestral haplotype (Fig. 6 and Table B in S1 File).

Species delimitation

The PTP species delimitation model supports 9 species or Operational Taxonomic Units (OTU's) based on our single marker COI. One of the supported OTU's was the outgroup *Euthore fasciata* ($p = 1$). Within the *Polythore,* some of the OTU's were highly supported, with probabilities > 0.70, while others were supported with probabilities < 0.69 (Fig. 2B). The Colombian species, *P. gigantea* and *P. procera,* were consistent with our

expectations. *P. procera* was divided into two OTU's (one supported with 0.658, and the other one with 0.903), which is consistent with the results previously obtained by Sánchez Herrera et al. 2010 (Fig. 2B). *P. gigantea* was recovered as an OTU with a high probability (0.705). The Peruvian species show incongruence with the morphological expectations. *P. aurora, P. spaeteri* and *P. ornata/neopicta* were highly supported OTU's, with probabilities of 0.988, 0.759 and 0.731, respectively (Fig. 2B). The *P. victoria*/*P. neopicta* clade was supported with a low probability (0.474) as only one OTU (Fig. 2B). Despite the latter, two individuals of *P. victoria* were considered as another OTU with a high of probability 0.701 (Fig. 2B).

Discussion

Patterns of Diversity

Our analyses of wing color patterns in *Polythore* demonstrate that both the complexity of wing patterns—with some wingforms incorporating particular bands while others do not—and the interchanging of colors within those bands, come together to create a diverse range of phenotypes. Through our landmark analyses we show the influence of the different combination of bands on these phenotypes; for example, males of *P. victoria* and *P. ornata* are shown to be relatively similar to one another (Fig. 5A and Table 1), despite their obvious color differences (Fig. 1). In this case, both wingforms have very similar banding, but the colors of the bands differ. These striking differences in color are shown in our chromaticity results (Fig. 5B); while there is less resolution between the different wingforms, overall levels of melanization, in both the medial and distal parts of the wing, drive differences. Our GWT results incorporate both of these components; here *P. victoria* and *P. ornata* are shown to be quite different (as they are on visual

inspection). Males of *P. victoria* and *P. neopicta* show great similarity, sharing similar overall color patterns as they do, but differing in the presence (*P. victoria*) or absence (*P. neopicta*) of a single, medial band. There are also differences in the overall variability of the phenotype components—banding patterns are relatively invariant, as reflected through the tight clustering of individuals sharing a common wingform in the LM and GWT analyses, but we see greater differences in the chromaticity values within wingforms. It is of note that these differences among and within wingforms are driven most by the red and blue components of color; the green component did not contribute significantly. The combination of these analyses (Table 1 and Fig. F in S1 File) resolves all of the analyzed wingforms effectively, except for the male wingforms of *P. neopicta* versus *P. ornata*, and *P. neopicta* versus *P. victoria*; these wings all have black distal bands and differ only in the banding pattern preceding that shared band.

An interesting observation that can be made from these analyses concerns the way in which wing pattern diversity is generated in this group. While there are a number of distinct wingforms observed in *Polythore*, these do not represent unlimited complexity; as shown by the assembly of our 'default wing' for landmark analysis, there are a fixed number of repeated pattern elements within the wings, such that a particular band may be present or absent within a wingform, and if present may be of a different color within a different wingform. This suggests a fixed number of wing elements that can be expressed or suppressed, similar to the pattern elements observed in *Heliconius* butterflies (Joron et al. 2006a, 2006b). In *Heliconius*, these pattern element shifts are made through a small number of allele differences, and the same may be true of *Polythore*. Exploration of these wing pattern elements within this highly diverse group will allow for an understanding of

the mechanisms of wing pattern expression in the genus, and possibly more generally in odonates.

While distinct pattern elements can be identified through our morphometric analyses, our phylogenetic results are less clear. When considering the phylogenetic analyses of the morphological dataset alone (Fig. G in S1 File), individuals sharing a common wingform generally form well-supported clades, reflecting the distinctness of the different wingforms. The greatest exception to this are the males of *P. aurora*, which are found to be paraphyletic with respect to the remaining species; this is perhaps due to the rather extreme variability in the color intensity of individuals in our analyses (see the 3 examples at the top of Fig. 1), Two individual males of *P. ornata* clustered with *P. victoria* males in the morphological phylogeny; this is likely due to variation in the hindwing banding patterns and forewing color patterns. Our molecular phylogenetic analyses (Figs. 2B and 7) and species delimitation analyses reveal that, for the Peruvian species studied here, there are some wingforms that correspond to well-defined species--such as *P. spaeteri* and *P. aurora*--while the wingforms associated with *P. victoria*, *P. neopicta* and *P. ornata* do not resolve well. *P. victoria* and *P. ornata* emerge in different locations within the tree, but have *P. neopicta* individuals contained within each of these two clades; a number of *P. victoria* and *P. neopicta* individuals cannot be separated at all, and this clade with its two wingforms is identified as a species in our delimitation analysis, albeit with low support. Other specimens of *P. neopicta* are indistinguishable from *P. ornata*, and these individuals are identified as a species with high support by our delimitation analysis. Further, our delimitation analysis suggests that, similar to the cryptic speciation within *P. procera* highlighted by Sánchez Herrera *et al.* (2010) and

recovered in our own results (Fig. 2B) we have a small clade of individuals from one site (Pozuzo 6) that, despite having the characteristic *P. victoria* wingform, are supported as a separate species from the other *P. victoria*. The lack of molecular separations between *P. neopicta* and *P. victoria*/*P. ornata* are at the heart of this lack of congruence between analyses. These preliminary analyses of the COI sequence suggest that a more extensive phylogenetic exploration may be necessary to elucidate species relationships.

Topography is potentially very important in the distribution of *Polythore*. The localities for *P. victoria*, *P. neopicta* and *P. ornata* are all within steep river valleys with high ridges separating them (Fig. 2A); *P. spaeteri*, while at lower elevation between the Andes and Sira ranges, is also isolated from the other populations sampled in Peru. Thus, while the distances between these populations are not large, there are significant barriers to movement between these regions. In our haplotype network (Fig. 6 and Table 2), *P. spaeteri* from Panguana, with its single wingform, shows relatively high genetic diversity in comparison to other groups that have multiple wingforms, but little morphological diversity. Other haplotypes within the Peruvian *Polythore* in our study appear to be derived from these *P. spaeteri* haplotypes, possibly due to the highest genetic diversity present in that population.

Most of the species in this study were taken from the drainage basin of the Río Ucayali, one of the most water-rich headwaters of the Amazon (Fig. 2A); the one exception is *P. aurora* taken along the Río Marañón near Iquitos (see below). The *P. spaeteri* specimens in this study were physically closest to the Río Ucayali confluence, taken at the Panguana field station, on the Río Llullapichis, a tributary of the Río Pachitea, which discharges into the Río Ucayali. The other *Polythore* wingforms/species found in Peru, are all taken

from river valleys (Pozuzo, Santa Cruz, Perené) that like the Pachitea, drain to the Río Ucayali. It is possible that there is some connectivity on the landscape through these river corridors, connecting *P. spaeteri* to the *P. neopicta*, *P. ornata* and *P. victoria* populations in higher-elevation streams, though some of the patterns seen from our high F_{ST} suggests that there is significant genetic isolation between the Pachitea river and Pozuzo River valleys (Figs. 5 inset and 6). Individuals in the putative cryptic species with *P. victoria* wingforms identified by our delimitation analysis were taken from site Pozuzo 6, which is actually in the valley of the Río Santa Cruz, a tributary of the Río Pozuzo; this latter river valley is where all of the other sample populations with *P. victoria* wingforms are found. Within the higher-elevation *P.ornata* from Pampa Hermosa near the Perené River Valley shows a high genetic isolation with all the other populations from the Pozuzo Valley, except the Oxapampa. Finally, the Perené River Road population shows no differentiation with the Pozuzo Valley populations; this may represent an ancestral polymorphism, rather than more recent gene flow due to the lack of connectivity between these regions (Fig. 2A). Populations containing these latter three wingforms (Fig. 1, *P. neopicta*, *P. victoria* and *P. ornata*) are genetically less diverse, despite the greater morphological diversity (Fig. 6 and Table 2).

The Ucayali flows north from central Peru to the Amazon and the region where *P. aurora* is found. It is also of note that the haplotype of *P. aurora*, is derived from the *P. neopicta*/*P. victoria* haplotype group, rather than from those of the Colombian *Polythore*; sampling of other *Polythore* populations in Peru would help to better elucidate this relationship, but it is again possible that river corridors may be involved in establishing flow between these populations.

Why do we see such high wing pattern diversity that does not correlate to our molecular phylogenetics? A few explanations are available for these patterns; one is that these groups are currently speciating, and as yet are difficult to distinguish through molecular genetic techniques (Mallet 1989; Mallet and Barton 1989; Brower 1996, 2011; Hill et al. 2012). If this is the explanation for our pattern, then wing color phenotypes have already diversified, but fully assortative mating has not yet established (Feder et al. 2012; Martin et al. 2013). This is a potential explanation for the *P. neopicta* wingform, which does not emerge as a separate species in our analyses, but as polymorphic forms of two other species, *P. victoria* and *P. ornata*. If this is the case, then we have potentially two new species forming which share a common wing phenotype. There is also the possibility that wingform is associated with species identity, but that introgression between individuals with different wingforms occurs regularly. This scenario begs the question of why hybrid wingforms are not observed in these zones: regular mixing has apparently not diminished wing phenotypic diversity (Mavárez et al. 2006; Salazar et al. 2008).

The final picture, drawn from our analyses, is of a group of damselflies with highly distinct, complex and divergent wing phenotypes, but for which molecular phylogenetic species determinations are not clear, suggesting significant levels of polymorphism within this group, as well as the possible existence of cryptic species, as also found by Sánchez Herrera and colleagues in their studies of *P. procera* in Colombia (Sánchez Herrera et al. 2010). While this genus has a broad geographic distribution, local site wingform diversity is quite low, with usually only one predominant wingform found at any one locality. In some regions within the sampling area, a particular wingform is common in one zone, another common in an adjoining zone, and a narrow border zone

exists between the two where the two wingforms are encountered; these wingforms appear to remain distinct, even in these overlapping zones. These distribution differences appear to persist across years and seasons, suggesting that these wing colors are not influenced by the age of the individual or climatic conditions. Our haplotype analysis suggests that there may be gene flow between some of these localities with different wingforms (for example, between the sites in the Pozuzo Valley where the *P. victoria* and *P. neopicta* clade is found) and as such we would consider these as a single population that is polymorphic.

In their recent review paper on the study of lineage divergence and speciation in insects, Mullen and Shaw suggest that a comprehensive understanding of the speciation process requires demonstrating the axes of differentiation in the system, the speciation phenotypes (i.e., traits whose divergence somehow limits gene flow, either directly or indirectly) and which evolutionary forces cause the divergence of a speciation phenotype, followed by an investigation of the genetic architecture of the speciation phenotypes and how they trigger further genome evolution in establishing species boundaries (Mullen and Shaw 2014). Here we have identified wing color patterning as a primary axis of differentiation, and the establishment of different wingforms as the phenotypes that may be associated with speciation. Now we must ask, what are the evolutionary forces driving this phenotypic divergence?

Hypotheses to Explain Color Polymorphism in Polythore

Why did this extensive wing diversity arise in the first place? As has been noted previously, the majority of damselfly species that possess wing coloration display a single color in bands or spots on an otherwise clear wing, with much research supporting

that this coloring functions to attracting mates or fend off conspecific male competitors (Honkavaara et al. 2011; Hassall 2014). If, similar to these other calopterygoid damselflies, sexual selection is also the main driver of wing coloration in *Polythore*, it remains to be explained why in this group it has resulted in such elaborate wing patterns. Further exploration of this potential selective force would require mating behavior experiments within and among individuals of *Polythore* with different wingforms. Some diversity in mating behavior, such as differences in tendency for males to mate guard while the female oviposits, have been observed among different *Polythore* forms (MSH and CDB, unpublished data) and quantitative natural observations combined with experimental pairing between males and females of different wingforms will determine how much wing coloration is a factor in mate choices in these damselflies. If it is found that mating preference is a function of wing color and pattern, this suggests that sexual selection is at least a factor maintaining wing diversity.

Another possibility that has been suggested (at least anecdotally) for *Polythore*, is that some of the wingforms may be under selection to resemble co-occurring toxic Ithomiinae and Heliconiinae (clearwing) butterflies (De Marmels 1982; Louton et al. 1996; Beccaloni 1997; Corbet 1999) (K. Tennessen, pers. comm.). Even if wing colors were initially under sexual selection, selection by predators for similarity to local defended butterflies might have influenced wing color and pattern, in at least some species. It is of note that much recent work on speciation, introgression and wing ornamentation cited above comes from work on the *Heliconius* model system; comparative studies of the distribution of *Polythore* wingforms and butterfly wingforms may help to determine the feasibility of this hypothesis. Further investigation of this hypothesis will require

analysis of the wing color and patterning of co-occuring butterflies in the regions where different *Polythore* wingforms are found. If selection for mimetic resemblance is a factor in this system, we predict that morphometric analysis of butterfly and damselfly wings would find significant correlations between these two groups in each locality where they are found, a requirement for the model/mimic relationship.

Work on the diversification and genomics of *Heliconius* butterflies has identified interesting patterns that are worth considering in the case of *Polythore*, regardless of whether mimetic resemblance may be involved in the evolution of the wing colors of these damselflies. Research suggests that *Heliconius* color patterning loci are tightly linked to alleles underlying variation in male preference(Kronforst et al. 2006). In *Heliconius* tight physical linkage reduces recombination between loci associated with mating preference and color evolution and may facilitate the maintenance of positive assortative mating in this system. Introgression between different *Heliconius* species, while under strong selection from predators, may also provide the wing color diversity and adaptive novelty through wing color diversification(Consortium 2012), thus supporting the hypothesis that hybridization is an important source of adaptive novelty in this system. Considering what we now know about wing color diversity and species definitions in the *Polythore* damselflies, a further exploration of behavior, color diversity and the genomics of wing coloration in this group may elucidate more generally the factors that can influence the development of CP, in damselflies as well as other organisms.

Acknowledgments

The authors would like to thank Juan Grados, Gerardo Lamas Müller and colleagues at

the Natural History Museum in Peru for guidance and assistance with collections. We also thank many people for their hospitality during field work: Juliane Koepcke and Carlos Vásquez "Moro" Módena of the Panguana field station, the people of the villages of San Martín de Tipishca and Pozuzo, and Ernesto Lajara Loechle for assistance with transportation. We would like to thank David Polly and Gareth Russell for assistance with manuscript preparation.

Chapter 1: Tables

Table 1. Mahalanobis distances (MDs; calculated from first 6 DAPCs) between wingforms using for different combinations of morphological coefficients.

Wingform Pair	LM	CHRM	GWT	ALL	MEAN
auroraM—neopictaF	5.92	4.92	5.8	5.88	5.63
auroraM—neopictaM	4.82	4.58	4.74	4.8	4.74
auroraM—ornataF	5.66	5.17	5.58	5.65	5.52
auroraM—ornataM	4.9	4.57	4.83	4.89	4.80
auroraM—spaeteriM	5.14	4.82	5.03	5.12	5.03
auroraM—victoriaM	4.96	4.58	4.88	4.93	4.84
neopictaF—neopictaM	4.39	3.18	4.32	4.36	4.06
neopictaF—ornataF	5.3	4.12	5.27	5.32	5.00
neopictaF—ornataM	4.49	3.35	4.43	4.47	4.19
neopictaF—spaeteriM	4.75	3.64	4.68	4.74	4.45
neopictaF—victoriaM	4.56	3.19	4.5	4.54	4.20
neopictaM—ornataF	4.02	3.49	4.02	4.05	3.90
neopictaM—ornataM	2.88	2.7	2.85	2.87	2.83
neopictaM—spaeteriM	3.27	3.13	3.23	3.25	3.22
neopictaM—victoriaM	2.98	2.09	2.87	2.93	2.72
ornataF—ornataM	4.14	3.64	4.15	4.15	4.02
ornataF—spaeteriM	4.36	4.08	4.4	4.41	4.31
ornataF—victoriaM	4.21	3.46	4.2	4.22	4.02
ornataM—spaeteriM	3.4	3.22	3.35	3.39	3.34
ornataM—victoriaM	3.11	2.25	3.08	3.1	2.89

spaeteriM—victoriaM	3.49	2.91	3.41	3.48	3.32
MEAN	**4.32**	**3.67**	**4.27**	**4.31**	**4.14**

M = male, F = female, LM = landmark coefficients, CHRM = chromaticity coefficients, GWT = Gabor wavelet transformation coefficients, and ALL = combined LM, CHRM, & GWT. MD is measured in standard deviations.

Table 2. Peruvian geographical population polymorphism statistics.

Population	N	h	Hd	π	θ(S)	Tajima's D	Significance
Panguana	14	8	0.901	0.0027	0.00383	-1.06599	> 0.10
Pampa Hermosa	11	1	0	0	0	NA	NA
Pozuzo	24	4	0.536	0.0235	0.00326	-0.91249	> 0.10

Number of individuals (N), Number of haplotypes (h), haplotype diversity (Hd), genetic diversity (π), genetic diversity per segregating sites (θ(S)), and Tajima's D test including significance.

Chapter 1: Figures

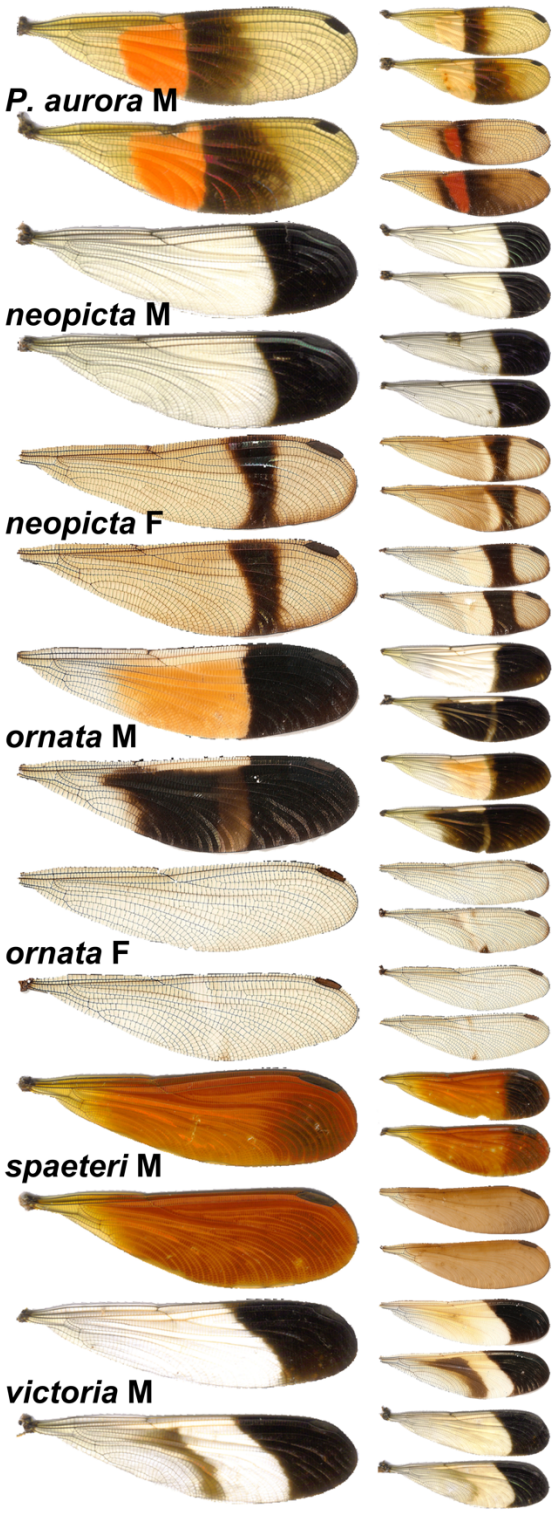

Figure 1. Examples of color polymorphism in *Polythore* taxa used in this study. For each wingform, the typical form is shown on the left, and extremes are shown on the right.

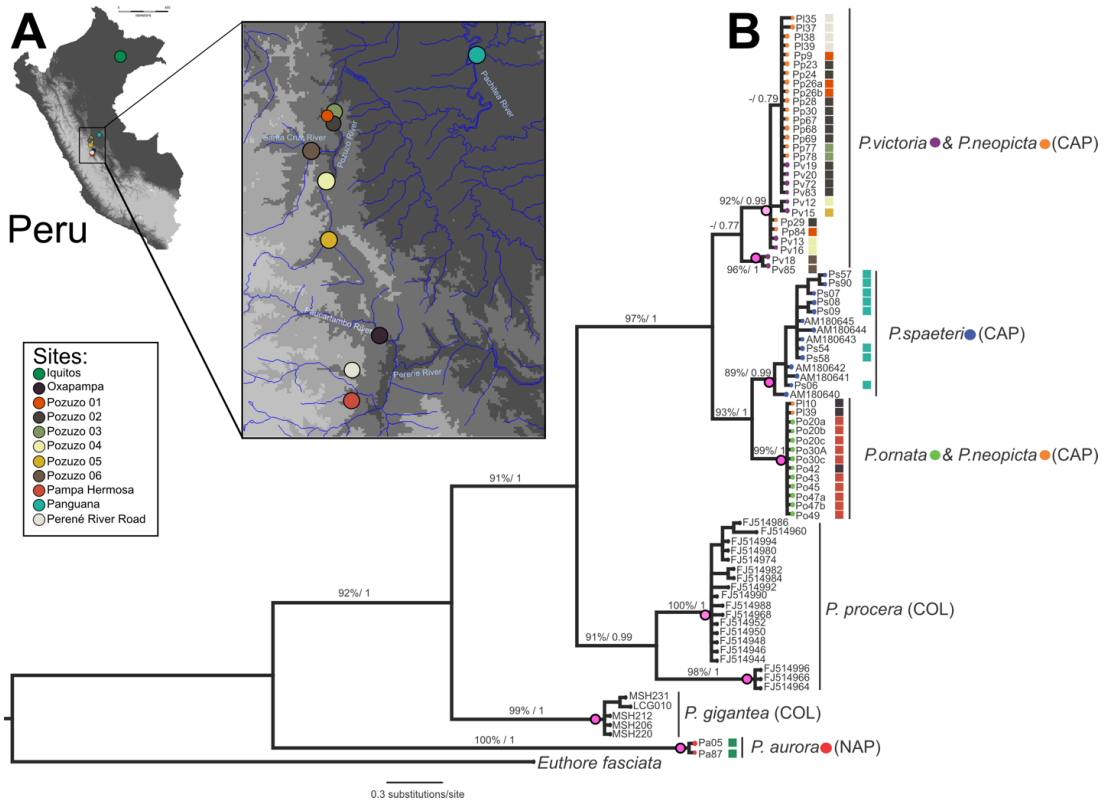

Figure 2. Collection localities of *Polythore* used in this study and phylogenetic reconstruction using Cytochrome oxidase I (COI). (A) map of collection localities of and (B) phylogenetic reconstruction (best ML phylogram) using COI data, values above the branches represent bootstraps support (ML) and posterior probabilities (BI). The magenta dots on the nodes represent the OTUs or species boundaries estimated by the PTP species delimitation model; lighter color represents less-supported probability for that OTU.

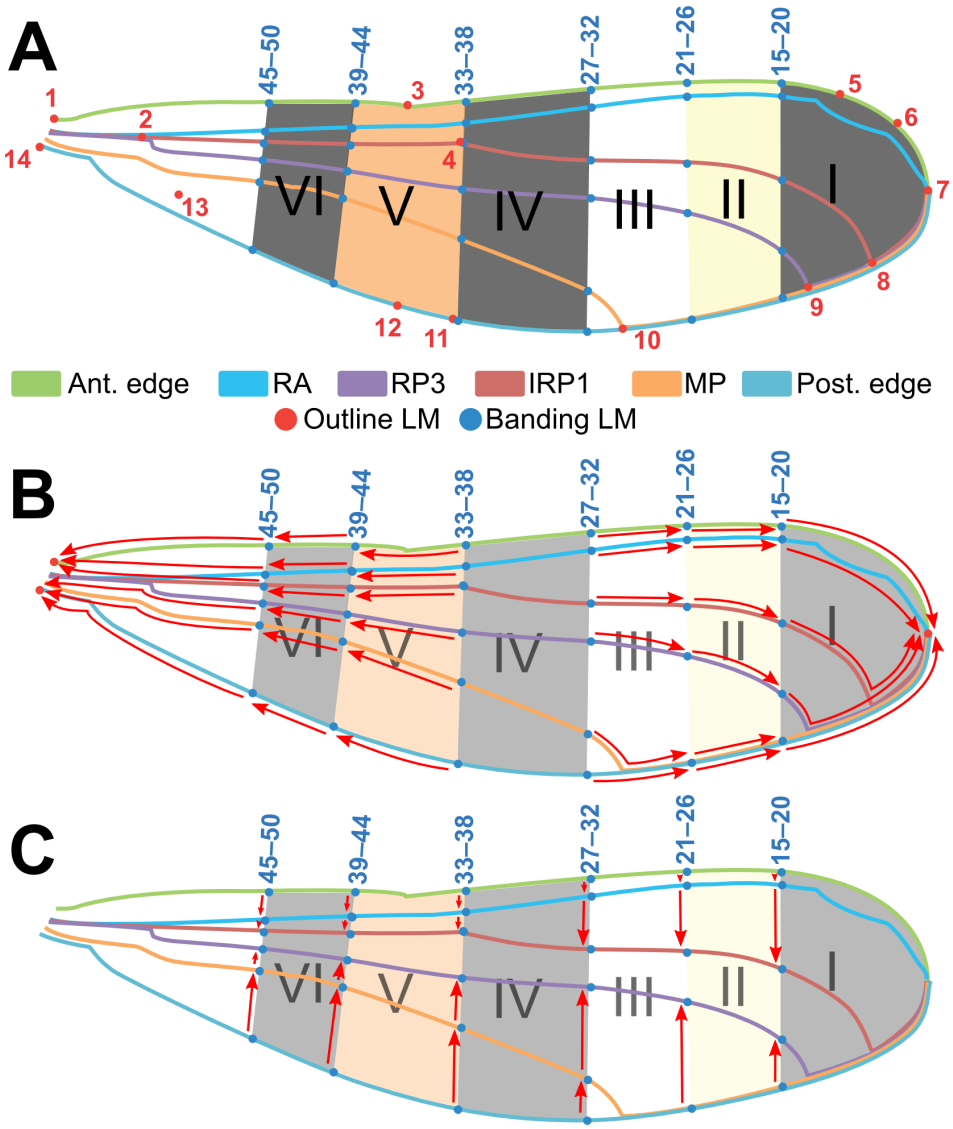

Figure 3. "Default wing" used as a template for landmarking analysis of fore- and hindwings of *Polythore* wingform. The positions of six major bands (I–VI) are marked as the cross six longitudinal veins: anterior edge or costa (C), radius anterior (RA), second branch of radius posterior (RP2), third branch of radius posterior (RP3), media posterior (MP), and posterior edge (venation terminology per Riek & Kukalová-Peck (1984)). (A) LMs 1–14 are major morphological points representing the basic venation pattern (~outline) of the wing, and LMs 15–50 represent the proximal edges of the six bands. (C–D) red arrows depict protocol for "collapsing" LMs in (C) proximodistal and (D) anteroposterior directions in wings where bands are missing or do not extend the full width of the wing (see Methods text for full description).

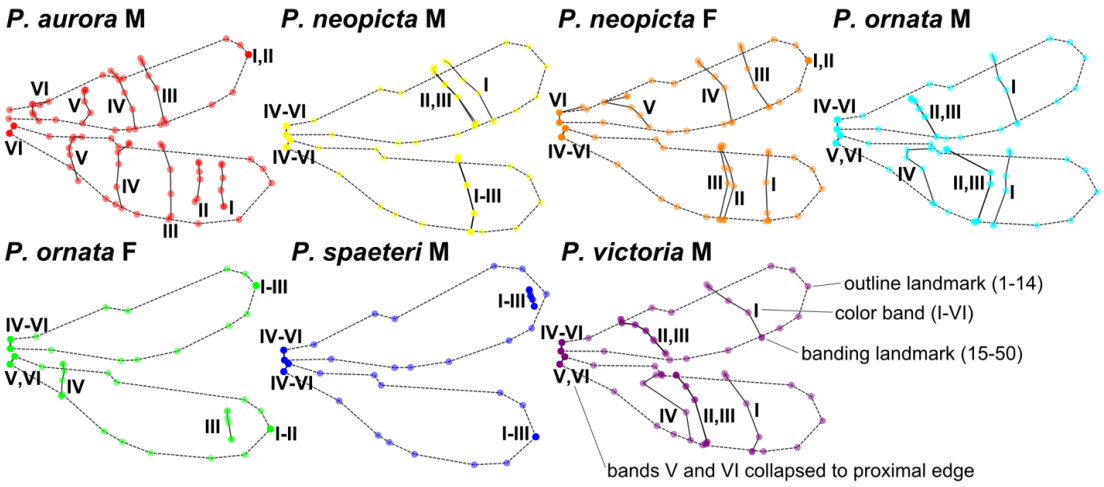

Figure 4. Mean wing shapes for *Polythore* wing morphs from landmark analysis. Fifty landmarks were taken from individuals of the 7 wing morphs, Procrustes superimposed, and averaged together for each wing morph. Outline landmarks (LMs 1–14) are dashed; color bands (LMs 15–50) are solid lines and numbered from I to VI. See Fig. 2 and text for detailed description of landmarking protocol. M = male, and F = female.

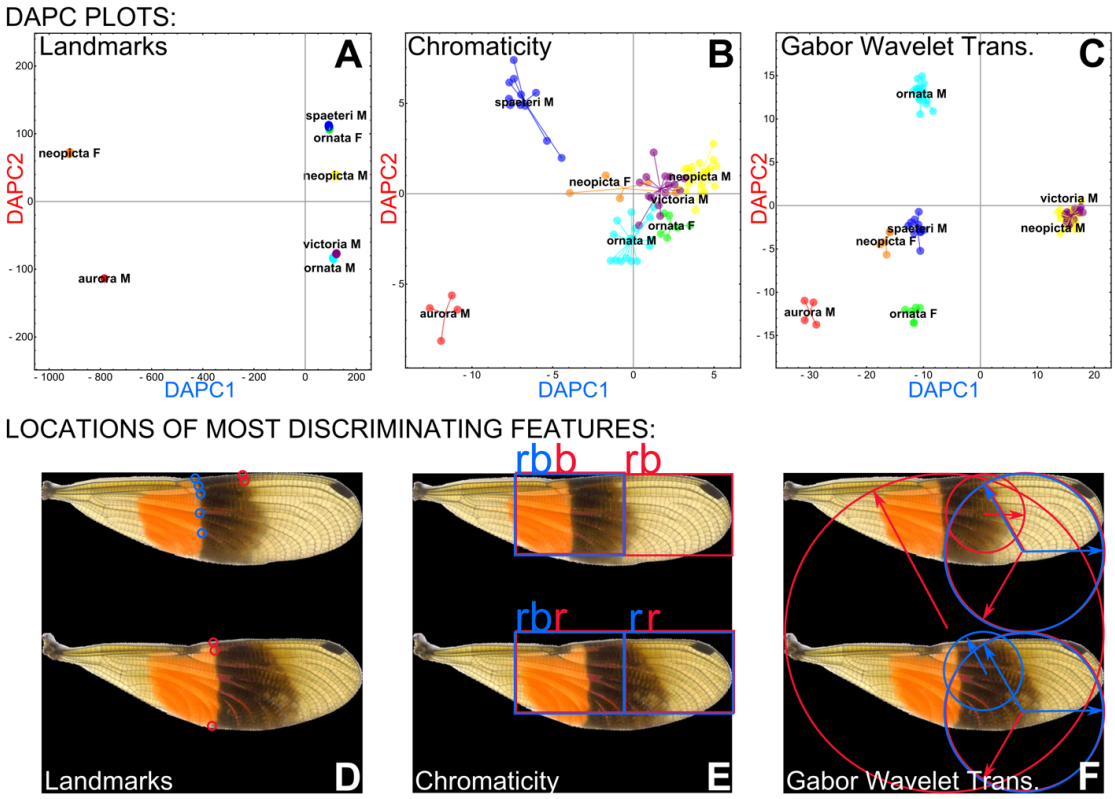

Figure 5. Discriminant analysis of morphological results. Discriminant analysis of principal components (DAPC) plots for (A) landmarking, (B) chromaticity, and (C) GWT analyses. (D–F) areas of the wings corresponding to the 5 most discriminating coefficients for DAPC axes 1 and 2 for each of the analyses (see Results text for further explanation of D–F). Note: here, these locations are superimposed onto an image of a *P. aurora* male, for presentation, but represent variation among all individuals/wingsforms.

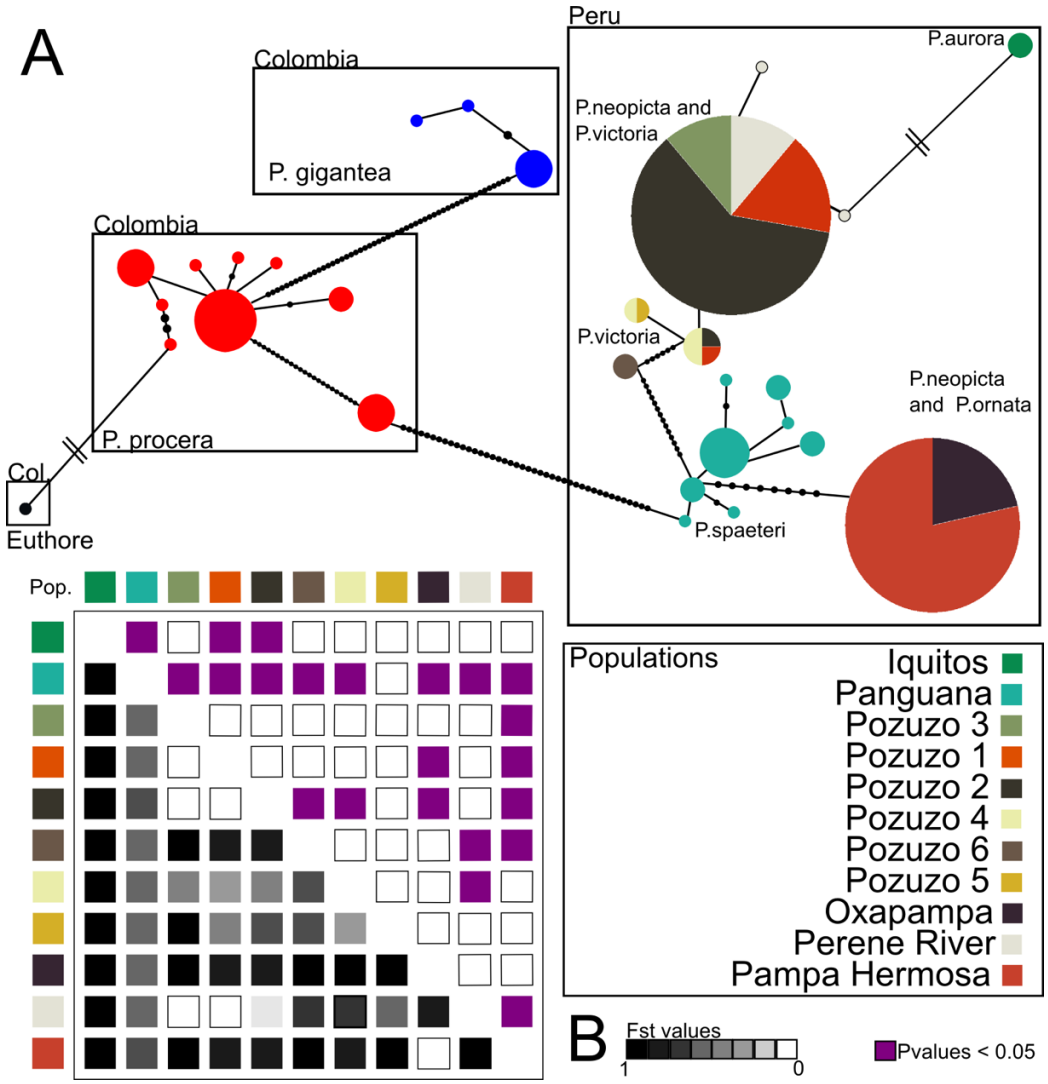

Figure 6. Comparison of mtDNA haplotypes among *Polythore*. (A) mtDNA haplotype network and (B) F_{ST} values across the geographical population. The COI haplotype network shows the relationships among 29 haplotypes. Each circle represent an haplotype, the size of the circles represents the number of individuals sharing the haplotype, colors represent the geographical population, black small circles show missing or unsampled haplotypes, branch lengths are fixed and represent the genetic distance between the haplotypes, parallels lines represent more than 100 missing haplotypes and high genetic distance between the haplotypes. The population matrix is organized from Northern to Southern geographic location, colors underneath the diagonal represent the F_{ST} values (i.e. gradient) and above the diagonal shows the significant p-values.

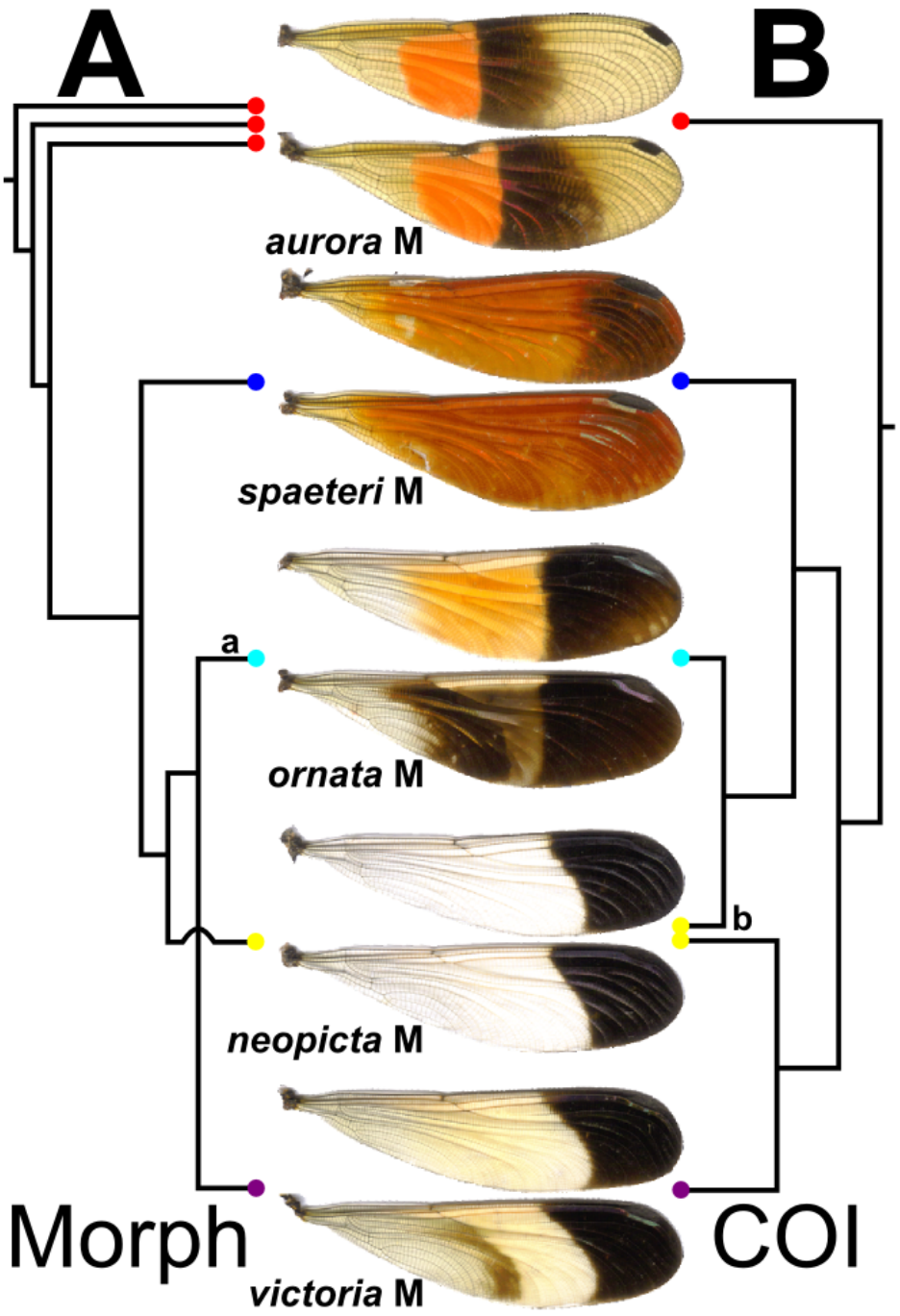

Figure 7. Comparison of the differing topologies among phylogenetic reconstructions. Simplified topologies are shown based on (A) morphological and (B) COI data, showing typical examples of each wing morph (center). Only males were included in these analyses. For full trees, see Fig. 5 and S1 Fig. G. Note: (a) *P. ornata* was recovered as monophyletic (although with low, 9% bootstrap branch support) except for two specimens, which were recovered within *P. victoria* (see S1 Fig. G); (b) in B, some *P. neopicta* grouped with *P. ornata*, while others grouped with *P. victoria*.

References

Beccaloni G.W. 1997. Ecology, natural history and behaviour of ithomiine butterflies and their mimics in Ecuador (Lepidoptera: Nymphalidae: Ithomiinae). Trop. Lepidoptera. 8:103–124.
Bick G.H., Bick J.C. 1985. A revision of the *picta* group of Polythore, with a description of a new species, *P. lamerceda* spec. nov., from Peru (Zygoptera: Polythoridae). Odonatologica. 14:1–28.
Bick G.H., Bick J.C. 1986. The genus *Polythore* exclusive of the *picta* group (Zygoptera: Polythoridae). Odonatologica. 15:245–273.
Brower A.V.Z. 1996. A new mimetic species of *Heliconius* (Lepidoptera: Nymphalidae), from southeastern Colombia, revealed by cladistic analysis of mitochondrial DNA sequences. Zool. J. Linn. Soc. 116:317–332.
Brower A.V.Z. 2011. Hybrid speciation in Heliconius butterflies? A review and critique of the evidence. Genetica. 139:589–609.
Cain A.J., Sheppard P.M. 1954. Natural Selection in *Cepaea*. Genetics. 39:89–116.
Chapman R.F. 1998. The insects: Structure and function. Cambridge, MA: Cambridge University Press.
Consortium T.H.G. 2012. Butterfly genome reveals promiscuous exchange of mimicry adaptations among species. Nature. 487:94–98.
Contreras-Garduño J., Lanz-Mendoza H., Córdoba-Aguilar A. 2007. The expression of a sexually selected trait correlates with different immune defense components and survival in males of the American rubyspot. J. Insect Physiol. 53:612–621.
Corbet P.S. 1999. Dragonflies: Behaviour and ecology of Odonata. Colchester, UK: Harley Books.
Córdoba-Aguilar A. 2002. Wing pigmentation in territorial male damselflies, *Calopteryx haemorrhoidalis*: a possible relation to sexual selection. Anim. Behav. 63:759–766.
Córdoba-Aguilar A. 2008. Dragonflies and damselflies: Model for ecological and evolutionary research. Cary, NC: Oxford University Press.
Darriba D., Taboada G., Doallo R., Posada D. 2012. jModelTest 2: more models, new heuristics and parallel computing. Nat. Methods. 9:772.
Daugman J.G. 1980. Two-dimensional spectral analysis of cortical receptive field profiles. Vision Res. 20:847–856.
Daugman J.G. 1988. Complete discrete 2-D Gabor transforms by neural networks for image analysis and compression. IEEE Trans. Acoust. Speech Signal Process. 36:1169–1179.
Davison A., Clarke B. 2000. History or current selection? A molecular analysis of "area effects" in the land snail *Cepaea nemoralis*. Proc. R. Soc. Lond. B Biol. Sci. 267:1399–1405.
De Marmels J. 1982. The genus *Euthore* Selys in Venezuela, with special notes on *Euthore fasciata fasciata* (Hagen, 1853)(Zygoptera: Polythoridae). Adv. Odonatol. 1:39.
Doyle J., Doyle J.L. 1987. Genomic plant DNA preparation from fresh tissue-CTAB method. Phytochem. Bull. 19:11–15.
Excoffier L., Lischer H.E.L. 2010. Arlequin suite ver 3.5: a new series of programs to perform population genetics analyses under Linux and Windows. Mol. Ecol. Resour. 10:564–567.

Feder J.L., Gejji R., Yeaman S., Nosil P. 2012. Establishment of new mutations under divergence and genome hitchhiking. Philos. Trans. R. Soc. B Biol. Sci. 367:461–474.
Fitzstephens D.M., Getty T. 2000. Colour, fat and social status in male damselflies, *Calopteryx maculata*. Anim. Behav. 60:851–855.
Ford E.B. 1957. Polymorphism in plants, animals and man. Nature. 180:1315–1319.
Franks D.W., Oxford G.S. 2009. The evolution of exuberant visible polymorphisms. Evolution. 63:2697–2706.
Garrison R.W., Ellenrieder N. von, Louton J.A. 2010. Damselfly genera of the New World: An illustrated and annotated key to the Zygoptera. Baltimore, MD: Johns Hopkins University Press.
Gillespie A.R., Kahle A.B., Walker R.E. 1987. Color enhancement of highly correlated images. II. Channel ratio and "chromaticity" transformation techniques. Remote Sens. Environ. 22:343–365.
Goloboff P., Farris J., Nixon K. 2008. TNT, a free program for phylogenetic analysis. Cladistics. 24:774–786.
Gray S.M., McKinnon J.S. 2007. Linking color polymorphism maintenance and speciation. Trends Ecol. Evol. 22:71–79.
Grether G.F. 1996a. Intrasexual competition alone favors a sexually dimorphic ornament in the rubyspot damselfly *Hetaerina americana*. Evolution. 50:1949–1957.
Grether G.F. 1996b. Sexual selection and survival selection on wing coloration and body size in the rubyspot damselfly *Hetaerina americana*. Evolution. 50:1939–1948.
Grether G.F. 1997. Survival cost of an intrasexually selected ornament in a damselfly. Proc. R. Soc. Lond. B Biol. Sci. 264:207–210.
Guindon S., Gascuel O. 2003. A simple, fast and accurate method to estimate large phylogenies by maximum-likelihood. Syst. Biol. 52:696–704.
Hammer Ø., Harper D.A.., Ryan P.D. 2001. PAST: paleontological statistics software package for education and data analysis. Palaeontol. Electron. 4:9.
Hassall C. 2014. Continental variation in wing pigmentation in *Calopteryx* damselflies is related to the presence of heterospecifics. PeerJ. 2.
Hill R.I., Elias M., Dasmahapatra K.K., Jiggins C.D., Koong V., Willmott K.R., Mallet J. 2012. Ecologically relevant cryptic species in the highly polymorphic Amazonian butterfly *Mechanitis mazaeus* s.l. (Lepidoptera: Nymphalidae; Ithomiini). Biol. J. Linn. Soc. 106:540–560.
Honkavaara J., Dunn D.W., Ilvonen S., Suhonen J. 2011. Sympatric shift in a male sexual ornament in the damselfly *Calopteryx splendens*. J. Evol. Biol. 24:139–145.
Hooper R.E., Tsubaki Y., Siva-Jothy M.T. 1999. Expression of a costly, plastic secondary sexual trait is correlated with age and condition in a damselfly with two male morphs. Physiol. Entomol. 24:364–369.
Jombart T., Devillard S., Balloux F. 2010. Discriminant analysis of principal components: a new method for the analysis of genetically structured populations. BMC Genet. 11:94.
Joop G., Mitschke A., Rolff J., Siva-Jothy M.T. 2006. Immune function and parasite resistance in male and polymorphic female *Coenagrion puella*. BMC Evol. Biol. 6:19.
Joron M., Jiggins C.D., Papanicolaou A., McMillan W.O. 2006a. *Heliconius* wing patterns: an evo-devo model for understanding phenotypic diversity. Heredity. 97:157–167.

Joron M., Papa R., Beltrán M., Chamberlain N., Mavárez J., Baxter S., Abanto M., Bermingham E., Humphray S.J., Rogers J., Beasley H., Barlow K., H. ffrench-Constant R., Mallet J., McMillan W.O., Jiggins C.D. 2006b. A conserved supergene locus controls colour pattern diversity in *Heliconius* butterflies. PLoS Biol. 4:e303.
Kronforst M.R., Young L.G., Kapan D.D., McNeely C., O'Neill R.J., Gilbert L.E. 2006. Linkage of butterfly mate preference and wing color preference cue at the genomic location of wingless. Proc. Natl. Acad. Sci. 103:6575–6580.
Lees D.R., Creed E.R. 1975. Industrial melanism in *Biston betularia*: The role of selective predation. J. Anim. Ecol. 44:67–83.
Librado P., Rozas J. 2009. DnaSP v5: A software for comprehensive analysis of DNA polymorphism data. Bioinformatics. 25:1451–1452.
Lorenzo-Carballa M.O., Watts P.C., Cordero-Rivera A. 2014. Hybridization between *Calopteryx splendens* and *C. haemorrhoidalis* confirmed by morphological and genetical analyses. Int. J. Odonatol. In press.
Louton J.A., Garrison R.W., Flint O.S. 1996. The Odonata of Parque Nacional Manu, Madre de Dios, Peru; natural history, species richness and comparisons with other Peruvian sites. Manu, the biodiversity of southeastern Peru. Washington DC: Smithsonian Institution Press. p. 431–449.
Maddison W.P., Maddison D.R. 2011. Mesquite: A modular system for evolutionary analysis. .
Mallet J. 1989. The Genetics of warning colour in Peruvian hybrid zones of *Heliconius erato* and *H. melpomene*. Proc. R. Soc. Lond. B Biol. Sci. 236:163–185.
Mallet J., Barton N.H. 1989. Strong natural selection in a warning-color hybrid zone. Evolution. 43:421–431.
Martin S.H., Dasmahapatra K.K., Nadeau N.J., Salazar C., Walters J.R., Simpson F., Blaxter M., Manica A., Mallet J., Jiggins C.D. 2013. Genome-wide evidence for speciation with gene flow in *Heliconius* butterflies. Genome Res. 23:1817–1828.
Mavárez J., Salazar C.A., Bermingham E., Salcedo C., Jiggins C.D., Linares M. 2006. Speciation by hybridization in *Heliconius* butterflies. Nature. 441:868–871.
Mullen S.P., Shaw K.L. 2014. Insect Speciation Rules: Unifying Concepts in Speciation Research. Annu. Rev. Entomol. 59:339–361.
Polly P.D. 2014. Geometric Morphometrics for Mathematica, version 11.1. Bloomington, Indiana: Department of Geological Sciences, Indiana University.
Posada D., Crandall K.A. 2001. Intraspecific phylogenetics: Trees grafting into networks. Trends Ecol. Evol. 16:37–45.
Rambaut A. 2014. FigTree v 1.4.1, A Tree Figure Drawing Tool. .
Rambaut A., Suchard M.A., Xie D., Drummond A.J. 2014. Tracer v1.6. .
Riek E.F., Kukalová-Peck J. 1984. A new interpretation of dragonfly wing venation based upon Early Upper Carboniferous fossils from Argentina (Insecta: Odonatoidea) and basic character states in pterygote wings. Can. J. Zool. 62:1150–1166.
Robertson H.M., Paterson H.E.H. 1982. Mate recognition and mechanical isolation in *Enallagma* damselflies (Odonata: Coenagrionidae). Evolution. 36:243–250.
Rohlf F.J. 2005. tpsDig, digitize landmarks and outlines, version 2.05. Dep. Ecol. Evol. State Univ. N. Y. Stony Brook.

Ronquist F., Teslenko M., Mark P. van der, Ayres D.L., Darling A., Höhna S., Larget B., Liu L., Suchard M.A., Huelsenbeck J.P. 2012. MrBayes 3.2: Efficient Bayesian phylogenetic inference and model choice across a large model space. Syst. Biol.:sys029.
Russell K., Huff J., Do M.T., Plantnick, MacLeod N. 2007. Introducing SPIDA-web: wavelets, neural networks and internet accessibility in an image-based automated identification system. Automated taxonidentification in systematics: Theory, approaches and applications. Boca Raton, FL: CRC Press. p. 131–152.
Salazar C., Jiggins C.D., Taylor J.E., Kronforst M.R., Linares M. 2008. Gene flow and the genealogical history of *Heliconius heurippa*. BMC Evol. Biol. 8:132.
Sánchez Herrera M., Realpe E., Salazar C. 2010. A Neotropical polymorphic damselfly shows poor congruence between genetic and traditional morphological characters in Odonata. Mol. Phylogenet. Evol. 57:912–917.
Sánchez-Herrera M., Realpe E. 2010. Population structure of *Polythore procera* at a Colombian stream (Odonata: Polythoridae). Int. J. Odonatol. 13:27–37.
Simon C., Frati F., Beckenbach A., Crespi B., Liu H., Flook P. 1994. Evolution, weighting, and phylogenetic utility of mitochondrial gene sequences and a compilation of conserved polymerase chain reaction primers. Ann. Entomol. Soc. Am. 87:651–701.
Sinervo B., Lively M. 1996. The rock-paper-scissors game and the evolution of alternative male strategies. Nature. 380:240–243.
Siva–Jothy M.T. 2000. A mechanistic link between parasite resistance and expression of a sexually selected trait in a damselfly. Proc. R. Soc. Lond. B Biol. Sci. 267:2523–2527.
Sonnentag O., Hufkens K., Teshera-Sterne C., Young A.M., Friedl M., Braswell B.H., Milliman T., O'Keefe J., Richardson A.D. 2012. Digital repeat photography for phenological research in forest ecosystems. Agric. For. Meteorol. 152:159–177.
Sukumaran J., Holder M.T. 2008. SumTrees: Summarization of Split Support on Phylogenetic Trees. Version 1.0. 2. DendroPy Phylogenetic Comput. Libr. Version 20. 3.
Svensson E.I., Eroukhmanoff F., Friberg M. 2006. Effects of natural and sexual selection on adaptive population divergence and premating isolation in a damselfly. Evolution. 60:1242–1253.
Svensson E.I., Friberg M. 2007. Selective predation on wing morphology in sympatric damselflies. Am. Nat. 170:101–112.
Svensson E.I., Sinervo B. 2004. Spatial scale and temporal component of selection in side-blotched lizards. Am. Nat. 163:726–734.
Szeliski R. 2010. Computer Vision: Algorithms and Applications. Springer Science & Business Media.
Tajima F. 1989. Statistical method for testing the neutral mutation hypothesis by DNA polymorphism. Genetics. 123:585–595.
Tamura K., Peterson D., Peterson N., Stecher G., Nei M., Kumar S. 2011. MEGA5: Molecular evolutionary genetics analysis using maximum likelihood, evolutionary distance, and maximum parsimony methods. Mol. Biol. Evol. 28:2731–2739.
Teacher A.G.F., Griffiths D.J. 2011. HapStar: Automated haplotype network layout and visualization. Mol. Ecol. Resour. 11:151–153.
Thompson J.D., Higgins D.G., Gibson T.J. 1994. CLUSTAL W: Improving the sensitivity of progressive multiple sequence alignment through sequence weighting, position-specific gap penalties and weight matrix choice. Nucleic Acids Res. 22:4673–4680.

Tynkkynen K., Grapputo A., Kotiaho J.S., Rantala M.J., Väänänen S., Suhonen J. 2008a. Hybridization in *Calopteryx* damselflies: the role of males. Anim. Behav. 75:1431–1439.
Tynkkynen K., Kotiaho J.S., Svensson E.I. 2008b. Interspecific interactions and premating reporductive isolation. In: Cordoba-Aguilar A., editor. Dragonflies and damselflies: Model organisms for ecological and evolutionary research. Cary, NC: Oxford University Press. p. 139–152.
Vukusic P., Sambles J.R. 2003. Photonic structures in biology. Nature. 424:852–855.
Weldon T.P., Higgins W.E., Dunn D.F. 1996. Efficient Gabor filter design for texture segmentation. Pattern Recognit. 29:2005–2015.
Wellenreuther M., Tynkkynen K., Svensson E.I. 2010a. Simulating range expansion: Male species recognition and loss of premating isolation in damselflies. Evolution. 64:242–252.
Wellenreuther M., Vercken E., Svensson E.I. 2010b. A role for ecology in male mate discrimination of immigrant females in *Calopteryx* damselflies? Biol. J. Linn. Soc. 100:506–518.
Woebbecke D.M., Meyer G.E., Von Bargen K., Mortensen D.A. 1995. Color indices for weed identification under various soil, residue, and lighting conditions. Trans. ASAE. 38:259–269.
Wolfram Research. 2010. Mathematica Edition: Version 8.0. Champaign, Illinois: Wolfram Research Inc.
Zelditch M.L., Swiderski D.L., Sheets H.D. 2004. Geometric morphometrics for biologists: A primer. Waltham, MA: Academic Press.
Zhang J., Kapli P., Pavlidis P., Stamatakis A. 2013. A general species delimitation method with applications to phylogenetic placements. Bioinformatics. 29:2869–2876.
Zwickl D. 2006. Genetic algorithm approaches for the phylogenetic analysis of large biological sequence datasets under the maximum likelihood criterion.

Chapter Two: Testing species diversity in the highly polymorphic Neotropical *Polythore* damselflies.

Abstract

Identifying and discovering species is one of the most important tasks when assessing biodiversity. Traditionally, morphological traits were used to evaluate species delimitation, but recent advances in the molecular data collection have led us to discover new, previously undetected, or cryptic, lineages. Often, new molecular data agrees with the classical morphology described by alpha taxonomists, but occasions, when there is a disagreement between these data sources, can highlight interesting evolutionary patterns. Odonates (dragonflies and damselflies) are one of the oldest groups of flying insects. They possess distinctive reproductive behaviors, which often maintain species boundaries; traditional odonate taxonomy has relied heavily on morphological characters in describing diversity. The Neotropical damselflies of the genus *Polythore* are stunningly colorful; their wings display varying shades of orange, black and white in intricate patterns. Despite this color diversity, they lack variation in the classical reproductive traits (e.g. male genitalia) commonly used for species description. The genus comprises 21 described morphospecies distributed along the eastern slopes of the Andes cordillera and the Amazon basin, from Colombia to northern Bolivia. Here I present the first multi-locus species tree (e.g. COI, ND1, 16S) for thirteen of the described morphospecies. I recovered a total of fifteen lineages and additionally tested with a coalescent Bayesian species delimitation model as independent operational taxonomic units (OTU's). The genetic diversity within these damselflies seems to be explained by geography. Additionally, shallow coalescent times suggest a recent

radiation, which has an incredible diversity in wing color pattern. Finally, I show that *Polythore* damselflies can be a unique and novel model to study evolutionary ecology in the Neotropics.

Key words: damselflies, *Polythore*, species delimitation, polymorphisms

Introduction

Species delimitation, the process of identifying and discovering species boundaries, is an important task in systematics (De Queiroz 2007; Carstens et al. 2013). Accuracy in delimitation allows for defined, reliable evolutionary units that correspond to species, and is essential for furthering our understanding of how species arise, adapt and persist. However, the continuous nature of speciation can make setting boundaries of species a difficult task (Shaw and Mullen, 2014). It remains unclear how much gene flow or genetic divergence (e.g. constrained to specific regions or widespread in the genome) may occur among related populations before they can be upgraded to the "species" status (Bolnick and Fitzpatrick 2007; Hey and Pinho 2012; Powell et al. 2013). Several species concepts have arisen in an attempt tackle this issue directly, or to circumvent it using practical strategies (Braby et al., 2012). These concepts rely on 'biological properties' or 'operational criteria' to define species: for example, characteristic morphology, monophyly, unique ecology, the overall degree of reproductive isolation, reproductive isolation restricted to specific loci, etc. (Mallet 1995; Hey 2001, 2014; Coyne and Allen Orr 2004; De Queiroz 2007; Hausdorf 2011). The process of speciation is a continuous sequence of genetically- based events that happen as two lineages diverge from another on the path to reproductive isolation (Shaw and Mullen, 2014). Within this context, to establish lineages through this speciation continuum, we need to test how distinct

reproductive barriers across different stages of divergence in several geographic populations may contribute to genetic isolation and variation (in alleles or frequency differences of shared alleles, (Wu and Chung-I 2001; Powell et al. 2013). For many taxa, however, it is not feasible to do so, due to the absence of apparent "biological properties" or technical limitations (e.g. if their life cycle precludes them from being quickly raised under experimental conditions, or if there are few genomic resources available). Given these limitations, other strategies are required to approximate and delimit evolutionary units. Recently, new methods to estimate Operational Taxonomic Units (OTUs) can be a robust approximation to establish lineages as "candidate" species using phylogenetic and population genetics algorithms (DeSalle et al. 2005; Pons et al. 2006; Fujisawa and Barraclough 2013; Rannala and Yang 2013; Zhang et al. 2013). Despite the fact that there are limitations in performance for these methods (Reid and Carstens 2012; Carstens et al. 2013; Burbrink and Guiher 2015), their use is a good first step toward understanding species limits. These methods could be one of the multiple independent lines of evidence, that at the end can lead to reliable species identification in taxa for which there is an absence of distinct 'biological properties' (Dayrat 2005; Will et al. 2005; Padial et al. 2010; Schlick-Steiner et al. 2010; Yeates et al. 2011). Furthermore, there are cases where the inclusion of morphology data in the species delimitation algorithm improves the credibility of the lineages that can be treated as species (Solis-Lemus et al. 2015; Pyron et al. 2016; Eberle et al. 2016).

These new species delimitation models are useful with the discovery of cryptic diversity (Pons et al. 2006; Katz et al. 2015; Lin et al. 2015), or with the corroboration of "biological properties" (i.e., morphological, ecological, behavioral; Drotz et al. 2015; Li

et al. 2015; Wade et al. 2015), for the most speciose organisms on Earth, insects. Within Insecta, odonates (dragonflies and damselflies) are the oldest flying insects, sister to the remaining Pterygota (Misof et al. 2014). Odonate species descriptions heavily rely on the size and shape of reproductive traits. Globally, the Neotropical region is home to the highest diversity of odonate species (Sanchez Herrera and Ware 2012), yet it is understudied, and species diversity remains poorly understood.

The Neotropical damselflies from the genus *Polythore* Calvert are stunningly colorful; their wings display orange, black and/or white (Fig 1). Despite this color diversity, they lack variation in classical reproductive traits (e.g. male genitalia) commonly used for species description (Bick and Bick 1985, 1986, 1990). The genus comprises 21 described morphospecies distributed along the Eastern slopes of the Andes cordillera and the Amazon basin, through Colombia to Northern Bolivia and Brazil. They dwell in small, fast flowing creeks with highly oxygenated waters; their larvae are the only Mesoamerican damselflies that possess abdominal gills and highly modified caudal lamellae that may provide stability in fast flowing waterfalls (Etscher et al., 2006; Corbet, 1999). This genus was first described as *Thore* by Hagen in Selys (1853) using a few thorax and wing features of a single male specimen of *P. gigantea*. Later on, Calvert (1917) changed it to *Polythore* to avoid confusion with a spider genus previously described by Koch, 1850. But until Montogomery (1967) and Bick and Bick (1985, 1986) there were not morphological characters to diagnose this genus. Rojas-Riaño (2011) in her master dissertation, wrote a formal diagnosis for *Polythore* based on the presence of supplementary sectors in the hindwings of the males (HW) between the Radius posterior second branch vein (RP2) and the Intercalar vein 2 (IR2) as the diagnostic character for

Polythore (Rojas-Riaño 2011). The first attempt to delimit the species within this genus was proposed by Bick and Bick (1985, 1986). They suggested six species groups within *Polythore*: ***batesi, boliviana, picta, victoria*** and ***vittata***. They proposed to delimit these groups based on the differences in the hindwing length, wing color pattern, numbers of cells under the pterostigma, length of the apical horns of the male secondary genitalia and lateral lobe segmentation. However, they acknowledge high variation for these characters within most of the suggested groups (Bick and Bick, 1986). Recent studies of Colombian and Peruvian species show a lack of congruence between wing color morphs and genetic markers (COI), supporting the presence of possible cryptic species and/or polytypic species (Sánchez Herrera et al. 2010; Sánchez Herrera et al. 2015). Here I used population data to explore the genetic variation of thirteen of twenty-one proposed species. Additionally, I estimated the first species tree using a multi-locus coalescent analysis and finally tested if the obtained OTUs correspond to independent lineages using a coalescent species delimitation approach. My findings suggest a total of fifteen separate lineages, including the presence of cryptic species and possible polymorphic complexes, strongly related to geographic location. Furthermore, short coalescence times indicate a rapid radiation of *Polythore*, suggesting incomplete lineage sorting among some species.

Methods

Taxon sampling

I used a total of 201 individuals from 17 populations (Fig 2) of fifteen morphospecies for the analyses; specimen details (geographic origin, collector, and Genbank Accession Numbers) are summarized in Supplementary Table 1.

DNA amplification, sequencing, and alignment: I extracted DNA from either the legs or ¼ of the pterothorax using a DNeasy Tissue Kit (QIAGEN) from each sample following the manufacturer's protocol. I amplified three mitochondrial fragments: Cytochrome Oxidase I (~799bp), NAD dehydrogenase (~548 bp), and 16S, (~340bp) (see Supplementary Table 2 for primer details). All these genes fragments were amplified using PCR conditions described in the studies that developed each pair of primers and as outlined in Supplementary Material Appendix 1. Macrogen USA Inc. laboratories (NY) performed the purification protocol for the PCR products (15µl final volume for each primer) and the Sanger DNA sequencing. Primer contig assembly, peak chromatogram verification and the generation of per-individual consensus sequences were done using Geneious v 7 (Kearse et al. 2012). All fragments were aligned using MAFFT (Katoh and Standley 2013) and then manually aligned in Mesquite (Maddison and Maddison 2015). The 16S fragment was aligned manually using the structural methods described in Kjer (1995) and Kjer et al. (2007).

Population Genetics Analyses

To visualize the genetic diversity present in all the morphospecies, I estimated the minimum spanning haplotype networks for each gene fragment using PopArt (Leigh and Bryant 2015). I calculated the genetic diversity statistics (i.e. Genetic diversity ($\theta\pi$), Segregating sites (SS)) and tested for the neutral evolution of each fragment with the Tajima D test for each of the lineages using Arlequin v 3.5 (Excoffier and Lischer 2010), assuming the well-accepted premise the mtDNA does not recombine. Additionally, I estimated uncorrected pairwise distances and the genetic structure F_{ST} values (i.e. adapted to DNA sequence data) between the populations and morphospecies with Arlequin

(Excoffier and Lischer 2010). I performed a total of 10,000 permutations to establish the 95 % statistical significance for each Tajima D test and F_{ST} values in Arlequin v 3.5 (Excoffier and Lischer 2010). To detect the source of genetic variation among the phylogenetic clusters estimated in the species tree (see below) I ran an Analysis of Molecular Variance (AMOVA) in Arlequin v 3.5 (Excoffier and Lischer 2010).

Species Tree Inference

Based on a combination of the significance of the F_{ST} values and distinct morphology (i.e. color pattern), I selected the 24 unique haplotypes for each gene fragment representing fifteen possible independent lineages. I estimated a species tree using three partitions, one for each fragment, using a coalescent-based approach implemented in *BEAST v 2.3.2 (Heled and Drummond 2010; Bouckaert et al. 2014). I performed two independent runs of 1 x 10^8 generations, sampled every 5000 generations, and discarded the first 10% as burn-in period. The models of substitutions (i.e. estimated in IQ-tree, Trifinopoulos et al. 2016) and priors are specified as follow (otherwise as default): COI, HKY + G4; ND1, TN93 + G4; 16S, HKY + I (models); Relaxed Uncorrelated Lognormal Clock (Estimate); Yule process of speciation; population mean gamma distribution (i.e. $\alpha = 1, \beta = 2$), all gene tree ploidy were mitochondrial (priors). I assessed the convergence of the model examining the trace files in Tracer v 1.6 (Rambaut et al. 2014), after obtaining an effective sample size (ESS) > 200 for all the parameters. I combined the tree files using LogCombiner (Heled and Drummond 2010), the uncertainty of the trees was visualized in DensiTree (Bouckaert 2010). However, the maximum credibility tree with the coalescent divergent time scalar and 95% highest probability densities

(HPDs) were produced in Tree Annotator (Heled and Drummond 2010). I visualized the tree using the R package ggtree (Yu et al. 2016).

Distinguishing between incomplete lineage sorting and hybridization

To assess if the low genetic variation present among the estimated species tree can be attributed to incomplete lineage sorting, I used the posterior predictive checking approach in the software JML (Joly 2012) developed by Joly et al. (2009). This method uses simulated datasets of gene trees and sequence alignments generated under a coalescent model that assumes no migration for a given species tree. The proportion of simulations for which the minimum pairwise distance is lower than the observed, can be interpreted as the posterior probability that the model is correct. Meaning that if the posterior probabilities are small values, the model of no hybridization (no migration) doesn't fit the data, suggesting hybridization as a possible cause of the lower genetic variation. To account for uncertainty, I performed simulations for each gene fragment using the 10,000 trees from the *BEAST species tree estimation.

Species delimitation

In order to test the estimated species tree, I ran a coalescent species delimitation model using the platform Bayesian Phylogenetics and Phylogeography (BBP) v 3.2, (Yang and Rannala 2010; Yang 2015). This genealogical method uses a Markov Chain Monte Carlo (rjMCMC) method to estimate the following population parameters: θa (i.e., effective population size (N_e) x the mutation rate (μ)), τa (i.e., time of origin for each species) and τd (i.e., time of diversification for each species; Yang and Rannala 2010; Rannala and Yang 2013). The posterior probabilities indicate whether two or more predefined lineages can be differentiated accounting for coalescent uncertainty (Ruane et al. 2014). I included

five individuals representing each of the fifteen lineages of the estimated species tree within the analysis. I ran BPP v 3.2 (Yang 2015) for species delimitation using a fixed guided tree (A10). The fine-tuning parameters were adjusted to ensure swapping rates, allowing the rjMCMC to mix properly among the species delimitation models. I parameterized two models and using a gamma distribution, assuming in the first, a large population ($\alpha = 1, \beta = 10$) and shallow divergences ($\alpha = 2, \beta = 2000$); and in the second a small population ($\alpha = 2, \beta = 2000$) and shallow divergences ($\alpha = 2, \beta = 2000$). The last assumptions are the most conventional models favoring speciation events (Leaché and Fujita 2010). I ran four independent analyses with different start seeds to ensure convergence in the posterior probabilities for 1 x 10^5, burning of 2 x 10^4, and thinning every five generations for each model.

Results

Population Genetic Analyses

The minimum spanning haplotype networks of all mitochondrial fragments (Fig 2) show that the Cytochrome oxidase I gene (COI) has a higher genetic diversity in comparison with either the NADH dehydrogenase subunit 1 (ND1) or the ribosomal 16S. However, all the fragments showed a consistent pattern of geographical distribution of the included morphospecies. The Amazonian species, *Polythore aurora* and *P. mutata,* were always recovered clustered together (Fig. 2). However, this particular group shows a low number of haplotypes suggesting little genetic diversity within these morphospecies. On the other hand, I recovered the following three geographical clusters related to the slopes of the Andes Cordillera: the Western (W), the Northeastern (NE) and the Southeastern (SE). The Western cluster is represented by populations of the species *Polythore gigantea* from

Colombia and Ecuador (Fig 2). The number of haplotypes within this group shows genetic diversity within this morphospecies. Both the NE and SE encompassed more morphospecies and showed a higher genetic diversity.

The NE cluster is composed by *Polythore procera*, *P. derivata*, *P. williamsoni sp. nov*, *P. concinna* and *P. terminata* shows a significant haplotype diversity in each fragment network. The morphospecies *P. procera*, in particular, shows non-monophyletic highly divergent haplotypes for the three fragments (Fig 2). The SE cluster comprising *P. picta*, *P. spaeteri*, *P. ornata*, *P. neopicta*, *P. victoria*, and *P. boliviana* also shows higher diversity. However, *P. neopicta* seems to share haplotypes with *P. ornata* and *P. victoria* (Fig 2).

The F_{ST} values for the populations sampled for each locus show a significant degree of genetic differentiation (Fig 3). Both Amazon morphospecies, *P. aurora* and *P. mutata*, show a significant differentiation between them and each of them with other morphospecies showed a similar high structure (Fig 3). For both COI and 16S, the two populations of *Polythore gigantea* showed high and significant F_{ST} values, suggesting that there is genetic structure between Colombian and Ecuadorian populations (Fig 3, A). Several NE populations have low or no genetic differentiation among them (Supplementary Table 1, Fig 3). In contrast, *P. procera* populations from Colombia (e.g. Chirajara-CH and Guayabetal-G), showed high and significant genetic structure. The population from Ecuador (Rio Negro-RN) showed a weak genetic structure with Chirajara-CH, but robust with Guayabetal-G (Fig 3). While, for the SE Andean populations, there appears to be a higher degree of genetic differentiation among them in

comparison with the NE populations, consistent with the haplotype networks previously observed.

Species tree estimation

The estimated species tree for *Polythore* supports fifteen lineages, based on the haplotype selection with shallow coalescent scalar times (Fig 4). I recovered two well-supported monophyletic clades; one encompasses the two Amazon morphospecies (*P. aurora* and *P.mutata*, pp = 0.9995), while the other clusters all the morphospecies distributed in the Andes Cordillera (pp = 1, fig 4). Within the Andean Clade, *P. gigantea* was recovered with a high posterior probability as sister to two well-supported monophyletic clades, the Northeastern and Southeastern clades (Fig 4). The NE clade groups the following morphospecies: *P. procera*, *P. derivata*, *P. terminata, P. concinna* and *P. williamsoni sp.nov.* However, I recovered *P.procera* and *P.derivata* morphospecies as paraphyletic (Fig 4 A). The Colombian Guayabetal-G population of *P. procera* was recovered as sister to all the other members within the clade. I recovered the following morphospecies as sister lineages: *P. terminata* and the Peruvian Tarapoto-TAR population (pp = 0.9892); *P. williamsoni* and the Colombian (Chirajara-CH) and Ecuadorian (Rio Negro-RN) populations of *P.procera* (pp = 0.6614); and *P. concinna* and Ecuadorian (Tiputini-T) and Colombian (Florencia-FL) populations of *P. derivata* (pp = 0.8989). Despite the high posterior probabilities there is uncertainty on coalescent relationships; some of the recovered topologies show different patterns between *P.williamsoni*, *P. derivata* (T-FL), *P. procera* (CH-RN) and *P. concinna* (Fig 4 A).

The SE clade clusters the following morphospecies: *P. neopicta*, *P. victoria*, *P. picta*, *P. spaeteri* and *P. ornata*. I recovered the Peruvian Pozuzo population of *P. neopicta* and *P.*

victoria sister to the Santa Cruz-STAC population of *P.victoria* and *P.picta* (Fig X, pp = 0.4143). And the following as sister lineages: *P. victoria* and *P. picta* (pp =0.9796); and *P. spaeteri* and *P.ornata* (pp = 0.5422). For these species, the recovered topologies show a higher uncertainty in the coalescent relationships in comparison with the NE (i.e. a major density of crossed color lines are observed among taxa; Fig 4A).

Species Delimitation

The JML analyses for each gene fragment, based on 5000 simulations, showed no significant evidence of hybridization (Supplementary Table 2). For both set of parameters (i.e., small and large population) BBP tested 149 species delimitation models, and found the posterior probability values were low overall. The large population and shallow divergence assumption estimated 0.027 as the highest posterior probability, which supports the presence of 15 operational units. On the other hand, the small population and shallow divergence support the same species delimitation model, however the posterior probability is higher than for the previous parameter assumption, 0.37. The large population and shallow divergence model recovered lower posterior probabilities for the following nodes than with small population and shallow divergence times: *P. aurora* and *P. mutata*; *P. procera* - CH and *P. williamsoni*; *P. derivata* - TAR and *P. terminata*; *P. neopicta* and *P. ornata*; and *P. picta* and *P. victoria* (Figure 5). All the other nodes were highly supported by both assumptions (Figure 5).

P. derivata (T), *P. procera* (CH, G), *P. neopicta* - *victoria* (POZ), *P. concinna* and *P. gigantea* show high genetic diversity for the three loci (Table 1). The Tajima's D < 0, is significant in some lineages (i.e. *P. mutata*, *P. procera* - G, *P. neopicta* - *victoria*, *P. ornata*) in particular gene fragments (Table 1), which means that these DNA sequences

might be evolving under a non-random process. In Tables 2, 3 and 4 the F_{ST} values and their significance among the lineages are presented. The pairwise genetic and Nei distances recovered a similar pattern to the F_{ST} values (Supplementary Table 3). There are lower F_{ST} and short distances among the lineages within each clade (see NE and SE, Table 2, 3 and 4). Analysis of molecular variance for each gene (AMOVA's), show high and significant fixation indices (i.e. genetic structure) among the geographical clades, among the lineages within each clade and within each independent lineage (Table 5).

Discussion

Taxonomic remarks

The estimated species tree shows fascinating patterns within these Neotropical damselflies. The thirteen morphospecies assessed suggests that the morphological delimitation proposed by Bick and Bick (1985, 1986) is not consistent with all the recovered independent lineages within the genus (Fig 4). I recovered *P. aurora* and *P. mutata* as sister lineages; this might the only consistent cluster with the morphological group proposed by Bick and Bick. Although, I am missing from these analyses some of the species clustered, *P. beata, P. batesi* and *P. chibiriquete*, to actually assessed if the morphological traits suggested by Bick and Bick (1985). The suggested *picta, concinna, victoria* and *boliviana* groups were not recovered in the species tree. The ***picta*** group comprises *P. gigantea, P. procera, P. derivata, P. lamerceda, P. neopicta*, and *P. picta*; all these morphospecies show a similar pattern in both fore and hind-wings, however there some dissimilarities in the secondary genitalia shape among them (Fig 5). Due to fragility of the secondary genitalia, Bick and Bick relied mostly on the melanic band gradient covering the wings to delimit these morphospecies. The recovered species tree

topology shows that all the species within these morphological groups are actually scattered throughout all the Andean subclades (Figs 4,5). Species in the ***concinna*** group, represented only by *P. conccina* (Bick and Bick 1985) and *P. spaeteri*, have similar amber wing coloration pattern. Neotropical taxonomists have considered synonymizing these two morphospecies due to their similarities in wing coloration and male genitalia (pers.comm. R. Garrison). Although, the estimated genealogy shows that each of these lineages belongs to two divergent clades (Fig 4). In the case of ***victoria***, which was only represented by *P. victoria*, we see a paraphyletic pattern within the SE Andean clade, where individuals from Pozuzo are almost genetically identical to *P. neopicta* and the Santa Cruz population seems to be an independent lineage sister to *P. picta*. Finally, the ***boliviana*** group which comprises *P. ornata, P. boliviana, P. manua,* and *P. williamsoni*, shows the most sophisticated wing coloration patterns with the exception of *P. williamsoni*. *P. ornata* was recovered sister to *P. neopicta*, whose wing coloration is simpler (Fig 5). Rojas-Riaño (2011), reported Colombian populations of *P. williamsoni*, which we include in our analyses. However, these populations were recovered in the NE Andean clade, and when I revised the male secondary genitalia morphology to Kennedy's drawings (1919) from the holotype, the lateral lobes are different between them. The Colombian populations show short lateral lobes, while the holotypes described from Machu Picchu, Peru show significantly long and segmented lateral lobes (Supplementary Fig 1). Overall, the recovered species tree suggests that wing color pattern in not a reliable trait, for the species delimitation of this genus as previously proposed by Sanchez Herrera *et al.* (2010, 2015). *P. procera* and *P. derivata*, showed multiple common ancestors within the NE Andean clade (Fig 4, 5) due to highly divergent haplotypes from

different populations coalescing with various lineages (Fig 2, 4). For *P. procera* the Colombian population of Guayabetal (G) is an entirely different lineage in comparison with the other two Colombian Chirajara (CH) and Ecuadorian Rio Negro (RN) populations. The Guayabetal populations are sister to all the other members of the clade, while the Chirajara-Rio Negro is sister to *P. williamsoni sp.nov*. Sanchez et al. 2010 reported these two lineages as possible cryptic species, due to the high variability of morphological traits (i.e., wing banding pattern and secondary genitalia shape). In the case of *P. derivata*, I recovered the populations distributed in the Amazon Basin in lower elevations (e.g. Tiputini), usually coexisting with *P. mutata*, to be sister to *P. conccina*. While the populations distributed in the Andean foothills of Northern Peru (e.g. Tarapoto) sister to *P. terminata*, which spreads into higher elevations in the Ecuadorian foothills.

Geography as the source of genetic variation

The recovered topology suggests a clear geographical pattern between the independent lineages (Fig 4B, 5). There are two major geographic clades retrieved with high posterior probabilities (Fig 4B): The Amazonian and Andean clades. The Andean clade is further divided up into West (W), Northeastern (NE) and Southeastern (SE) Andean slopes (Fig 4B, 5). These geographic clades explain most of the genetic variation present within *Polythore*, (AMOVA's, Table 3). Paleogeographic studies suggest that the Andes uplift caused a lot of changes in the landscape of Neotropical lowlands; including the formation of the Amazon watershed system, the closure of the Central America Seaway, east and west montane Andes habitats and the aridification of the Caribbean lowlands in Northern South America (Hoorn et al. 2010, Montes et al. 2012). The fact that geography explains

most of the genetic variation implies the possibility that the speciation of *Polythore* is influenced by some of these important geological changes. However, recent studies in Passerines birds acknowledged that landscape changes alone cannot explain speciation events in the Neotropics; the time a lineage has persisted in the landscape and its ability to move through it are important factors that explain the spatial and temporal patterns of genetic differentiation among taxa (Smith et al. 2014). The North and South divergence can be explained by the presence of one the most prominent barrier to dispersal in the Andes is the arid valley of the Marañon River in Northern Peru (Vuilleumier 1969, 1984; Weir 2009, Winger and Bates 2015). Future studies testing the influence of lineage persistence, ancestral areas, and dispersal ability traits (i.e. territoriality) will be needed to understand the speciation process in *Polythore*. For now, I was able to recognize a strong influence of geography on the current genetic diversity within the genus.

Species delimitation

The Amazonian clade, which includes *P. mutata* and *P.aurora*, contains populations showing the deepest coalescent divergence, suggesting that these two lineages have been separated for a longer time in comparison to the other lineages. The inclusion of other morphospecies distributed in the Amazon watershed, such as *P. batesi, P. beata, P. chibiriquete* and *P. vittata*, will allow testing if the Amazon clade lineages have deeper coalescent times than the Andean clade. On the other hand, the Andean clade's most profound coalescent event reveals the only species distributed at the West slope of the Andes, *P. gigantea* (Fig 4). Then the NE and SE Andean clades coalesce; and the lineages within each show strikingly shallow coalescent divergence times (Fig 4B);

considering those mtDNA markers are fast-evolving in comparison to nuclear markers (Brown et al. 1979), I do not expect the power of resolution in the last ones. To explore if the shallow coalescent times are due introgression (i.e. hybridization, recent gene flow) or incomplete lineage sorting that might be obscuring the relationships within them, I ran the hybridization test. JML suggest that the low genetic divergence among the lineages within the NE and SE Andean clades is more likely to be due to incomplete lineage sorting of the selected mtDNA markers. This pattern suggests that the speciation has been very recent, and there has not been enough time for the lineages to accumulate mutations, at least in the mtDNA genome. For the Andean clade the divergent morphology of the secondary genitalia of some lineages (Fig 5) suggests that there might be reproductive isolation among some of the lineages, however, cryptic species like *P. procera, P. neopicta*, and *P. picta* might be able to interbreed. To assess reproductive isolation between sister lineages sexual selection assays should be performed. Additionally, we will be able to test if the individuals are sexually selecting the wing coloration as a prezygotic barrier of reproductive isolation.

The coalescent species delimitation tests to corroborate the estimated species tree, showed highest posterior probability support for the presence of fifteen lineages. However, from the two sets parameters, the small population, and slight divergences fit the data better based on the considerably higher posterior probabilities. However, the large population and shallow divergences tend to be a more conservative parameter (Leaché and Fujita 2010). Both models show high posterior probabilities supporting most of the geographical clades (Fig 5). Only the Amazon clade might show a lower probability due to lack of individuals for *P. aurora*. For the large population and shallow

divergence, the lowest posterior probabilities for the most recent coalescent species were slightly above 0.5. For the small population and shallow divergences, show posteriors > 0.8, except of *P. picta* and *P. victoria* node (pp = 0.63).

My analysis suggests the redescription of *P. derivata* and *P. procera* into four distinct lineages and the description of a new species *P. williamsoni sp.nov*. Furthermore, *P. neopicta* and *P. victoria* from Pozuzo show a lack of genetic variation that might suggest this is a polymorphic species; further morphological assessments of the secondary genitalia are needed to corroborate this hypothesis. Additionally, further analysis increasing the taxon sampling (i.e., other eight morphospecies) and with better-resolved markers (i.e. SNP's derived from NGS sequencing) are required to understand the evolutionary history of this enigmatic damselfly group.

Conclusion

The Neotropical damselflies of the genus *Polythore* are a mysterious and challenging group for species delimitation. The lack of variability of classical isolating structures (e.g. males' abdomen appendages) in this group caused previous taxonomists to rely on wing color pattern as a classification trait. However, my analysis demonstrates that wing color pattern is not a good predictor of species. The secondary genitalia of males seem to be consistent for each lineage, and can be used as a diagnostic character for some of the lineages where there are not cryptic species. Further studies that incorporate quantitative data that assesses the variability in the shape of this structure within and among lineages are needed to test its reliability as a diagnostic character. I was able to establish the presence of 15 lineages, 5 of which will be described as new species to science.

Additional studies increasing the taxon sampling and genetic markers will clarify the evolutionary relationships within this group.

The speciation of *Polythore* damselflies is unusual due to the shallow divergence coalescent times, the incredible diversity of wing color patterns, the presence of cryptic species suggests a possible recent radiation within these damselflies. New behavioral studies are needed to test the selection forces shaping (e.g. sexual selection, mimicry) this morphological diversity. Furthermore, I was able to show that the genetic variation within *Polythore* seems to be influenced by geographical location, making this group an excellent model for biogeographical studies. Overall, these damselflies will be a unique and novel model to study evolutionary ecology of the Neotropics.

Chapter 2: Tables

Table 1. Summary of the genetic diversity statistics and Tajima's neutrality test per gene fragment for the recovered lineages. N # of individuals, θ (π) nucleotide diversity, θ (SS) segregating sites. Bolded values represent significant p-values for the Tajima's D.

Statistics		NE Clade							W Clade	SE Clade				Amazon Clade	
		derivata -T	*derivata* - TAR	*concinna*	*procera* - G	*procera* - CH	*terminata*	*williamsoni sp. nov*	*gigantea*	*neopicta*	*ornata*	*victoria*	*spaeteri*	*aurora*	*mutata*
COI	**N**	5	4	8	45	20	3	6	31	36	7	6	13	2	12
	θ (π)	21.900	3.333	8.750	2.532	11.005	5.333	1.533	8.305	10.311	0	3.000	5.808	0	1.167
	s.d θ (π)	13.668	2.566	5.151	1.541	5.832	4.400	1.224	4.399	5.354	0	2.098	3.339	0	0.908
	θ (SS)	19.680	3.273	9.256	8.233	11.839	5.333	1.314	8.260	40.272	0	3.942	9.990	0	2.318
	s.d θ (SS)	10.138	2.088	4.318	2.653	4.326	3.528	0.910	2.853	12.176	0	2.180	4.089	0	1.200
	Tajima's D	0.849	0.180	-0.287	**-2.374**	-0.281	0.000	0.862	0.020	**-2.795**	0	-1.423	-1.839	0	**-1.944**
	p-value D	0.772	0.723	0.430	**0.000**	0.446	0.754	0.845	0.582	**0.000**	1	0.042	0.015	1	**0.006**
ND1	**N**	5	8	9	54	29	2	3	34	42	20	11	6	NA	17
	θ (π)	2.000	0.250	3.722	4.068	6.316	0	0	4.278	3.912	1.689	0	2.333	NA	6.235
	s.d θ (π)	1.571	0.355	2.351	2.286	3.502	0	0	2.416	2.223	1.153	0	1.704	NA	3.486
	θ (SS)	2.400	0.386	1.386	6.803	4.292	0	0	2.446	9.296	4.510	0	1.752	NA	14.494
	s.d θ (SS)	1.513	0.386	1.386	2.178	1.791	0	0	1.036	2.990	1.848	0	1.128	NA	5.417
	Tajima's D	-1.124	-1.055	0.254	**-1.526**	0.795	0	0	2.310	**-2.232**	**-2.324**	0	-1.295	NA	**-2.512**
	p-value D	0.105	0.202	0.687	**0.031**	0.809	1	1	0.994	**0.000**	**0.001**	1	0.084	NA	**0.000**
16S	**N**	3	10	11	33	13	2	3	24	22	8	11	5	2	12
	θ (π)	2.667	0	2.618	1.701	3.436	0	0	0.685	0	0	0	0	0	5.379
	s.d θ (π)	2.393	0	1.708	1.135	2.109	0	0	0.602	0	0	0	0	0	3.141
	θ (SS)	2.667	0	0.509	1.725	2.900	0	0	0.803	0	0	0	0	0	9.603
	s.d θ (SS)	1.919	0	0.685	0.808	1.407	0	0	0.509	0	0	0	0	0	4.021
	Tajima's D	0.000	0	-1.300	-0.618	0.205	0	0	-0.371	0	0	0	0	0	**-2.054**
	p-value D	1.000	1	0.097	0.278	0.610	1	1	0.370	1	1	1	1	1	**0.004**

Table 2. Cytochrome oxidase I (COI) F_{ST} values among all lineages. Under the diagonal are the F_{ST} and above the diagonal are the p-values of 10000 permutations, black means $p < 0.05$.

Lineage	NE Clade							W Clade	SE Clade					Amazon Clade	
	derivata - T	*derivata - TAR*	*concinna*	*procera - G*	*procera - CH*	*terminata*	*williamsoni sp. nov*	*gigantea*	*neopicta*	*ornata*	*victoria*	*spaeteri*	*picta*	*aurora*	*mutata*
derivata - T															
derivata - TAR	0.28														
concinna	0.31	0.72													
procera - G	0.80	0.90	0.87												
procera - CH	0.32	0.61	0.22	0.75											
terminata	0.21	0.28	0.69	0.89	0.60										
williamsoni sp. nov	0.42	0.89	0.32	0.90	0.27	0.88									
gigantea	0.83	0.88	0.86	0.91	0.85	0.88	0.88								
neopicta	0.77	0.81	0.81	0.89	0.80	0.82	0.83	0.86							
ornata	0.82	0.97	0.91	0.95	0.84	0.97	0.99	0.89	0.68						
victoria	0.77	0.93	0.87	0.95	0.82	0.93	0.95	0.88	0.33	0.93					
spaeteri	0.80	0.90	0.87	0.94	0.83	0.90	0.92	0.88	0.66	0.77	0.78				
picta	0.67	0.95	0.85	0.95	0.80	0.93	0.97	0.87	0.31	1	0.03	0.77			
aurora	0.83	0.97	0.93	0.97	0.90	0.96	0.99	0.91	0.89	1	0.97	0.95	1		
mutata	0.94	0.99	0.96	0.98	0.94	0.98	0.99	0.94	0.93	0.99	0.98	0.97	0.99	0.98	

Table 3. 16S fragment F_{ST} values among all lineages. Under the diagonal are the F_{ST} and above the diagonal are the p-values of 10000 permutations, black means $p < 0.05$.

Lineage	SE Clade				NE Clade							W Clade	Amazon Clade	
	boliviana	*neopicta*	*spaeteri*	*ornata*	*derivata - T*	*derivata - TAR*	*concinna*	*procera - G*	*procera - CH*	*terminata*	*williamsoni sp. nov*	*gigantea*	*aurora*	*mutata*
boliviana														
neopicta	1													
spaeteri	1	1												
ornata	1	1	1											
derivata -T	0.954	0.976	0.912	0.936										
derivata - TAR	1	1	1	1	0.775									
concinna	0.954	0.917	0.817	0.843	0.156	0.451								
procera - G	0.972	0.926	0.892	0.898	0.736	0.796	0.668							
procera - CH	0.941	0.890	0.776	0.795	0.161	0.167	0.112	0.535						
terminata	1	1	1	1	0.368	0	0.191	0.745	-0.1228					
williamsoni sp. nov	1	1	1	1	0.5	0	0.269	0.757	-0.012	0				
gigantea	0.990	0.982	0.962	0.971	0.942	0.968	0.908	0.911	0.886	0.957	0.959			
aurora	0.932	0.942	0.869	0.898	0.815	0.894	0.850	0.910	0.844	0.828	0.842	0.925		
mutata	1	1	1	1	0.945	1	0.9283	0.9516	0.9049	1	1	0.980	0.846	

Table 4. NADH Dehydrogenase I (ND1) fragment F_{ST} values among all lineages. Under the diagonal are the F_{ST} and above the diagonal are the p-values of 10000 permutations, black means $p < 0.05$.

	NE Clade							W Clade	SE Clade				Amazon Clade
Lineage	*derivata* - T	*derivata* - TAR	*concinna*	*procera* - CH	*procera* - G	*terminata*	*williamsoni sp. nov*	*gigantea*	*neopicta*	*ornata*	*victoria*	*spaeteri*	*mutata*
derivata - T													
derivata - TAR	0.91												
concinna	0.55	0.74											
procera - CH	0.53	0.58	0.44										
procera - G	0.74	0.70	0.67	0.56									
terminata	0.86	0.81	0.66	0.51	0.69								
williamsoni sp. nov	0.87	0.98	0.70	0.47	0.72	1.00							
gigantea	0.88	0.89	0.87	0.86	0.86	0.87	0.89						
neopicta	0.85	0.86	0.84	0.83	0.82	0.85	0.86	0.85					
ornata	0.93	0.96	0.91	0.86	0.86	0.94	0.94	0.89	0.75				
victoria	0.97	1.00	0.92	0.84	0.83	1.00	1.00	0.88	0.65	0.89			
spaeteri	0.91	0.96	0.89	0.82	0.86	0.94	0.94	0.88	0.76	0.84	0.94		
mutata	0.89	0.91	0.89	0.88	0.90	0.89	0.89	0.90	0.90	0.93	0.92	0.90	

Table 5. Summary table for the AMOVA's by geographic clades, among and within lineages (COI, ND1 and 16S). * means is p-values after 10,000 permutations < 0.05.

COI					
Source of Variation	d.f	Sum of squares	Variance components	% of variation	Fixation Indices
Among geographical clades	3	3475.157	21.93631	66%	**0.65511***
Among species within clades	11	912.13	8.27714	24.72%	**0.71671***
Within species	185	605.269	3.27172	9.77%	**0.86855***
Total	199	4992.556	33.48517		
ND1					
Source of Variation ND1	d.f	Sum of squares	Variance components	% of variation	Fixation Indices
Among geographical clades	3	1834.417	9.67514	61%	**0.61482***
Among species within clades	9	495.317	4.15737	26.42%	**0.68588***
Within species	217	413.161	1.90397	12.10%	**0.87901***
Total	229	2742.895	15.73648		
16S					
Source of Variation 16S	d.f	Sum of squares	Variance components	% of variation	Fixation Indices
Among geographical clades	3	673.829	5.17794	58%	**0.56517***
Among species within clades	9	261.369	3.2354	33.84%	**0.81212***
Within species	135	101.043	0.74847	8.44%	**0.91831***
Total	147	1036.241	9.16181		

Chapter 2: Figures

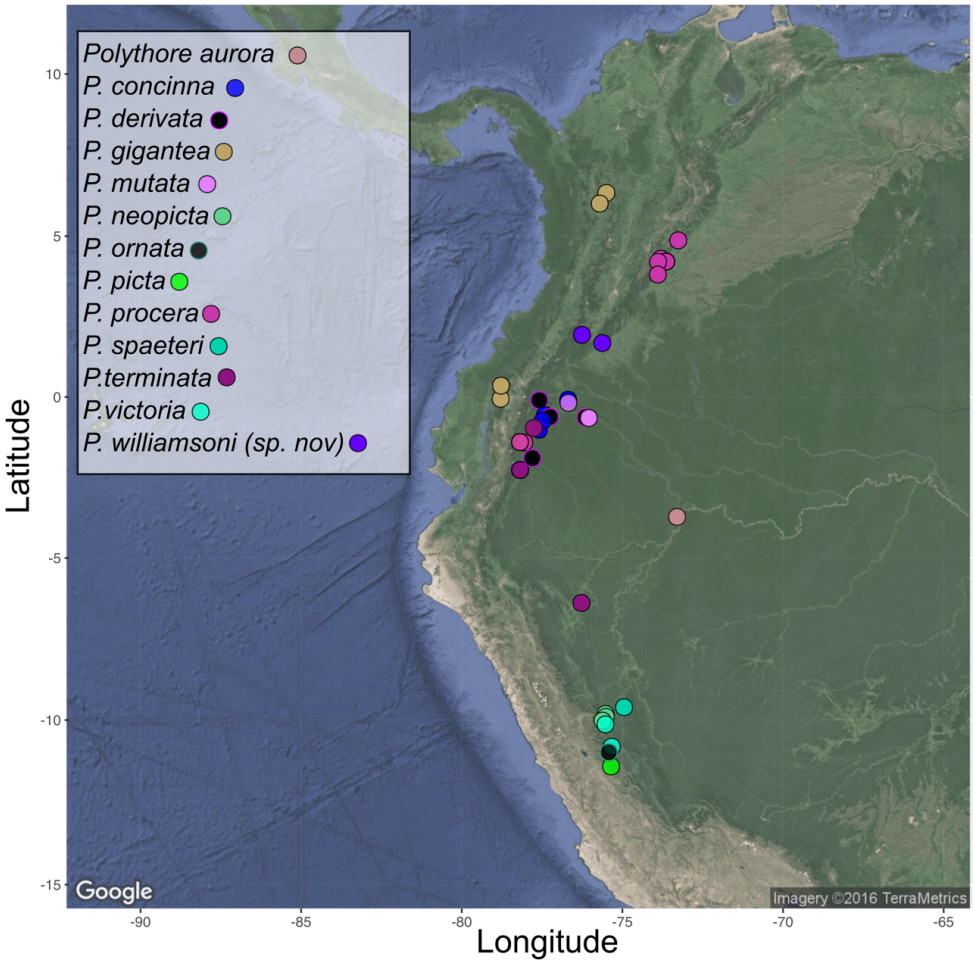

Figure 1. Map of the all the populations sampled, colored by morphospecies.

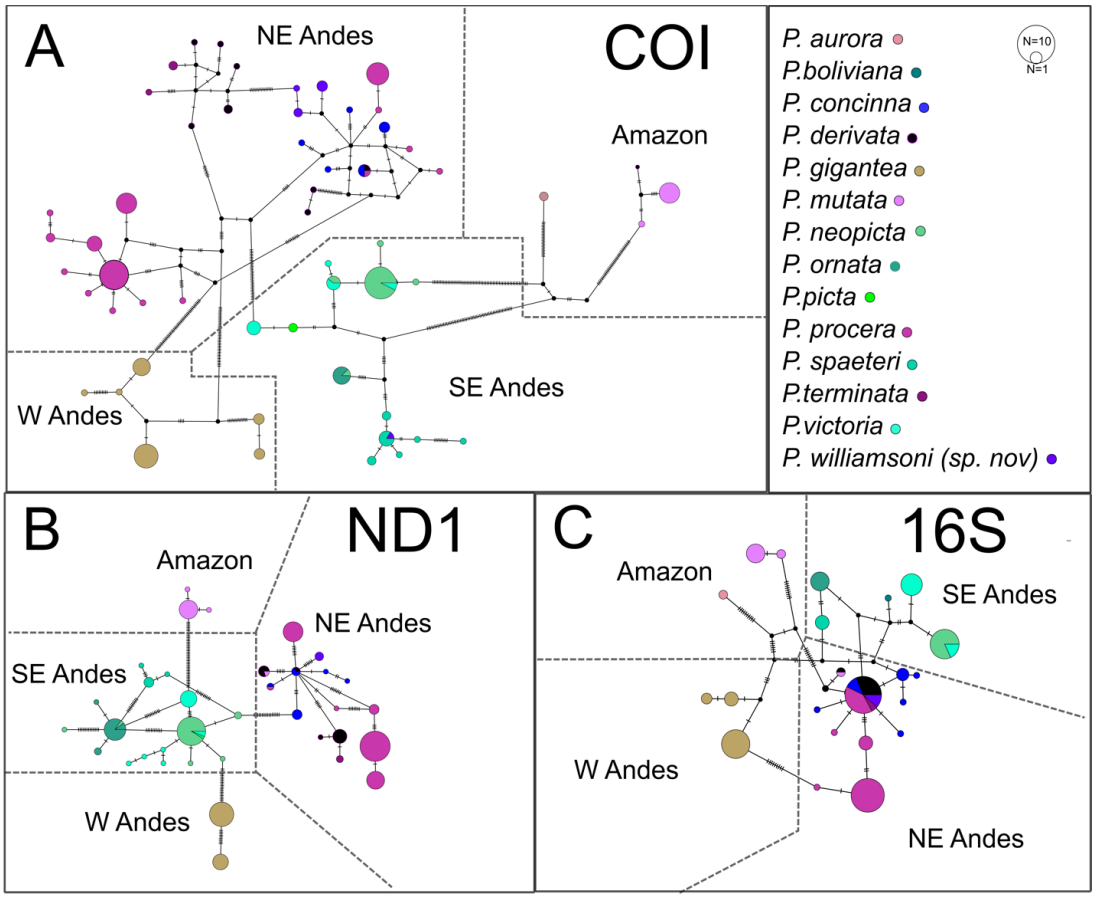

Figure 2. Haplotype networks of the three gene fragments. A) COI, B) ND1 and C) 16S.

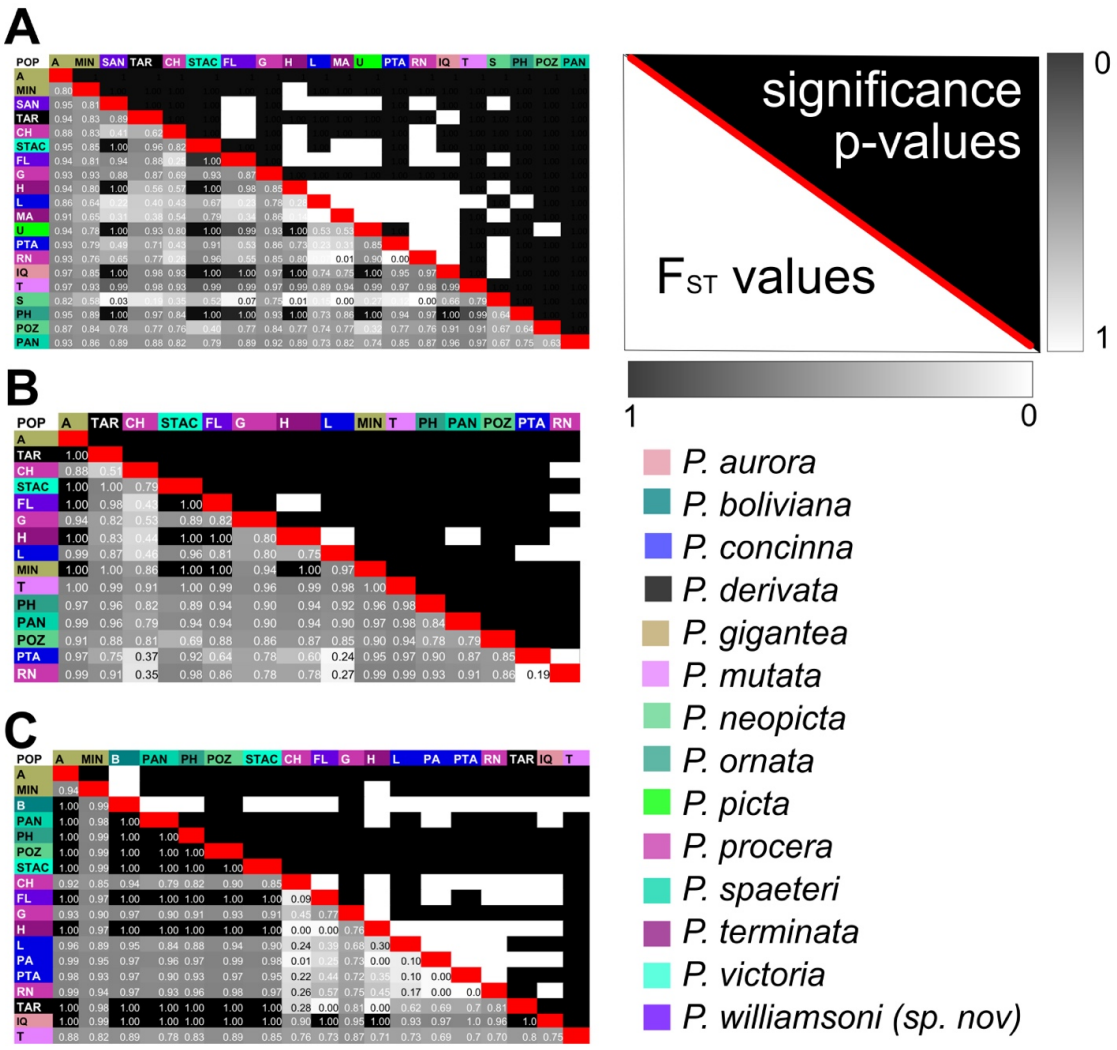

Figure 3. F_{ST} among all the populations sampled for all gene fragments. A) COI, B) ND1 and C) 16S.

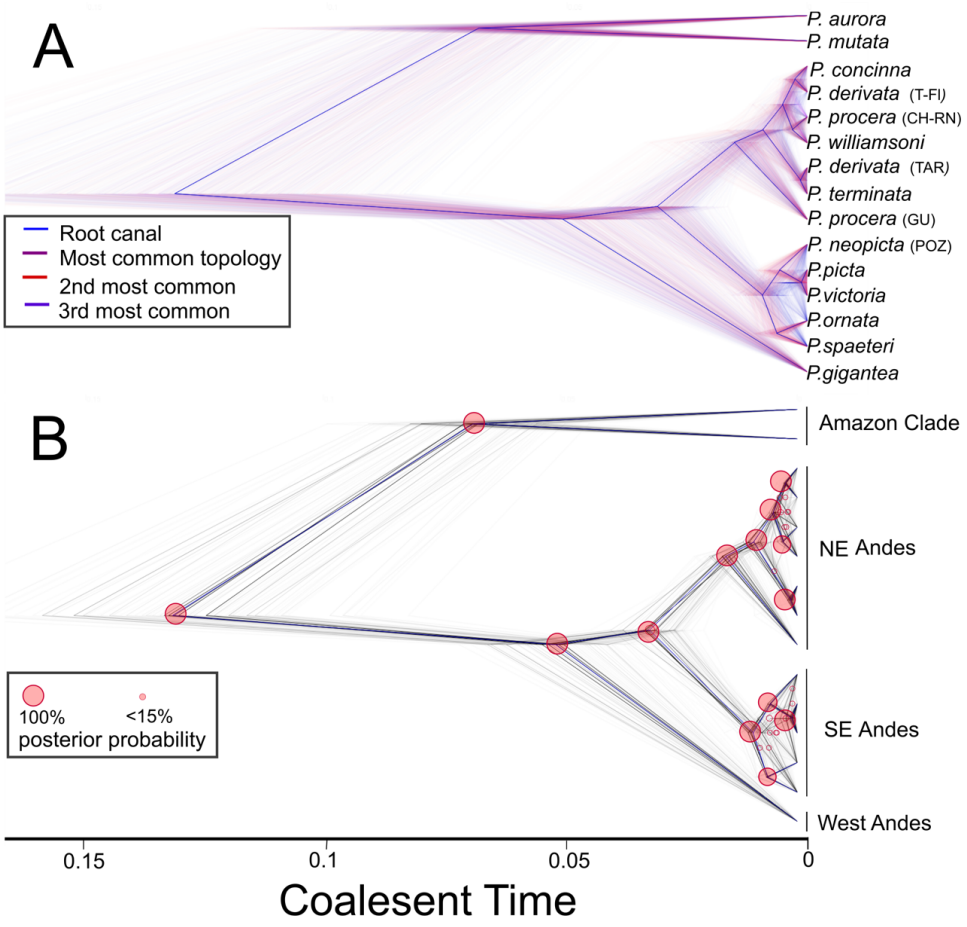

Figure 4. Estimated Species trees by *BEAST, topologies display after 90% of burning. A) Species Tree Uncertainty B) Consensus tree and posterior probabilities for the geographic clades.

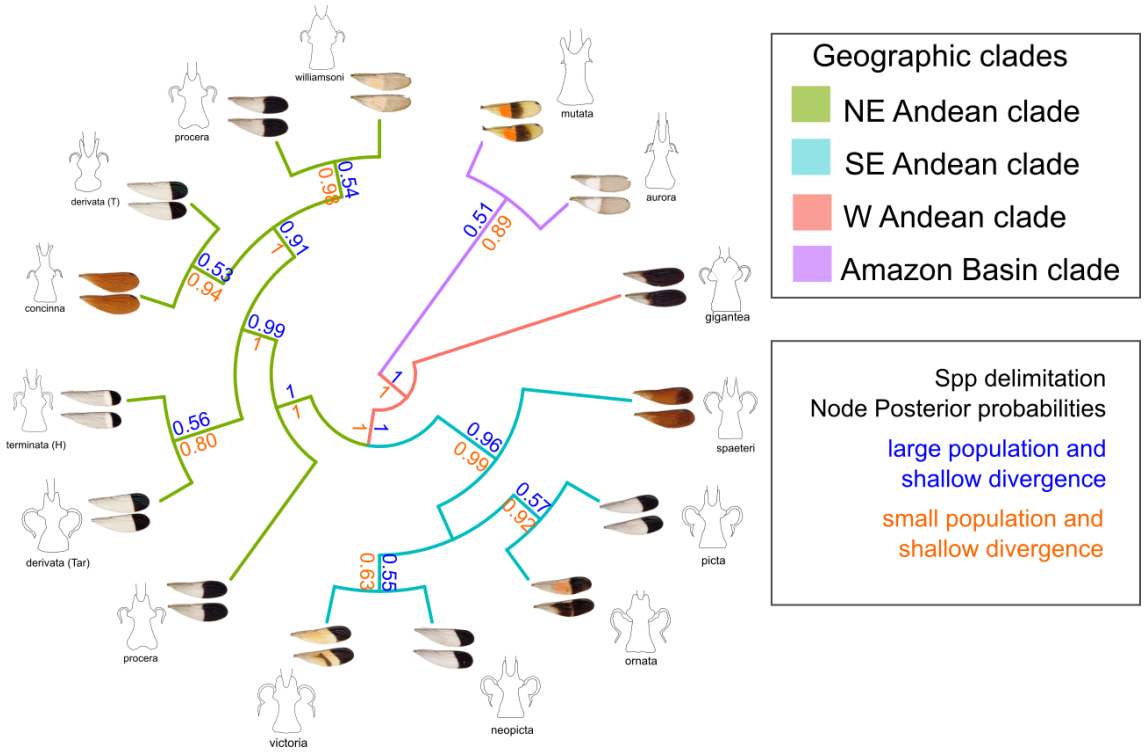

Figure 5. Maximum credibility species tree showing the geographic clades, species delimitation supports, males wing color pattern and male secondary genitalia ectal views.

References

Bick G.H., Bick J.C. 1985. A revision of the picta group of Polythore, with a description of a new species, P. lamerceda spec. nov., from Peru (Zygoptera: Polythoridae). Odonatologica. 14:1–28.

Bick G.H., Bick J.C. 1986. The genus Polythore exclusive of the picta group (Zygoptera: Polythoridae). Odonatologica. 15:245–273.

Bick G.H., Bick J.C. 1990. Polythore manua spec. nov. from southern Peru (Zygoptera: Polythoridae). Odonatologica. 19:367–373.

Bolnick D.I., Fitzpatrick B.M. 2007. Sympatric Speciation: Models and Empirical Evidence. Annu. Rev. Ecol. Evol. Syst. 38:459–487.

Bouckaert R., Heled J., Kühnert D., Vaughan T., Wu C.-H., Xie D., Suchard M.A., Rambaut A., Drummond A.J. 2014. BEAST 2: a software platform for Bayesian evolutionary analysis. PLoS Comput. Biol. 10:e1003537.

Bouckaert R.R. 2010. DensiTree: making sense of sets of phylogenetic trees. Bioinformatics. 26:1372–1373.

Brown W.M., George M. Jr, Wilson A.C. 1979. Rapid evolution of animal mitochondrial DNA. Proc. Natl. Acad. Sci. U. S. A. 76:1967–1971.

Burbrink F.T., Guiher T.J. 2015. Considering gene flow when using coalescent methods to delimit lineages of North American pitvipers of the genus Agkistrodon : Agkistrodon Species Delimitation. Zool. J. Linn. Soc. 173:505–526.

Carstens B.C., Pelletier T.A., Reid N.M., Satler J.D. 2013. How to fail at species delimitation. Mol. Ecol. 22:4369–4383.

Coyne J.A., Allen Orr H. 2004. Speciation. W.H. Freeman.

Dayrat B. 2005. Towards integrative taxonomy: INTEGRATIVE TAXONOMY. Biol. J. Linn. Soc. Lond. 85:407–415.

De Queiroz K. 2007. Species Concepts and Species Delimitation. Syst. Biol. 56:879–886.

DeSalle R., Egan M.G., Siddall M. 2005. The unholy trinity: taxonomy, species delimitation and DNA barcoding. Philos. Trans. R. Soc. Lond. B Biol. Sci. 360:1905–1916.

Drotz M.K., Brodin T., Nilsson A.N. 2015. Changing Names with Changed Address: Integrated Taxonomy and Species Delimitation in the Holarctic Colymbetes paykulli

Group (Coleoptera: Dytiscidae). PLoS One. 10:e0143577.

Excoffier L., Lischer H.E.L. 2010. Arlequin suite ver 3.5: a new series of programs to perform population genetics analyses under Linux and Windows. Mol. Ecol. Resour. 10:564–567.

Fujisawa T., Barraclough T.G. 2013. Delimiting species using single-locus data and the Generalized Mixed Yule Coalescent approach: a revised method and evaluation on simulated data sets. Syst. Biol. 62:707–724.

Hausdorf B. 2011. Progress toward a general species concept. Evolution. 65:923–931.

Heled J., Drummond A.J. 2010. Bayesian inference of species trees from multilocus data. Mol. Biol. Evol. 27:570–580.

Hey J. 2001. The mind of the species problem. Trends Ecol. Evol. 16:326–329.

Hey J. 2014. Species Concepts. .

Hey J., Pinho C. 2012. Population genetics and objectivity in species diagnosis. Evolution. 66:1413–1429.

Joly S. 2012. JML: testing hybridization from species trees. Mol. Ecol. Resour. 12:179–184.

Joly S., McLenachan P.A., Lockhart P.J. 2009. A statistical approach for distinguishing hybridization and incomplete lineage sorting. Am. Nat. 174:E54–70.

Katoh K., Standley D.M. 2013. MAFFT multiple sequence alignment software version 7: improvements in performance and usability. Mol. Biol. Evol. 30:772–780.

Katz A.D., Giordano R., Soto-Adames F.N. 2015. Operational criteria for cryptic species delimitation when evidence is limited, as exemplified by North American Entomobrya (Collembola: Entomobryidae) : Collembola Species Delimitation. Zool. J. Linn. Soc. 173:818–840.

Kearse M., Moir R., Wilson A., Stones-Havas S., Cheung M., Sturrock S., Buxton S., Cooper A., Markowitz S., Duran C., Thierer T., Ashton B., Meintjes P., Drummond A. 2012. Geneious Basic: an integrated and extendable desktop software platform for the organization and analysis of sequence data. Bioinformatics. 28:1647–1649.

Kjer K.M. 1995. Use of rRNA secondary structure in phylogenetic studies to identify homologous positions: an example of alignment and data presentation from the frogs. Mol. Phylogenet. Evol. 4:314–330.

Kjer K.M., Gillespie J.J., Ober K.A. 2007. Opinions on multiple sequence alignment, and an empirical comparison of repeatability and accuracy between POY and structural alignment. Syst. Biol. 56:133–146.

Leaché A.D., Fujita M.K. 2010. Bayesian species delimitation in West African forest geckos (Hemidactylus fasciatus). Proc. Biol. Sci. 277:3071–3077.

Leigh J.W., Bryant D. 2015. popart: full-feature software for haplotype network construction. Methods Ecol. Evol. 6:1110–1116.

Lin X., Stur E., Ekrem T. 2015. Exploring Genetic Divergence in a Species-Rich Insect Genus Using 2790 DNA Barcodes. PLoS One. 10:e0138993.

Li Y., Gunter N., Pang H., Bocak L. 2015. DNA-based species delimitation separates highly divergent populations within morphologically coherent clades of poorly dispersing beetles: Species delimitation in Chinese Lycidae. Zool. J. Linn. Soc. 175:59–72.

Maddison W.P., Maddison D.R. 2015. Mesquite: a modular system for evolutionary analysis. .

Mallet J. 1995. A species definition for the modern synthesis. Trends Ecol. Evol. 10:294–299.

Misof B., Liu S., Meusemann K., Peters R.S., Donath A., Mayer C., Frandsen P.B., Ware J., Flouri T., Beutel R.G., Niehuis O., Petersen M., Izquierdo-Carrasco F., Wappler T., Rust J., Aberer A.J., Aspöck U., Aspöck H., Bartel D., Blanke A., Berger S., Böhm A., Buckley T.R., Calcott B., Chen J., Friedrich F., Fukui M., Fujita M., Greve C., Grobe P., Gu S., Huang Y., Jermiin L.S., Kawahara A.Y., Krogmann L., Kubiak M., Lanfear R., Letsch H., Li Y., Li Z., Li J., Lu H., Machida R., Mashimo Y., Kapli P., McKenna D.D., Meng G., Nakagaki Y., Navarrete-Heredia J.L., Ott M., Ou Y., Pass G., Podsiadlowski L., Pohl H., von Reumont B.M., Schütte K., Sekiya K., Shimizu S., Slipinski A., Stamatakis A., Song W., Su X., Szucsich N.U., Tan M., Tan X., Tang M., Tang J., Timelthaler G., Tomizuka S., Trautwein M., Tong X., Uchifune T., Walzl M.G., Wiegmann B.M., Wilbrandt J., Wipfler B., Wong T.K.F., Wu Q., Wu G., Xie Y., Yang S., Yang Q., Yeates D.K., Yoshizawa K., Zhang Q., Zhang R., Zhang W., Zhang Y., Zhao J., Zhou C., Zhou L., Ziesmann T., Zou S., Li Y., Xu X., Zhang Y., Yang H., Wang J., Wang J., Kjer K.M., Zhou X. 2014. Phylogenomics resolves the timing and pattern of insect evolution. Science. 346:763–767.

Padial J.M., Miralles A., De la Riva I., Vences M. 2010. The integrative future of taxonomy. Front. Zool. 7:16.

Pons J., Barraclough T., Gomez-Zurita J., Cardoso A., Duran D., Hazell S., Kamoun S., Sumlin W., Vogler A. 2006. Sequence-Based Species Delimitation for the DNA Taxonomy of Undescribed Insects. Syst. Biol. 55:595–609.

Powell T.H.Q., Hood G.R., Murphy M.O., Heilveil J.S., Berlocher S.H., Nosil P., Feder J.L. 2013. Genetic divergence along the speciation continuum: the transition from host race to species in rhagoletis (Diptera: tephritidae). Evolution. 67:2561–2576.

Rambaut A., Suchard M.A., Xie D., Drummond A.J. 2014. Tracer. .

Rannala B., Yang Z. 2013. Improved reversible jump algorithms for Bayesian species delimitation. Genetics. 194:245–253.

Reid N.M., Carstens B.C. 2012. Phylogenetic estimation error can decrease the accuracy of species delimitation: a Bayesian implementation of the general mixed Yule-coalescent model. BMC Evol. Biol. 12:196.

Rojas-Riaño N.C. 2011. Sistematica de genero POLYTHORE Calvert, 1917 (ODONATA: POLYTHORIDAE). Master Thesis.

Ruane S., Bryson R.W. Jr, Pyron R.A., Burbrink F.T. 2014. Coalescent species delimitation in milksnakes (genus Lampropeltis) and impacts on phylogenetic comparative analyses. Syst. Biol. 63:231–250.

Sánchez Herrera M., Realpe E., Salazar C. 2010. A neotropical polymorphic damselfly shows poor congruence between genetic and traditional morphological characters in Odonata. Mol. Phylogenet. Evol. 57:912–917.

Sánchez Herrera M., Ware J. L. 2012. Biogeography of Dragonflies and Damselflies: Highly Mobile Predators. In: Stevens L., editor. Global Advances in Biogeography. InTech.

Sánchez Herrera M., Kuhn W.R., Lorenzo-Carballa M.O., Harding K.M., Ankrom N., Sherratt T.N., Hoffmann J., Van Gossum H., Ware J.L., Cordero-Rivera A., Beatty C.D. 2015. Mixed signals? Morphological and molecular evidence suggest a color polymorphism in some neotropical polythore damselflies. PLoS One. 10:e0125074.

Schlick-Steiner B.C., Steiner F.M., Seifert B., Stauffer C., Christian E., Crozier R.H. 2010. Integrative taxonomy: a multisource approach to exploring biodiversity. Annu. Rev. Entomol. 55:421–438.

Trifinopoulos J., Nguyen L.-T., von Haeseler A., Minh B.Q. 2016. W-IQ-TREE: a fast online phylogenetic tool for maximum likelihood analysis. Nucleic Acids Res. 44:W232–W235.

Wade E.J., Hertach T., Gogala M., Trilar T., Simon C. 2015. Molecular species delimitation methods recover most song-delimited cicada species in the European Cicadetta montana complex. J. Evol. Biol. 28:2318–2336.

Will K.W., Mishler B.D., Wheeler Q.D. 2005. The perils of DNA barcoding and the need for integrative taxonomy. Syst. Biol. 54:844–851.

Wu C.-I., Chung-I W. 2001. The genic view of the process of speciation. J. Evol. Biol. 14:851–865.

Yang Z. 2015. The BPP program for species tree estimation and species delimitation.

Curr. Zool. 61:854–865.

Yang Z., Rannala B. 2010. Bayesian species delimitation using multilocus sequence data. Proc. Natl. Acad. Sci. U. S. A. 107:9264–9269.

Yeates D.K., Seago A., Nelson L., Cameron S.L., Joseph L., Trueman J.W.H. 2011. Integrative taxonomy, or iterative taxonomy? Syst. Entomol. 36:209–217.

Yu G., Smith D., Zhu H., Guan Y., Lam T.T. 2016. ggtree: an R package for visualization and annotation of phylogenetic tree with different types of meta-data. Under review .

Zhang J., Kapli P., Pavlidis P., Stamatakis A. 2013. A general species delimitation method with applications to phylogenetic placements. Bioinformatics. 29:2869–2876.

Chapter Three: Are *Polythore* damselflies monophyletic? A molecular systematic reconstruction of the phylogenetic relationships of the Neotropical Polythoridae damselflies.

Abstract

The Neotropics are a center for global diversity for many groups of organisms, including the dragonflies and damselflies (Insecta: Odonata). While the number of biodiversity surveys and new species descriptions for neotropical odonates is increasing, diversity in this region is still under-explored, and very few studies have looked at the genetic and morphological diversity within species. Here, I present an overview of the evolutionary history of the Neotropical damselfly family Polythoridae. The family comprises fifty-seven species across seven genera: *Chalcothore, Chalcopteryx, Cora, Euthore, Miocora, Polythore* and *Stenocora*. Using a multi-locus approach, mitochondrial (COI, ND1, 16S) and nuclear (18S, 28S, EF1, PMRT) genes were incorporated to estimate phylogenetic relationships. My results support five monophyletic clades, which were not always congruent with the genera currently considered to be monophyletic. *Cora* was found to be paraphyletic and as a consequence, several species currently assigned to this group likely belong to other genera. *Polythore* was found to be monophyletic, with geographical distribution strongly influencing within-genus relationships. Moreover, several of the *Polythore* clades may constitute a polymorphic complex (putative geographical races). Divergence time estimation analyses using fossil calibration suggest that the family appeared around the mid-Eocene (~40 Ma), and its diversification peak was around the mid-Miocene (~16 Ma). The recovered ages and diversification patterns strongly suggest

a correlation between diversification in this group and key geological events, including the Andes Uplift, Central American Seaway closure and the formation of the Amazon Basin.

Background

Odonates (dragonflies and damselflies) are one of the most basal nodes in the insect tree, perhaps the first to take to the skies (Misof et al. 2014). They comprise ~6000 species distributed in three suborders: Anisoptera ("true" dragonflies), Zygoptera (damselflies) and the strange looking Anisozygoptera (adults possess body characteristics similar to dragonflies, but with wing morphology resembling damselflies). Odonates are efficient predators in all of their life stages; they have unique and complex reproductive behaviors, and are dependent on freshwater ecosystems (Corbet 1999, Cordoba-Aguilar 2009). Their immature stages tend to live in either lotic (flowing) or lentic (static) water bodies, and display a number of morphological adaptations to their preferred habitats (Corbet 1999). With their strong habitat fidelity and relatively low species diversity in comparison with other insect orders (6000 species as compared to 350,000 beetle species), odonates are excellent bioindicators for freshwater ecosystems, which are rapidly becoming one of our most precious and limited resources. Odonate biodiversity varies with latitude and longitude, with the Neotropics holding the highest species richness (~1800 spp, Sanchez and Ware, 2012). Despite this high Neotropical diversity this region is understudied; by comparison, our current knowledge of taxonomic diversity and behavior is much greater for the North American fauna. Evolutionary relationships among endemic Neotropical taxa are at best poorly understood.

The damselfly family Polythoridae belongs to the superfamily Calopterygoidea (Zygoptera), commonly known as the broad-wing damselflies, and is distributed exclusively in the Neotropical region, from Southern Mexico to Bolivia and Northern Brazil (Figure 1). Polythoridae comprises 57 species within seven genera, *Chalcopteryx* Selys, *Chalcothore* De Marmels, *Cora* Selys, *Euthore* Selys, *Miocora* Calvert, *Polythore* Calvert and *Stenocora* Kennedy. These medium-to-large sized damselflies have a robust thorax and short abdomen, wings with dense venation, long pterostigma, and usually show colored wing bands, which are sometimes iridescent in sunlight (Garrison et al. 2010). Recent morphological and molecular intraordinal studies of Odonata support the monophyly of Polythoridae and suggest Euphaeidae as its sister taxon (Rehn 2003; Bybee et al. 2008; Dumont et al. 2009; Dijkstra et al. 2013).

During the 1980's and early 1990's, Drs. G.H. Bick and J.C. Bick summarized an unfinished monograph on Polythoridae that E.B. Montgomery was working on before he died (Bick and Bick 1985, 1992). They examined all the specimens that Montgomery had borrowed from several collections; commercial collectors had collected most of them from the Andes of Colombia, Ecuador, and Peru. After extensive examination, they published six manuscripts; these manuscripts revised and described new species of *Cora*, *Euthore* and *Polythore*, increasing our knowledge of Polythoridae (Bick and Bick 1985, 1986, 1990a, 1990b, 1991, 1992). Around the same time, Dr. J. De Marmels described the monotypic genus *Chalcothore* (De Marmels 1988), and documented the ecology and behavior of *Euthore* species (De Marmels 1982). In past discussions of *Chalcopteryx*, most studies have used information from original species descriptions (Rambur 1842; Selys Longchamps 1853; McLachlan 1870; Ris 1914), but recently new reports from

Brazil (Santos and Machado 1960; Costa 2005), have reopened discussions of their classification. All these revisions highlight the traditional characters' liability for species determination in Odonates within the family, including, male secondary genitalia (i.e. penis or ligula) or male abdominal appendages and the incredible diversity in wing coloration patterns, that includes sexual dimorphism. Recent studies of Colombian and Peruvian *Polythore* species show a lack of congruence between wing color morphs and genetic markers (COI), supporting the presence of possible cryptic species (Sánchez Herrera et al. 2010) or polytypic species (Sánchez Herrera et al. 2015). Here I reconstructed phylogenetic hypotheses of Polythoridae. I used four nuclear and three mitochondrial loci, and reconstructed trees with Maximum Likelihood and Bayesian Inference. I included a total of 36 species representing six of the seven genera in the analyses. I established the monophyletic nature of two of the genera (*Polythore* and *Euthore*). However, the other five show unexpected relationships, suggesting taxonomical revision is needed at the generic level. The first time-calibrated phylogeny is reconstructed here, estimated using fossil calibrations. In addition, I present estimates for the diversification ages within Polythoridae.

Methods

Taxon sampling

I included thirty-six species in the phylogenetic reconstruction presented here (geographic origin, collector details, and Genbank Accession Numbers are summarized in Supplementary Table 1). Other related Calopterygoid taxa, Philogangidae, Euphaeidae, and Pseudolestidae were used as outgroups (additional sequences from Bybee et al. 2008; Dumont et al. 2009; Dijkstra et al. 2013).

DNA amplification, sequencing, and alignment

I extracted DNA from either the legs or ¼ of the pterothorax using a DNeasy Tissue Kit (QIAGEN) from each specimen following the manufacturer's protocol. I amplified three mitochondrial and four nuclear fragments: Cytochrome Oxidase I (~799bp), NAD dehydrogenase (~548 bp), 16S, (~340bp), Elongation Factor (~900 bp), Arginine N-methyltransferase (~300bp), 28S (~340bp) and 18S (~600bp) (see Supplementary Table 2 for a list of primers used). All gene fragments were amplified using PCR conditions as described in the associated publications for each pair of primers (Supplementary Material Appendix 1). Macrogen USA Inc. laboratories (NY) performed the purification protocol for the PCR products (15µl final volume for each primer) and the Sanger DNA sequencing. Primer contig assembly, peak chromatogram verification and the generation of per-individual consensus sequences were done using Geneious v 7 (Kearse et al. 2012). All fragments were aligned using MAFFT (Katoh and Standley 2013) and then manually aligned in Mesquite (Maddison and Maddison 2015). Ribosomal genes were aligned manually with reference to secondary structure using the methods described in Kjer (1995) and Kjer et al. (2007). Finally, all genes were concatenated using Mesquite for the overall analyses.

Phylogenetic Methods

Phylogenetic relationships among the taxa were reconstructed using partitioned analyses in IQ-Tree (Nguyen et al. 2015; Trifinopoulos et al. 2016) for Maximum Likelihood (ML) and MrBayes 3.2.1 (Ronquist et al. 2012) for Bayesian Inference (BI). For each gene fragment, the substitution model was determined using both the Akaike Information

Criterion (AIC) and Bayesian Information Criterion (BIC) using the IQ-tree model selection option. For all mtDNA fragments the selected model was HKY+F+I+G4, for the 18S and PMRT the JC was the best fit, for EF1 the best-fit model was TIM3e + G4 and for 28S TIM+ASC was determined to have the best fit (Trifinopoulos et al. 2016). IQ-tree performed a total of 5,000 bootstrap pseudoreplicates (hereafter bs) to determine node support for the ML analysis. For the BI analysis, we implemented the closest possible models to those suggested by IQ-tree (e.g. EF1 and 28S, for example, we used GTR + G). I ran four different heated MCMC chains, and 1 x 10^7 million generations sampling every 100 cycles. I assessed chain convergence in posterior probabilities (hereafter pp) distribution of the multiple runs using Tracer v 1.6 (Rambaut et al. 2014), and topology convergence were determined using AWTY (Nylander et al. 2007). I estimated a majority rule 50% consensus posterior probability tree. Both ML and BI best and consensus trees were visualized using Figtree v. 1.4 (http://tree.bio.ed.ac.uk/software/figtree/) and the R package ggtree (Yu et al. 2016).

Divergence time estimation analyses

A relaxed-clock molecular dating analysis on the partitioned dataset was run using BEAST v 1.8.3 (Drummond et al. 2012). Specifically, I partitioned the gene fragments as follows: (i) I linked the sites and clock models for all mtDNA fragments and (ii) unlinked all nuclear ones their clock and site models. I implemented the appropriate model selection for each partition: HKY + G4 for all mtDNA, JC for 18S and PMRT, 28S and for EF1 we set the model to GTR + G. I used lognormal relaxed clock models for all partitions, under a Yule speciation model. I used the best ML phylogram with proportional branch lengths as the starting tree for the analysis. Table 1 shows the

calibrated nodes (4), stem fossils (10) and prior distributions selected for the analyses. Biogeographical events may not be reliable calibrations points in divergence estimation studies due to their reliance on *a priori* assumptions about ancestral distributions (Drummond et al. 2012). However, due to a lack of strong fossil calibrations in Polythoridae, we ran our analyses with and without an additional biogeographical calibration from the uplift of the Andes Cordillera to calibrate the *Polythore* clade (Table 1) to evaluate the impact of this calibration. For each treatment, with and without biogeography, we ran four independent analyses to ensure convergence of the MCMC; convergence was checked using Tracer 1.6 (Rambaut et al. 2014). Finally, the independent runs for each treatment were combined using LogCombiner v 1.8.3 (Drummond et al. 2012). The dated ultrametric tree was obtained using TreeAnnotator v 1.8.3 (Drummond et al. 2012) and visualized using Figtree v 1.4 (http://tree.bio.ed.ac.uk/software/figtree/) and the R package ggtree (Yu et al. 2016). The estimated mean node ages for both treatments were compared using paired t-tests in R (R Core Team 2013). I estimated the lineage divergence plots for both analyses using the package ape (Paradis et al. 2004) in R.

Results

The phylogenetic relationships recovered were congruent under both optimality criteria, ML and BI. The monophyly of the family Polythoridae clade was highly supported, with 100% bootstrap and 0.7 posterior probability (Figure 2). Within the Polythoridae, 5 major clades were recovered with high to moderate support values (Figure 2): 1) *Chalcopteryx* clade (node 54, bs 97 and pp 0.65), 2) *Cora* clade (node 58, bs 100 and pp 0.98), 3) *Cora* - *Miocora* clade (node 64, bs 90 and pp 0.93), 4) *Cora* - *Euthore* clade

(node 71, bs 80 and pp 0.51); and 5) *Polythore* clade (node 77, bs 95% and pp 0.52). The relationships within each of these clades is as follows: a) The *Chalcopteryx* clade includes the monospecific genus *Chalcothore*, however the support values within are not high enough to resolve intra-clade relationships (Fig 3A); b) The *Cora* clade comprises two well-supported monophyletic groups (Fig 3B):one encompasses *C. xanthostoma*, *C.cyane* and *C.irene*, while the other includes just *C. inca*. c) The *Cora* - *Miocora* clade also supports two reciprocally monophyletic clades (Fig 3C), one represents members of *C.aurea*, while the other groups *C. chirripa* and *Miocora peraltica* together. d) Two reciprocally monophyletic clades include the *Cora* - *Euthore* lineages (Fig 3D): one groups all *Euthore* species and *C. terminalis*, (however, the support for this relationship is low (bs and pp < 50%)), while the species *C. klenei* is recovered as the sister clade to *Euthore* and *C. terminalis*. Finally, the *Polythore* clade consists of four highly supported monophyletic clades (Fig 4) i) ***mutata-aurora*** clade (node 78, bs and pp 99%), ii) ***gigantea*** clade (node 95, bs 99% and pp 0.96), iii) **Southeastern (SE)** clade (node 90, bs 98% and pp 0.9) and iv) **Northeastern (NE)** clade (node 81, bs 98 and pp 0.8).

Within the *Polythore* clade, the *mutata-aurora* clade is sister to all the other *Polythore* species (Fig 4, node 77). Node 79, is composed by two highly-supported clades, one encompasses populations of the species *P.gigantea* (node 95) distributed through the western slopes of the Andes (Fig 4). The other clade includes all the other *Polythore* species (node 80) that are distributed along the eastern slopes of the Andes. Within this Andean clade, there are two groups, a Southeastern (SE, node 90) and a Northeastern clade (NE, Fig 4, node 81). Within the SE clade there are three subclades: a) ***picta-victoria-neopicta*** (bs 92% and pp 0.97), b) ***ornata-spaeteri*** (bs 98% and pp 0.95), and c)

boliviana (Fig 4). The northeastern clade shows a paraphyletic pattern of almost all the species that composed it, *P.procera, P.derivata, P.terminata, P.concinna* and *P.williamsoni* (Fig 4).

The divergence time analyses show significant differences in node age estimates (i.e. t-Test) between the two BEAST analyses treated with and without the secondary calibration of the Andean uplift (Table 4). With the Andean calibration, the age estimates are significantly younger showing differences ~1 to 5Ma depending on the node (Table 2). The estimated node age of the superfamily Calopterygoidea was Paleocene in both BEAST analyses, ~ 63Ma without and ~58 Ma with the Andean calibration (see Fig 5, Table 2). For the outgroup family Euphaeidae, the estimated ages were from the Late Eocene, showing a significant difference of ~ 1Ma between the treatments (Table 2). On the other hand, the family Polythoridae estimates Eocene in age (Fig 5, Table 2) ~ 9 to 7 Ma older than the Euphaeidae. The BEAST analysis with the Andean calibration yields an age which is ~3.5Ma younger than the BEAST analysis with just fossil calibrations (see Table 5). Within Polythoridae, the estimates for the *Chalcopteryx* clade suggest it is the oldest extant Polythoridae, having diverged around the Oligocene epoch (~22 Ma, Fig 5). The *Cora*, *Miocora*, *Euthore* and *Polythore* clades diverged somewhere around the mid Miocene (Fig 5). *Euthore* node age estimates suggest it is the youngest of the extant taxa which diverged during the Pliocene (Fig 5). Lineage through time plots based on both BEAST analyses indicate the Miocene (~ 23Ma) as the peak time for the diversification of this family (Fig 6).

Within the *Polythore* clade, the Andean clade (i.e. *P. gigantea*, Northeastern and Southeastern groups) was estimated to have arisen during the late Miocene (Fig 7). The

P. gigantea clade from the western slopes separated from the eastern clade sometime around the late Miocene, and later the Northeastern and Southeastern clades diverged during the Pliocene - Pleistocene (Fig 7).

Discussion

Systematics and Taxonomic Remarks

The molecular reconstructions corroborate the monophyly of the family Polythoridae (Fig 2), previously recovered by deep-level phylogenies of Odonata (Rehn 2003; Bybee et al. 2008; Dijkstra et al. 2013). Until this current study, there has been a lack of knowledge of the molecular and morphological evolutionary relationships among Polythoridae genera and species. There has been only one prior morphological phylogenetic evaluation of *Polythore;* the genus was recovered as monophyletic, however, it fails to resolve the species-level relationships due to high phenotypic polymorphism (Rojas-Riaño 2011) . Here, I reconstructed topologies support five monophyletic groups within Polythoridae that are not always consistent with the current classification based on morphological data alone (Fig. 2).

Chalcopteryx and Chalcothore

Within the *Chalcopteryx* clade (Fig 3A), the species *Chalcothore montgomery* (Racenis 1968) was recovered as sister to all *Chalcopteryx* species (Figs 2, 3A). *Chalcothore* De Marmels (1988) is a monotypic genus, previously described by Racenis (1968) as *Euthore*, using five females collected at the first terrace of the large table top mountain Auyan-Tepuy in Venezuela. He used only wing characters (i.e. trifurcate anal vein, proportions of the triangles of the fore- and hindwings, less dense venation and primary

antenodals) to place this species into the genus *Euthore*. However, he recognized that its overall small size and broadened anal fields in the wings were not shared with any other members of *Euthore*. De Marmels (1988) with new male specimens in hand, re-described this species and placed it into a new genus, *Chalcothore*. His comparative study of male secondary genitalia, anal appendages and wing venation with two species of *Euthore* and two of *Chalcopteryx* revealed that individuals of *Chalcothore* shared characters with both *Euthore* and *Chalcopteryx*, but also possessed unique features (De Marmels 1988). Most of the wing characteristics he assessed were found to be similar in the wings of *Euthore* except for the supplementary sectors arising from the main veins, which is a shared character with *Chalcopteryx* (De Marmels 1988). The secondary genitalia and anal appendages were similar to *Chalcopteryx*, but showed some divergent traits. De Marmels (1988) noticed a lack of sexual dimorphism in the color pattern of the wings. My recovered topology suggests that this *Chalcothore* is more closely related to *Chalcopteryx* than to *Euthore* (Fig 3A), which supports De Marmels (1988) discussion of shared ancestral habitat by *Chalcothore* and *Chalcopteryx* which is not shared with *Euthore*. Possibly more samples of *Chalcothore montgomery* and the missing three species of *Chalcopteryx* should be included in future analyses, to corroborate the relationships and revalidate both genera. Additionally, the inclusion of the specimens of *Stenocora* will be necessary because both genera share male appendage and female ovipositor morphological apomorphies.

Cora, Miocora and Euthore

Bick and Bick (Bick and Bick 1990a) revised the genus only using males and delimited three species groups based on distinct differences in the apex of the terminal segment of

the secondary genitalia (i.e. penis), nodus position, pterostigma length and color of the second abdominal segment. Here I will review Bick and Bick (1990a) proposed morphological groups:

MODESTA GROUP: Their secondary genitalia reflects the typical form of the other Polythoridae genera (*Chalcopteryx, Chalcothore, Stenocora, Miocora* and *Euthore*), with two apical horns of variable length (i.e. 0.05 - 0.35mm), forewing (hereafter FW) nodus position is equidistant or closer to the base of the wing than the tip of the wing; small pterostigma in the FW and the second abdominal segment is completely black (Bick and Bick 1990a). This group had two main distribution patterns, with some Central American species (*C. semiopaca, C. notoxantha, C. obscura, C. chirripa* and *C. skinneri*) and others species existing exclusively in South America (*C. dualis, C. modesta, C. lugubris, C. munda, C. terminalis, C. confusa* and *C. klenei*).

CYANE GROUP: These species have apical horns are completely lacking in the secondary genitalia; FW nodus is closer to the pterostigma, which is long, and the second segment of the abdomen is completely blue. Most of the members are distributed in South America, i.e., *C. cyane, C. jocosa, C. xanthostoma* and *C. irene*, except for *C. marina* which is broadly distributed across Central America (Bick and Bick, 1990).

INCA GROUP: It comprises only the species *C. inca*, which is distributed in Colombia and Ecuador. The secondary genitalia of this species shows an intermediate morphology between the Cyane and Modesta groups, while the other characters are the same as in the Cyane group (Bick and Bick, 1990).

My recovered topology shows that the described genus *Cora* Selys has a paraphyletic pattern. Species of several morphological groups were dispersed across three different clades (Fig 2). Here I discussed the following recovered monophyletic clades: The *Cora* sensu stricto, *Miocora* and *Euthore.*

***CORA* SENSU STRICTO:** The *Cora* clade (Fig 3B) comprises two of the proposed morphological groups by Bick and Bick (1990), the Inca and Cyane groups. Most of the species within *Cora* clade are distributed across eastern South America, except for *Cora marina*, which unfortunately we couldn't amplify for any gene fragment. So, the position of *C. marina* within the *Cora* should be assessed in further studies. I suggest the *Cora* clade be considered as the "true *Cora*" (*Cora sensu stricto*) based on its high phylogenetic support (Fig 3B), and in addition based on the following morphological features: concave morphology of the secondary genitalia (i.e. lack of distinctive apical horns), the position of the nodus, elongated pterostigma and geographical distribution.

***MIOCORA* CLADE:** Within the *Cora* - *Miocora* clade, I recovered the species *Cora aurea* as sister to *C. chirripa* and *Miocora peraltica* (Fig 3C). *Cora aurea* was initially described and placed by Ris (1918) within *Cora*. However, Kennedy (1940) erected a new genus (*Kalcora*) using the original description of Ris (1918), and argued that the CuA (i.e. cubitus anterior) vein was unbranched and that the metallic wing pattern was unlike other *Cora* species (Supplementary Fig A); Kennedy considered *C. aurea* to be unique enough to elevate it to a new generic designation. Nevertheless, Garrison (2007) revised this species using a bigger pool of specimens from Colombia; he discovered that the CuA did not always exist in an unbranched condition contra to Kennedy (1940); instead, this character was found to be extremely variable and Garrison decided to

synonymize *Kalcora* with *Cora*. He justified this based also on the metallic pattern of their wings, which he considered to makes them unique species, but not a new genus (Garrison 2007).

Miocora Calvert comprises two species: *M. peraltica* and *M.pellucida*. These species have an unbranched CuA in the FW and there is only one row of cells between the CuA and the margin of the wing (Calvert 1917), in contrast with *Cora sensu lato*, which usually has bi- or tri-branched CuA. The wings of both species are hyaline or with a subapical brown spot that in the sunlight displays a metallic blue iridescence (Garrison et al. 2010). *Cora chirripa* (i.e. member of the MODESTA GROUP) was recovered here in the *Miocora* group; it is found only in Central America, mostly in Costa Rica. Bick and Bick (1990) described two subspecies, *C. chirripa chirripa* and *C. chirippa donelly*, based on their geographical distribution within Costa Rica and the presence a brown band at the tip of the wings; these two species were later synonymized by Garrison et al. 2010. Each species in the clade have secondary genitalia with small apical horns (~0.07-0.15 mm), completely different than those of the *Cora sensu stricto* clade, which lack horns. Based on these morphological characters and the high phylogenetic support, I suggest to call all these species as *Miocora* (*Cora aurea* and *Cora chirripa*). All the other species showing small apical horns on their secondary genitalia, i.e., *C. semiopaca, C. notoxantha, C. obscura, C. skinneri, C. dualis, C. modesta* and *C. lugubris*, might be closely related to this clade, but until molecular data is available, I will consider them as *Miocora incertis sedis*.

***EUTHORE* CLADE:** The other members of *Cora* included in these analyses, *C. terminalis* and *C. klenei*, are sister to a small monophyletic clade composed of *Euthore fasciata*

fasciata and *Euthore fasciata fastigiata*. I called this cluster as the *Euthore* clade (Fig 3D). Phylogenetic support for this clade is not as compelling as that for the other recovered clades; however, reviewing the taxonomic history of these species, I discovered that *Cora terminalis* initially was placed under *Euthore* by Fraser, 1946 based on the presence of a proximal primary antenodal. Later Montgomery (1967) also assigned this species to *Euthore*; however, he stated his concern given that the basal antenodal is very hard to detect in some specimens, including the holotype. He offered other criteria, to separate *Euthore* and Cora; however, he kept *terminalis* within *Euthore*. Finally, Bick and Bick (1990) decided to return *C. terminalis* to *Cora*, because the only character supporting this species within the *Euthore* was the basal primary antenodal. Other diagnostic features of *Euthore* such as the broader, shorter petiole and the greater number of sector and peripheral cells between the media posterior and anal veins of the hindwings in comparison to *Cora*, were not observed in *C. terminalis* by Bick and Bick. The secondary genitalia of *C.terminalis* has long apical horns, in contrast to all the members of the *Miocora sensu lato* and *Cora sensu stricto* clade. The original description of *C. klenei* Karsch (1891) placed it under *Cora*; Kennedy (1940) removed them to a new genus, *Josocora*. The main character for the creation of this new genus was that the CuA vein was bifurcated and not trifurcated, as in other species of *Cora* (Kennedy, 1940; Bick and Bick, 1990). However, Bick and Bick (1990) returned both species to *Cora* due to the extreme variability across all *Cora* species in the CuA vein branching pattern. The secondary genitalia of *C. klenei* has the longest apical horns across of all the *Cora* species.

Selys (1869) establish the genus *Euthore*, comprising six species. The classification of species relies mostly on the wing coloration, due to a lack of variability in the secondary genitalia and male appendages. The apical horns of the penis are between 0.2-0.25mm across all of the species, so it is not considered a good diagnostic character for this genus. The most common species is *Euthore fasciata*, which shows a high polymorphism in the wing pattern, and it has five recognized subspecies. De Marmels (1982) made a few remarks on the ecology and distribution of *Euthore fasciata*. He found that these species live in the canyons of the Southern slope of the Coastal Cordillera in Caracas, on very steep slopes, parallel to the stream where small rivulets and seeping water walls keeping the rocks, roots, and small plants wet. They seemed to be more common during the rainy season than dry season, and he noticed the wing color pattern was unique in every canyon he explored. He suggested a possible Batesian mimicry between some clearwing butterflies and the males and females in some of the populations of the species, and he also suggests they have butterfly-like flight, evoking a similar flashing display to that of the ithomiinae butterflies in flight (De Marmels, 1982). The phylogenetic supports for *Euthore* are not very conclusive however the secondary genitalia show that all included members have longer apical horns in comparison with the *Miocora* clade. I suggest *C. terminalis*, *C. klenei* and *C. confusa* as incertis sedis of the genus *Euthore*, based on the apical horns of the penis between 0.2 - 0.35mm until we include all the current *Cora* species in the analysis.

Polythore

The genus *Polythore* Calvert was recovered as monophyletic with high support (Figs 2 and 4). Using a few thorax and wing features, Hagen in Selys (1853) described the genus

Thore using one male specimen of *P. gigantea*. Later on, Calvert (1917) proposed *Polythore* as a replacement to avoid confusion with the Arachnida genus previously described by Koch, 1850. But until, Montogomery (1967) and Bick and Bick (1985, 1986) there were not morphological characters to diagnose this genus. Until Rojas-Riaño (2011), the formal diagnosis for *Polythore* was very vague and scattered in the literature. She identified the presence of supplementary sectors in the hindwings of the males (HW) between the Radius posterior second branch vein (RP2) and the Intercalar vein 2 (IR2) as the diagnostic character for *Polythore* (Rojas-Riaño 2011). She reconstructed a morphological phylogeny based on 71 characters of venation, wing coloration, and male secondary genitalia; ~48% of the selected characters describe wing pattern coloration which is prone to polymorphism within this genus and can obscure the phylogenetic signal (Sánchez Herrera et al. 2015). Her results suggest that the genus is monophyletic based on only this synapomorphy. Bick and Bick (1985, 1986), suggested that there were six species groups within *Polythore*: ***batesi, boliviana, picta, victoria*** and ***vittata***. They delimited these groups based on the differences in the HW length, wing color pattern, numbers of cells under the pterostigma, and the apical horn length and lateral lobe segmentation on male secondary genitalia. However, they acknowledge high variation for these characters within most of the proposed groups. Sanchez Herrera et al. (2010, 2015), found a lack of congruence between the morphological characteristics and the genetic data (mtDNA) for several species within the genus.

The four recovered clades within *Polythore* in my present analysis are more consistent with geographical distribution than with the morphological groups proposed by Bick and Bick (1985, 1986). The *aurora-mutata* clade (Fig 4), is highly supported by our

phylogenetic analyses. McLachlan (1881) and Bick and Bick (1986) grouped the following species: *batesi, aurora, mutata*, and *beata*, due to their small size (e.g. HW length =26-37mm) and fewer number of cells under the pterostigma (i.e. ~ 3 - 9). They are distributed along streams and rivers in the Amazon watershed and are not present in the Andes Eastern slope foothills. Only the penis of *P.aurora* has apical horns of ~0.23 mm, while *mutata*, *beata*, and *batesi* are between ~0.1 -0.16 mm; additionally, this character might explain the long branches between *P. aurora* and *P. mutata* (Fig. 2). I predict—based on morphological traits (e.g. male penis, Fig 8) and their geographical distribution—that *P. batesi, P. beata, P.vittata*, and *P.chibiriquete* will be part of the *aurora-mutata* clade, (the Amazon clade). Based on the penis morphology long lateral lobes (Fig 8) I hypothesize that, *P. batesi* and *P.vittata,* are more closely related to each other, while the short lateral lobes in both *P.beata* and *P.chibiriquete* suggest they may be closer to *P.mututa* and *P. aurora*. However, their position within the tree remains uncertain until further genetic data of these species are included in future analyses.

P. gigantea is the only member of the *gigantea* clade (Figs 4,8), and it is the only *Polythore* distributed along the Western foothills of the Andes. Bick and Bick (1985, 1986) suggest that this species was within the **picta** group; however, all the proposed species of this group are scattered across the remaining clades. Within *P. gigantea* two strongly supported clades show genetic differentiation between populations from Colombia and Ecuador; I have noticed that wings of individuals from the Colombian populations are opaque, while those of the Ecuadorian populations show a bluish metallic iridescence (Supplementary Fig B). The male genitalia show rounded and rather small apical horns (~0.032 -0.128 mm), very distinct from the other species (see Fig 8). The

gigantea clade is sister to all the other species distributed along the Eastern slopes of the Andes.

The Northeastern (NE) and Southeastern (SE) clades comprise all the species distributed along the Eastern Andean slope (Fig 4). All the members of the SE clade were collected in Central and Southern Peru (Supplementary Table 1). The male secondary genitalia (see Fig 8) for this clade show relatively long, two-segmented lateral lobes, except for *P. spaeteri*, which has shorter lobes compared to all the other members of the clade. The NE clade includes all the species collected in Northern Peru, Ecuador and Colombia (see Supplementary Table 1). In contrast to the SE clade, male genitalia display relatively short, one-segmented lateral lobes, except *P. concinna* and *P.terminata*, which have a tiny, segmented projection (see Figure 8). Based on the following morphological characters and the geographic location, I expect *P. manua*, to be closely related to the SE Clade rather than the NE one. *P. williamsoni* was initially described by Forster (1903) based on several specimens of Vilcanota, Peru. The distant geographical location of the type specimens for *P.williamsoni* from the populations here sampled in Colombia, and also clustering in a different clades (Figure 4), suggests that they might be considered different species. Original illustrations of the male secondary genitalia from the type specimens from Kennedy (1919) show the lateral lobes to be long with two segments, as with most of the species of the SE clade (Supplementary Fig C). However, the specimens analyzed here, have the general secondary genitalia of the NE clade. In general, the species delimitation within these eastern Andean clades of *Polythore* is a difficult task. My results show that each species within the SE and NE, clades has very short branches, suggesting a small number of changes between the members of each clade (Fig 4).

Besides, the NE clade shows that species (e.g. *P.procera*, *P.derivata*, etc.) appear in more than one location within the clade, depending on the population to which they belong. Further studies (beyond here) as a coalescent species delimitation test with of multiple populations of the proposed clades, could help to define supported lineages within these species complex (see Chapter 2).

Biogeographical patterns and diversification of Polythoridae.

The estimated dating analyses for Polythoridae suggest the family started its diversification around the middle of the Eocene epoch (Table 2, Fig 5). During the Eocene, floral and faunal fossil records suggested that the Earth was warmer than today (Barron 1987). However, there has always been a discrepancy between the climate models and the oceanic (Lunt et al. 2012) and terrestrial (Huber and Caballero 2011) proxies. The mean annual temperatures for the Tropical areas are available from Tanzania drill excavation and indicate sea surface temperatures were ~33 °C around the 18 °S paleolatitudes, suggesting a stable warm climate through this epoch (Pearson et al. 2007). The warmer temperatures indicate that the habitat was suitable for the ancestors of Polythoridae to proliferate.

The lineage through time plots suggest a burst of speciation during the Miocene or a possible early extinction prior to the Miocene, regardless of my inclusion of the Andes uplift in the calibration (Fig 6). During the Miocene significant geological events occurred that could trigger the burst of speciation within this family. After the continental breakup (~135-100 Ma), the Atlantic Ocean and the plate tectonic adjustments along the Pacific margin caused deformations of the Amazon craton, and later the formation of the

Andes (Hoorn et al. 2010). During Paleogene times (~65 - 23Ma) the Amazon drainage that was initially situated at the eastern edge of Amazonia migrated westward and by the end of this period the continental divide was located in Central Amazonia and separated east- and west Amazonian rivers (Figueiredo et al. 2009). Around the same time, the subduction of the Pacific margin caused uplift in the Central Andes (Gregory-Wodzicki 2000; Poulsen et al. 2010). The Northern Andes started their formation prior to the breakup of the Pacific margin (~23 Ma) and its subsequent collision with the South American and Caribbean plates (Gregory-Wodzicki 2000; Hoorn et al. 2010). Mountains rising first peaked around ~23 Ma during late Oligocene and early Miocene; this is consistent with the recovered dates for the ancestral nodes of the Andean clades of Polythoridae, and this age also coincides with the diversification of the first montane flora and fauna (Hoorn et al. 2010). The next peak of mountain formation was during the middle of the Miocene (~12 Ma) and finalized with the Northeastern Cordillera during the Pliocene (~4.8 Ma, Gregory-Wodzicki 2000; Hoorn et al. 2010). All of this Andean uplift was a primary driver of the changes in the Amazonian landscape and biota around the Neogene and Quaternary periods (Hoorn et al. 2010). It changed from a lacustrine wetland to a fluvial tidal system (e.g. Pantanal region) to finally the forested habitats we see today (Hoorn et al. 2010). Overall the divergence dates for the Eastern clades are consistent with the geological, climatic and habitat changes of the Andean uplift, the Amazon Basin and the Isthmus of Panama. The recovered ages for the Amazon basin taxa (e.g. *Chalcopteryx, aurora-mutata* clades) were ~9 Ma (Fig 5); these are consistent with the full establishment of the Amazon watershed at ~7Ma (Figueiredo et al. 2010). The estimated ages and current distribution of the Andean clades of *Cora sensu stricto*,

Euthore, and *Polythore* correlate with the periods of mountain building in the Andes uplift (Fig 5, 7).

Recently, new evidence supports an earlier closure of the Central American Seaway (Montes et al. 2015). Traditionally, the closure age was thought to be around the Plio-Pleistocene (~ 3.5 - 3Ma) based on global oceanographic, atmospheric and biotic events (Molnar 2008). Uranium-lead geochronology suggests that the closure of the Isthmus was around the middle Miocene (13 -15 Ma) and that rivers originating in the Panama arc were transporting sediments to the shallow marine basins of South America (Montes et al. 2015). The recovered age for the *Miocora* clade, which distributes throughout Northwestern Colombia and Central America (e.g. Panama), matches this geological event (Figure 5). Recently, analyses of molecular and fossil data of multiple terrestrial and marine organisms by Bacon et al. (2015) showing the biota migrations across the Isthmus of Panama reject the more recent closure of the seaway.

Conclusions

The Neotropical family Polythoridae is a monophyletic group within the broad-wing damselflies (Calopterygoidea). The results here suggest congruence between morphological characters, geographic distribution and genetic data, and suggest the redefinition of several of the genera within this family. *Chalcothore* and *Chalcopteryx* are sister taxa; and despite their genetic similarity, I will keep them as separate genera due to their unique morphological features and the exclusive geographic distribution of *Chalcothore*. *Cora* showed a paraphyletic pattern across the reconstructed topologies. I suggest a redefinition of *Cora* based on strong phylogenetic support, male genitalia

characters and geographical distribution. Several previous species described as *Cora* are herein suggest to be moved to either *Miocora* or *Euthore*. Species not included in the phylogenetic reconstruction (but evaluated based on their distribution, male genitalia and original descriptions) I considered as *incertis sedis* within respective clades. *Cora, sensu stricto*, is restricted to those species distributed along the Eastern Slope of the Andes, whose secondary male genitalia lack apical horns. All species spread along the Northwest Andes and Central America, whose secondary genitalia have short apical horns and which were recovered as a group with strong phylogenetic support I consider to be *Miocora*. The *Cora s.l.* species distributed in South America and whose secondary genitalia possess long apical horns were found to be closely related to *Euthore*. However, the phylogenetic support was inconclusive, so I considered them *incertis sedis* within *Euthore*.

Finally, I recovered the genus *Polythore* as monophyletic. Within it, I find four well-support clades consistent with secondary genitalia and geographical distribution. The *aurora-mutata* (Amazonian) clades seem to be true independent lineages, similar species not tested should be included to observe the presence of geographical polymorphism in wing color pattern and the structure of male genitalia. The only species of *Polythore* distributed in the west of the Andes is *P. gigantea*; it is recovered as a unique clade, showing some degree of genetic differentiation at the population level. The Eastern Andeean species display two well-supported monophyletic clades based on their northern and southern distribution within the Andes, however within them, there might be a polymorphic species complex, based on the wing color pattern.

The estimated divergence age for Polythoridae was around mid-Eocene; however, the peak of its diversification was during the mid-Miocene. These estimated periods are possibly related to significant geological events including: The Andes uplift, Amazon basin formation, and the closure of the Central American seaway. *Chalcopteryx* and *Polythore* Amazonian species diversification may be related to geological changes produced by the formation of the Amazon watershed, which was heavily influenced by the Andes uplift. The Central American Seaway closure may have had an impact on the *Miocora* clade by allowing the interchange into new suitable habitats within the Northern hemisphere. Finally, all Andean species are related to the different mountain building events of the final Andean uplift.

Chapter 3: Tables

Table 1. Calibrated nodes with the fossils information supporting the prior distributions selected for the Divergence Time Analysis node calibration. * The influence of the biogeographical information of the Andes Cordillera was tested using two independent treatments with and without it.

Node/TAXA	Fossil Classification and estimated ages	Type Locality/PaleoDB	Prior distribution
Root *Calopterygoidea* (node 52)	Odonata, Zygoptera, Eosagrionidae, *Eosagrion risi* † , Early Jurassic, Toarcian, 183-182 Ma (Handlirsch, 1920)	Germany/ Dobbertin, Mecklenburg PaleoDB 123987	Uniform prior distribution max = **183** min = **47.8**
	Odonata, Zygoptera, Calopterygoidea, Calopterygidae *Sinocalopteryx shanyongensis †,* Eocene, Ypresian (56 - 47.8 Ma) NIGP 151367 (Lin *et al.*, 2010)	Yunnan, China PaleoDB 113892	
	Odonata, Zygoptera, Epallagidae, *Labandeiraia europae †,* Eocene, Ypresian (56 -47.8 Ma)	Island of Fur, Denmark PaleoDB 123998, 127173	
	Odonata, Zygoptera, Epallagidae, *Ejerslevia haraldi †,* Eocene, Ypresian (56 -47.8 Ma) (Zessin, 2011)	Ejerslev, Mors, Denmark PaleoDB 157041	
	Odonata, Zygoptera,		
Outgroup *Euphaeidae* (node 99)	Odonata, Zygoptera, Epallagidae, *Labandeiraia americaborealis †,* Eocene, Bridgerian (50 -46.2 Ma) 31.665A-B (Petrulevicius et al, 2007)	Colorado, USA PaleoDB = 107337	LogNormal; mean=41; std=0.15

	Odonata, Zygoptera, Epallagidae, *Litheuphaea coloradensis †,* Eocene, Bridgerian (50 -46.2 Ma) BMNH Pl II 562 (Petrulevicius et al, 2007)	Colorado, USA PaleoDB = 107337	
	Odonata, Zygoptera, Epallagidae, *Eodichroma mirifica †,* Late/Upper Eocene, (37.2 - 33.9) (Cockerell 1923)	Texas, USA PaleoDB = 130390	
	Odonata, Zygoptera, Epallagidae, *Litheuphaea ludwigi †,* Eocene, Priabonian (38 - 33.9 Ma) (Bechly,1990)	Baltic Amber, Russian Federation PaleoDB = 123911	
	Odonata, Zygoptera, Epallagidae, *Elektroeuphaea flecki †,* Eocene, Priabonian (38 - 33.9 Ma) (Nel et al., 2013)	Baltic Amber, Poland PaleoDB = 123215	
	Odonata, Zygoptera, Epallagidae, *Parazacallites aquisextanea †,* Oligocene, Chattian (28.1-23.03 Ma) MNHN IPM-R.06688 (Nel, 1988)	Bouches-Du-Rhone, France PaleoDB 123943	
Ingroup/ *Polythoridae* (node 53)	Odonata, Zygoptera, Polythoroidea, *Bolcathore colorata †*, Eocene, Lutetian (47.8 - 41.3 Ma) MCSNV I.G. 37582 (Gentilini, 2002)	Pesciara di Bolca, Italy PaleoDB = 122230	Uniform prior distribution max = **48** min = **33.9**
	Odonata, Zygoptera,	Isle of Wight, United Kingdom	

Polythoroidea, *Bolcathore sp. †*, Eocene, Priabonian (38 - 33.9 Ma) MCSNV I.G. 37582 (Nel and Fleck, 2014)	PaleoDB=123960	
Odonata, Zygoptera, *Protothore explicata †,* Eocene, Bartonian (41.3 - 38 Ma) (Cockrell, 1930)	California, USA PaleoDB = 117537	
Ingroup/ *Polythore** (node 77)	Andean Eastern Cordillera and uplift formation, ~10 - 5 Ma (Gregory-Wodzincki, 2000)	NA	LogNormal, Mean=7; std=0.25

Table 2. Comparison of the mean crown ages (in million years, with 95% HPD) with (WA) and without (WOA) the calibration of the *Polythore* clade with the Andes cordillera biogeographical information. * if the t-test there is a significant mean difference between treatments (p-values < 0.005).

Node	WA	Min	Max	WOA	Min	Max	HPD Overlapping
Calopterygoidea *	58.69	48	74	64.24	48	82	yes
Euphaeidae*	33.04	25	40	34.39	26	43	yes
Polythoridae*	40.39	34	48	43.72	36	50	yes
Polythore*	11.52	8	15	16.51	11	22	yes

Chapter 3: Figures

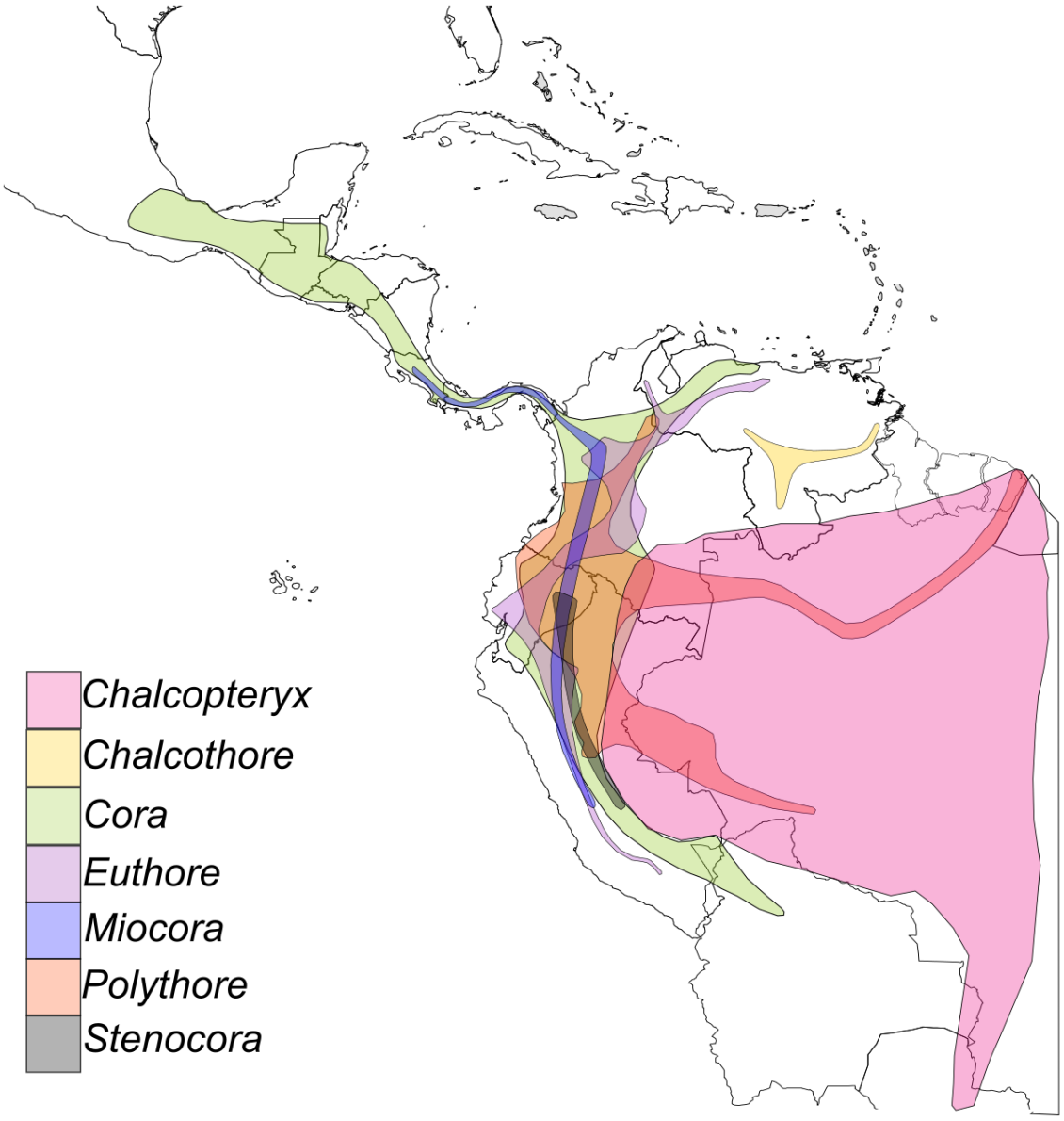

Figure 1. Geographical distribution of the family Polythoridae, each color represents a genus.

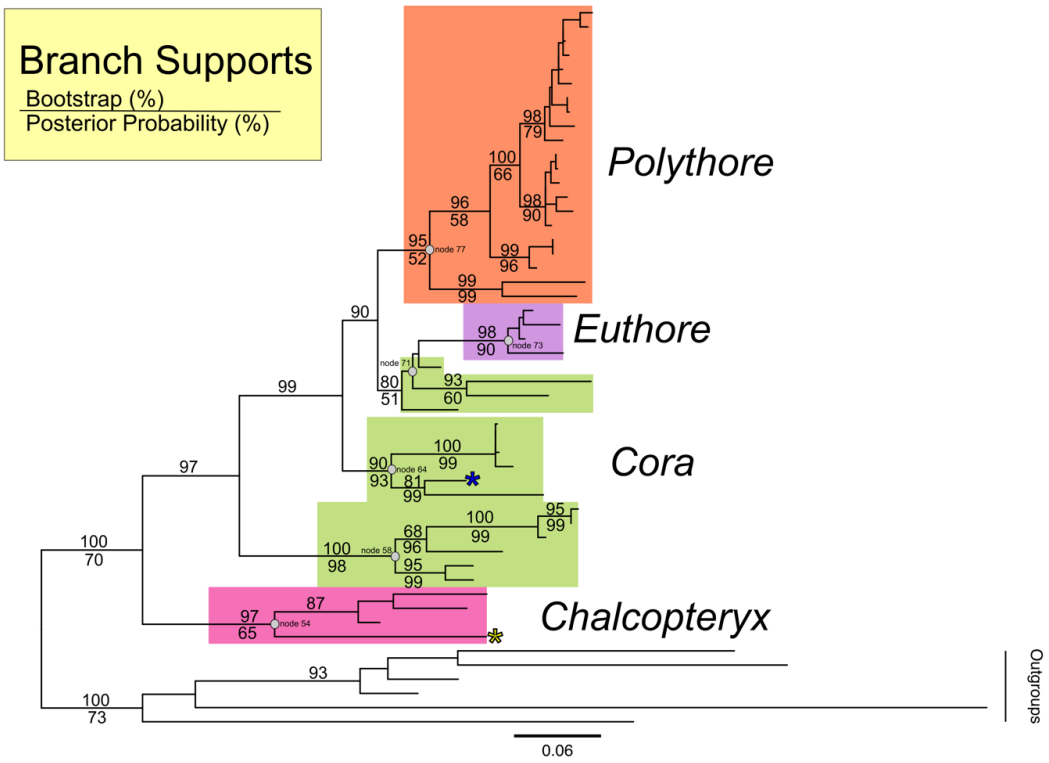

Figure 2. Best recovered ML phylogram for Polythoridae. Bootstrap and Posterior probabilities are shown on the branches. Each of the most representative genera (e.g. *Chalcopteryx, Cora, Euthore* and *Polythore*) are highlighted. The blue asterisk in the tree represents the position of the genus *Miocora,* while the yellow represents the genus *Chalcothore*. Important nodes are represented by a gray circle.

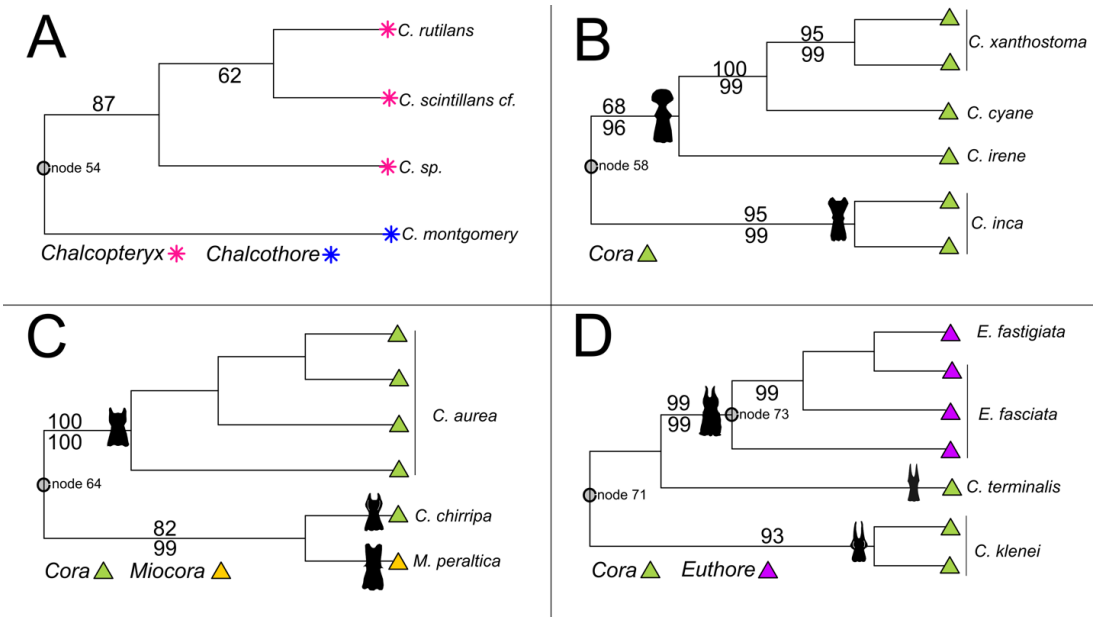

Figure 3. Cladograms of specific nodes of the best ML recovered. The bootstrap (on top) and posterior probabilities (below) the branches. Shared male secondary genitalia general shape represented at the node. **A**. *Chalcopteryx* clade, node 54. **B**. *Cora sensu stricto,* node 58. **C.** *Miocora* clade, node 64. **D.** *Euthore incertis sedis* clade, nodes 71 – 73.

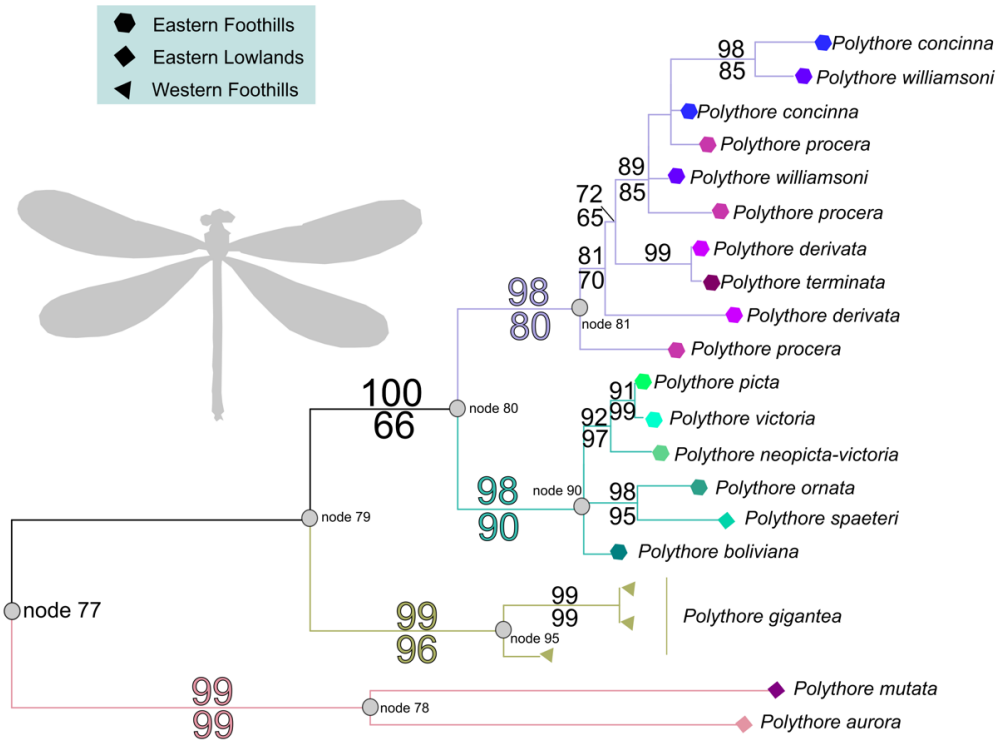

Figure 4. Expanded phylogram of the genus *Polythore,* node 77. The bootstrap (on top) and posterior probabilities (below) the branches.

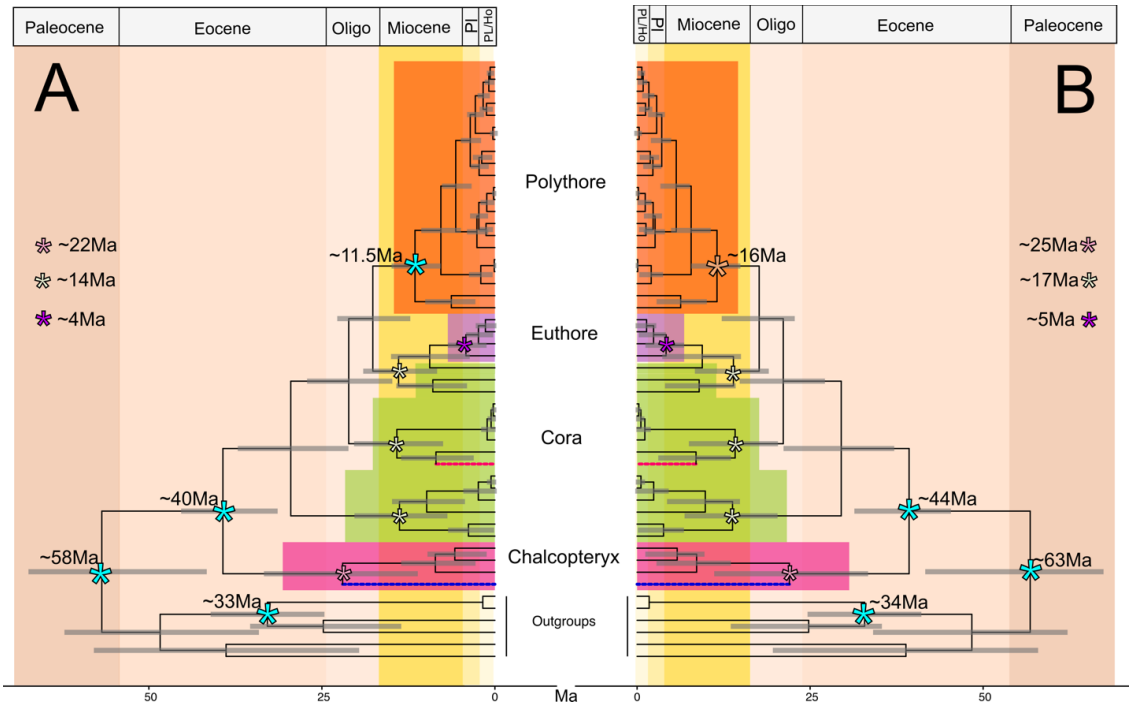

Figure 5. Estimated time calibrated topologies comparison. **A.** With and **B.** without the Andes uplift calibration. Grey bars in each node represents the 95% HPD (i.e. High Probability Density) uncertainty values. Blue asterisks correspond to the calibrated nodes; other asterisks represent estimated nodes. Approximate ages are shown in the figure; colors correspond to each genus. The blue and magenta dotted lines represent *Chalcothore* and *Miocora* respectively.

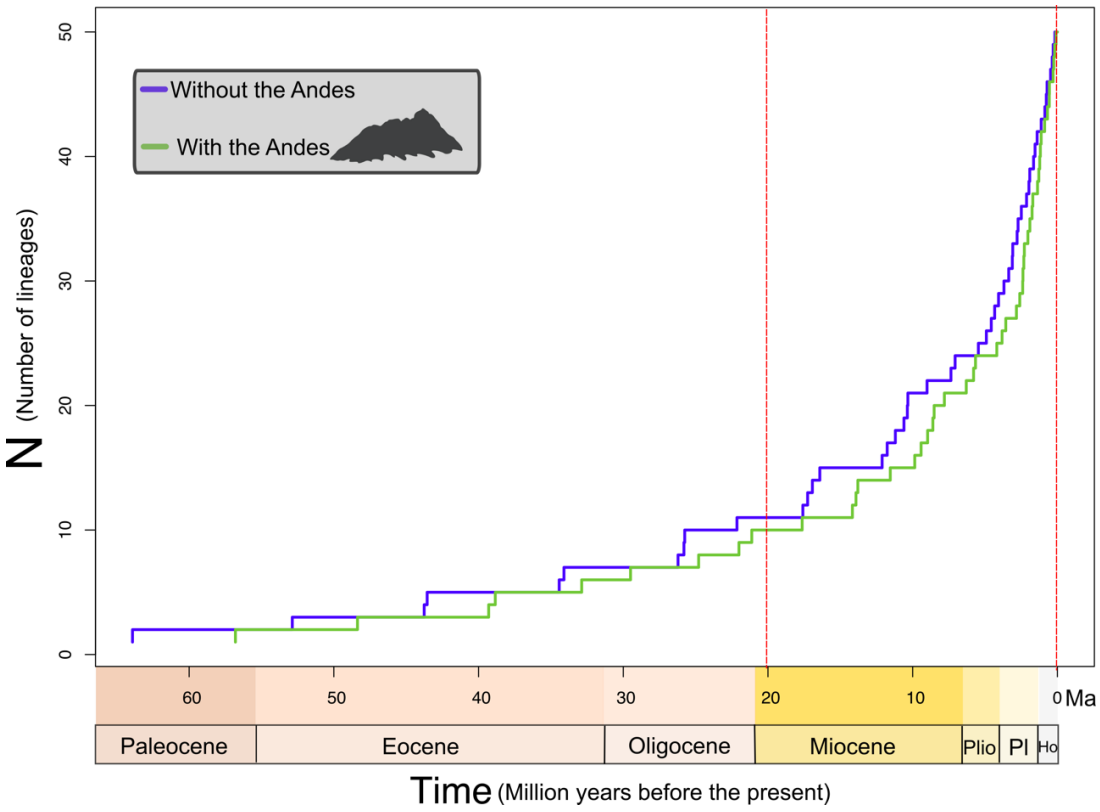

Figure 6. Lineage through time plots or for each analyses with (green) and without (blue) the Andes uplift calibration. Vertical red dotted line corresponds to the estimated peak time diversification (~23Ma) for Polythoridae.

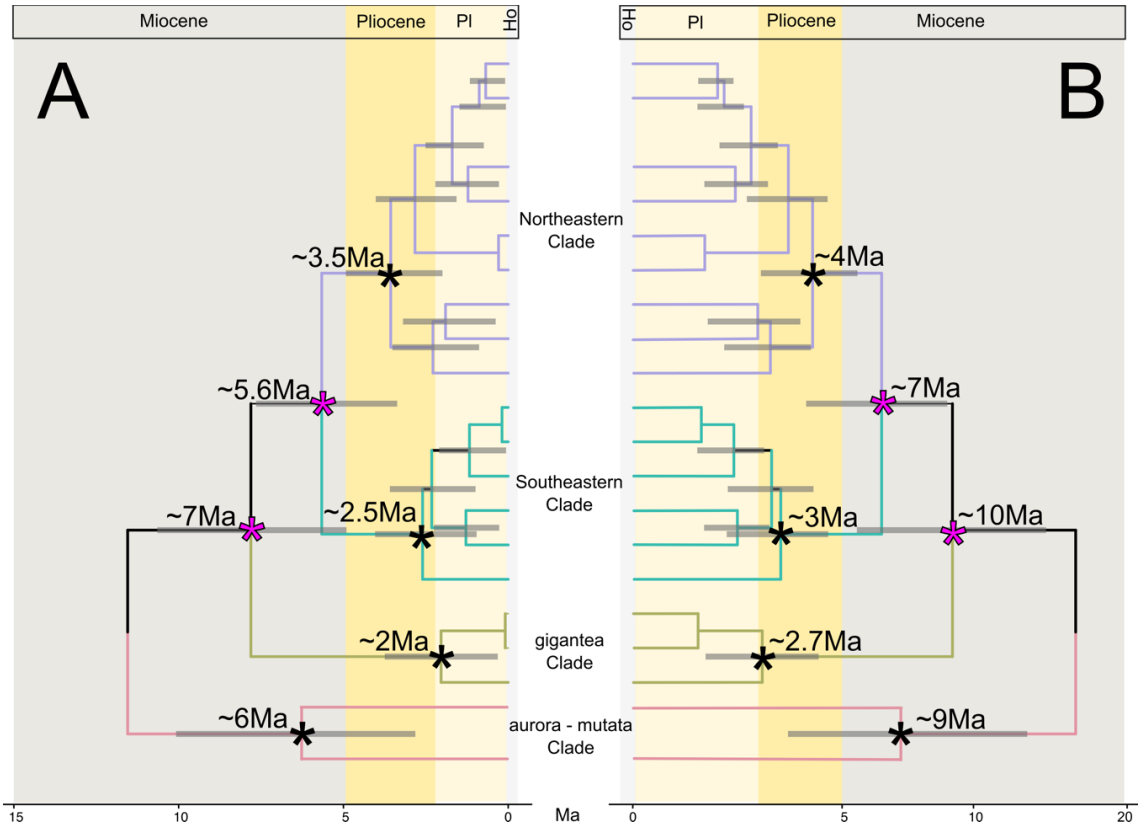

Figure 7. Expanded time calibrated topologies for the genus *Polythore*. **A.** With and **B.** without the Andes uplift calibration. Grey bars in each node represents the 95% HPD uncertainty values. All asterisks represent estimated ages; magenta represent the split of the Andean Cordillera.

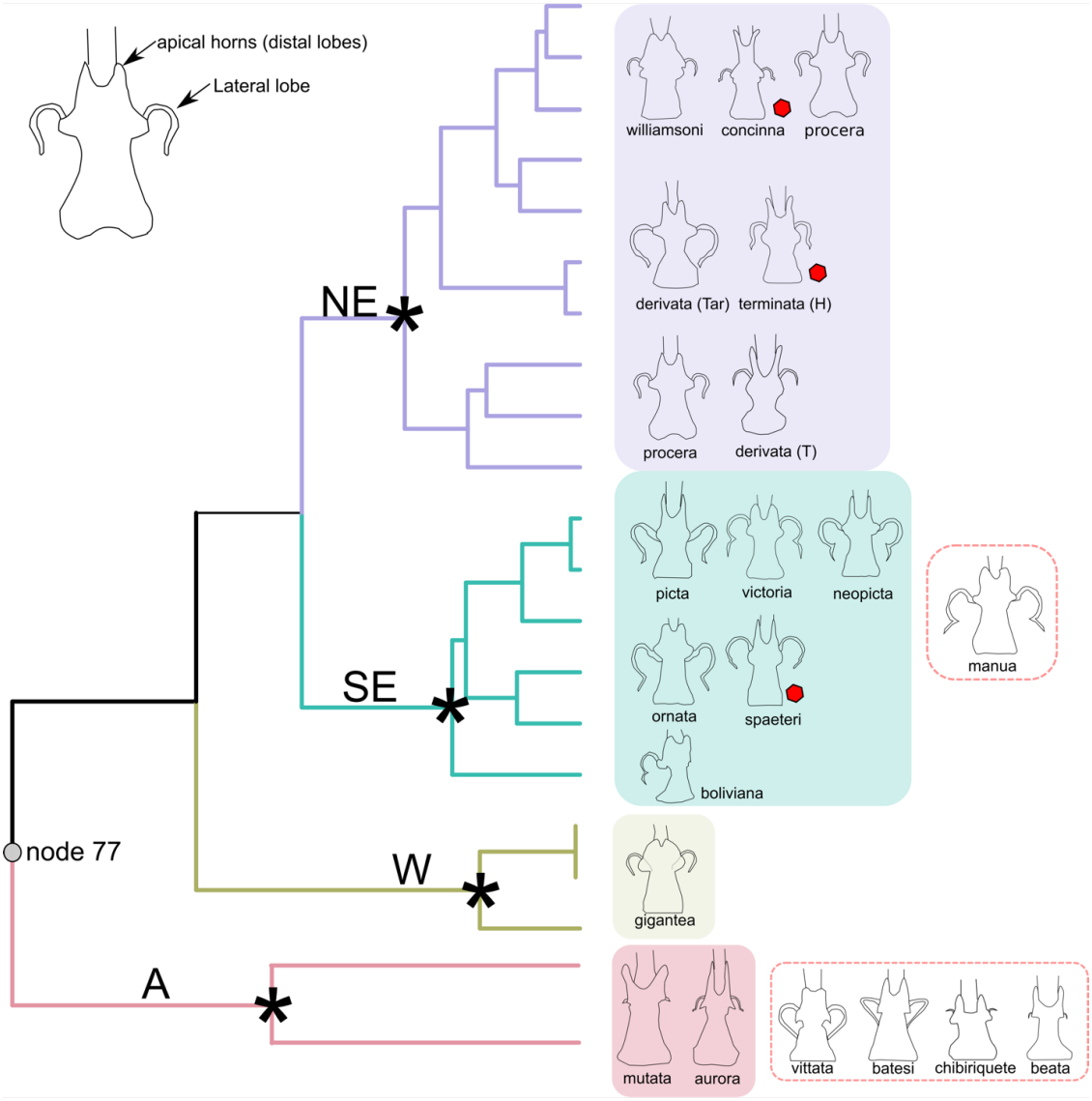

Figure 8. Male secondary genitalia of the males of *Polythore* mapped over the expanded ultrametric tree (node 77). Species in the red boxes are not included in the recovered molecular topology, they are placed in proximity to their possibly most closely related clade. Species with red hexagons indicate discrepancy with the lateral lobe morphology that prevails in the clade.

References

Bacon C.D., Silvestro D., Jaramillo C., Smith B.T., Chakrabarty P., Antonelli A. 2015. Biological evidence supports an early and complex emergence of the Isthmus of Panama. Proc. Natl. Acad. Sci. U. S. A. 112:6110–6115.

Barron E.J. 1987. Eocene equator-to-pole surface ocean temperatures: A significant climate problem? Paleoceanography. 2:729–739.

Bick G.H., Bick J.C. 1985. A revision of the picta group of Polythore, with a description of a new species, P. lamerceda spec. nov., from Peru (Zygoptera: Polythoridae). Odonatologica. 14:1–28.

Bick G.H., Bick J.C. 1986. The genus Polythore exclusive of the picta group (Zygoptera: Polythoridae). Odonatologica. 15:245–273.

Bick G.H., Bick J.C. 1990a. A revision of the neotropical genus Cora Selys, 1853 (Zygoptera: Polythoridae). Odonatologica. 19:117–143.

Bick G.H., Bick J.C. 1990b. Polythore manua spec. nov. from southern Peru (Zygoptera: Polythoridae). Odonatologica. 19:367–373.

Bick G.H., Bick J.C. 1991. Two new damselflies: Cora dorada spec. nov. from Ecuador and C. parda spec. nov. from Peru (Zygoptera: Polythoridae). Odonatologica. 20:453–458.

Bick G.H., Bick J.C. 1992. A study of family Polythoridae, with details on the genus Euthore Selys, 1869 (Zygoptera). Odonatologica. 21:275–288.

Bybee S.M., Heath Ogden T., Branham M.A., Whiting M.F. 2008. Molecules, morphology and fossils: a comprehensive approach to odonate phylogeny and the evolution of the odonate wing. Cladistics. 24:477–514.

Calvert P.P. 1917. Studies on Costa Rican Odonata VIII. A new genus allied to Cora. Entomol. News. 28:259–263.

Cockerell. 1930. A Fossil Dragon-fly from California (Odonata: Calopterygidae). Entomological News 41:49-50

Costa J.C. 2005. Chalcopteryx machadoi sp. n. da região norte do Brasil (Zygoptera: Polythoridae)with a key to the species of the genus. Lundiana. 6:37–40.

De Marmels J. 1982. The genus Euthore Selys in Venezuela, with special notes on Euthore fasciata (Hagen, 1853) (Zygoptera: Polythoridae). Advances on Odonatology. 1:39–41.

De Marmels J. 1988. Generic characters of Chalcothore De Marmels, 1985, with notes on

the male of C. montgomeryi (Racenis, 1968) and a description of the larva (Zygoptera: Polythoridae). Odonatologica. 17:379–384.

Dijkstra K.-D.B., Kalkman V.J., Dow R.A., Stokvis F.R., Van Tol J. 2013. Redefining the damselfly families: a comprehensive molecular phylogeny of Zygoptera (Odonata). Syst. Entomol. 39:68–96.

Drummond A.J., Suchard M.A., Xie D., Rambaut A. 2012. Bayesian phylogenetics with BEAUti and the BEAST 1.7. Mol. Biol. Evol. 29:1969–1973.

Dumont H.J., Andy V., Vanfleteren J.R. 2009. A molecular phylogeny of the Odonata (Insecta). Syst. Entomol. 35:6–18.

Figueiredo J., Hoorn C., van der Ven P., Soares E. 2009. Late Miocene onset of the Amazon River and the Amazon deep-sea fan: Evidence from the Foz do Amazonas Basin. Geology. 37:619–622.

Figueiredo J., Hoorn C., van der Ven P., Soares E. 2010. Late Miocene onset of the Amazon River and the Amazon deep-sea fan: Evidence from the Foz do Amazonas Basin: Reply. Geology. 38:e213–e213.

Garrison R.W. 2007. Kalocora , a junior synonym of Cora (Odonata: Polythoridae). Int. J. Odonatol. 10:185–188.

Garrison R.W., von Ellenrieder N., Louton J.A. 2010. Damselfly Genera of the New World: An Illustrated and Annotated Key to the Zygoptera. Johns Hopkins University Press.

Gentilini. 2002. Fossil damselflies and dragonflies from the Eocene of Monte Bolca (Insecta: Odonata). Studi e Ricerche sui Giacimenti Terziari di Bolca, Museo Civico di Storia Naturale di Verona 9:7-22

Gregory-Wodzicki K.M. 2000. Uplift history of the Central and Northern Andes: A review. Geol. Soc. Am. Bull. 112:1091–1105.

Handlirsch A. 1920. Palaeontologie. In C. Schröder (ed.), Handbuch der Entomologie 3:117-208 p 184. Fig. 140

Hoorn C., Wesselingh F.P., ter Steege H., Bermudez M.A., Mora A., Sevink J., Sanmartín I., Sanchez-Meseguer A., Anderson C.L., Figueiredo J.P., Jaramillo C., Riff D., Negri F.R., Hooghiemstra H., Lundberg J., Stadler T., Särkinen T., Antonelli A. 2010. Amazonia through time: Andean uplift, climate change, landscape evolution, and biodiversity. Science. 330:927–931.

Huber M., Caballero R. 2011. The early Eocene equable climate problem revisited. .

Katoh K., Standley D.M. 2013. MAFFT Multiple Sequence Alignment Software Version 7: Improvements in Performance and Usability. Mol. Biol. Evol. 30:772–780.

Kearse M., Moir R., Wilson A., Stones-Havas S., Cheung M., Sturrock S., Buxton S., Cooper A., Markowitz S., Duran C., Thierer T., Ashton B., Meintjes P., Drummond A. 2012. Geneious Basic: An integrated and extendable desktop software platform for the organization and analysis of sequence data. Bioinformatics. 28:1647–1649.

Kennedy C.H. 1940. The Miocora-like dragonflies from Ecuador with notes on Cora, Miocora, Kalocora, Josocora and Stenocora (Odonata:Polythorinae). Ann. Entomol. Soc. Am. XXXIII:406–436.

Kjer K.M. 1995. Use of rRNA secondary structure in phylogenetic studies to identify homologous positions: an example of alignment and data presentation from the frogs. Mol. Phylogenet. Evol. 4:314–330.

Kjer K.M., Gillespie J.J., Ober K.A. 2007. Opinions on multiple sequence alignment, and an empirical comparison of repeatability and accuracy between POY and structural alignment. Syst. Biol. 56:133–146.

Lin, J. F. Petrulevicius, D. Y. Huang, A. Nel, and M. S. Engel. 2010. First fossil Calopterygoidea (Odonata: Zygoptera) from Southeastern Asia: A new genus and species from the Paleogene of China. *Geobios* **43**:349-353

Lunt D.J., Dunkley Jones T., Heinemann M., Huber M., LeGrande A., Winguth A., Loptson C., Marotzke J., Roberts C.D., Tindall J., Valdes P., Winguth C. 2012. A model–data comparison for a multi-model ensemble of early Eocene atmosphere–ocean simulations: EoMIP. .

Maddison W.P., Maddison D.R. 2015. Mesquite: a modular system for evolutionary analysis. .

McLachlan R. 1870. Descriptions of a new genus and four new species of Calopterygidae and of a new genus and species of Gomphidae. Transactions of the Royal Entomological Society of London. 11:165–172.

Misof B., Liu S., Meusemann K., Peters R.S., Donath A., Mayer C., Frandsen P.B., Ware J., Flouri T., Beutel R.G., Niehuis O., Petersen M., Izquierdo-Carrasco F., Wappler T., Rust J., Aberer A.J., Aspöck U., Aspöck H., Bartel D., Blanke A., Berger S., Böhm A., Buckley T.R., Calcott B., Chen J., Friedrich F., Fukui M., Fujita M., Greve C., Grobe P., Gu S., Huang Y., Jermiin L.S., Kawahara A.Y., Krogmann L., Kubiak M., Lanfear R., Letsch H., Li Y., Li Z., Li J., Lu H., Machida R., Mashimo Y., Kapli P., McKenna D.D., Meng G., Nakagaki Y., Navarrete-Heredia J.L., Ott M., Ou Y., Pass G., Podsiadlowski L., Pohl H., von Reumont B.M., Schütte K., Sekiya K., Shimizu S., Slipinski A., Stamatakis A., Song W., Su X., Szucsich N.U., Tan M., Tan X., Tang M., Tang J., Timelthaler G., Tomizuka S., Trautwein M., Tong X., Uchifune T., Walzl M.G., Wiegmann B.M., Wilbrandt J., Wipfler B., Wong T.K.F., Wu Q., Wu G., Xie Y., Yang S., Yang Q., Yeates D.K., Yoshizawa K., Zhang Q., Zhang R., Zhang W., Zhang Y., Zhao J., Zhou C., Zhou L., Ziesmann T., Zou S., Li Y., Xu X., Zhang Y., Yang H., Wang J., Wang J., Kjer K.M., Zhou X. 2014. Phylogenomics resolves the timing and pattern of insect evolution. Science.

346:763–767.

Molnar P. 2008. Closing of the Central American Seaway and the Ice Age: A critical review: CENTRAL AMERICAN SEAWAY AND CLIMATE. Paleoceanography. 23.

Montes C., Cardona A., Jaramillo C., Pardo A., Silva J.C., Valencia V., Ayala C., Pérez-Angel L.C., Rodriguez-Parra L.A., Ramirez V., Niño H. 2015. Middle Miocene closure of the Central American Seaway. Science. 348:226–229.

Nel A. 1988. Parazacallitinae, nouvelle sous-famille et premier Epallagidae de l'Oligocène européen (Odonata, Zygoptera). Bulletin du Muséum National d'Histoire Naturelle. Section C, Sciences de la Terre, Paléontologie, Géologie, Minérologie 10:175-179

Nel A. and G. Fleck. 2014. Dragonflies and damselflies (Insecta: Odonata) from the Late Eocene of the Isle of Wight. Earth and Environmental Science Transactions of the Royal Society of Edinburgh 104:283-306

Nguyen L.-T., Schmidt H.A., von Haeseler A., Minh B.Q. 2015. IQ-TREE: a fast and effective stochastic algorithm for estimating maximum-likelihood phylogenies. Mol. Biol. Evol. 32:268–274.

Nylander J.A.A., A.A. Nylander J., Wilgenbusch J.C., Warren D.L., Swofford D.L. 2007. AWTY (are we there yet?): a system for graphical exploration of MCMC convergence in Bayesian phylogenetics. Bioinformatics. 24:581–583.

Paradis E., Claude J., Strimmer K. 2004. APE: Analyses of Phylogenetics and Evolution in R language. Bioinformatics. 20:289–290.

Pearson P.N., van Dongen B.E., Nicholas C.J., Pancost R.D., Schouten S., Singano J.M., Wade B.S. 2007. Stable warm tropical climate through the Eocene Epoch. Geology. 35:211.

Petrulevicius J.F, A. Nel, J. Rust, G. Bechly, and D. Kohls. 2007. New Paleogene Epallagidae (Insecta: Odonata) recorded in North America and Europe. Biogeographic Implications. *Alavesia* **1**:15-25

Poulsen C.J., Ehlers T.A., Insel N. 2010. Onset of convective rainfall during gradual late Miocene rise of the central Andes. Science. 328:490–493.

Racenis J. 1968. Los Odonatos de la region del Auyatepui y de la Sierra de Lema en la Guyana Venezolana 1. Superfamilia Agrionoidea. Memorias de la Sociedad de Ciencias Naturales “La Salle.” 28:151–176.

Rambaut A., Suchard M.A., Xie D., Drummond A.J. 2014. Tracer. .

Rambur P. 1842. Histoire Naturelle des Insects Nevroptéres. Paris: Librarie

Encyclopedique des Roret.

R Core Team. 2013. R: A language and environment for statistical computing. .

Rehn A.C. 2003. Phylogenetic analysis of higher-level relationships of Odonata. Syst. Entomol. 28:181–240.

Ris F. 1914. Zwei neue neotropische Calopterygiden. Entomol. Mitt. 3:282–285.

Ris F. 1918. Libellen (Odonata) aus der Region der amerikanishen Kordilleren von Costarica bis Catamarca. Archiv fur Naturgeschichte. A:1–197.

Rojas-Riaño N.C. 2011. Sistematica de genero POLYTHORE Calvert, 1917 (ODONATA: POLYTHORIDAE). .

Ronquist F., Teslenko M., van der Mark P., Ayres D.L., Darling A., Höhna S., Larget B., Liu L., Suchard M.A., Huelsenbeck J.P. 2012. MrBayes 3.2: efficient Bayesian phylogenetic inference and model choice across a large model space. Syst. Biol. 61:539–542.

Sánchez Herrera M., Kuhn W.R., Lorenzo-Carballa M.O., Harding K.M., Ankrom N., Sherratt T.N., Hoffmann J., Van Gossum H., Ware J.L., Cordero-Rivera A., Beatty C.D. 2015. Mixed signals? Morphological and molecular evidence suggest a color polymorphism in some neotropical polythore damselflies. PLoS One. 10:e0125074.

Sánchez Herrera M., Realpe E., Salazar C. 2010. A neotropical polymorphic damselfly shows poor congruence between genetic and traditional morphological characters in Odonata. Mol. Phylogenet. Evol. 57:912–917.

Santos N.D., Machado A.B.M. 1960. Contribuição ao conhecimento do gênero Chalcopteryx Selys, 1853, com a descrição de uma nova espécie. Boletim do Museu Paraense Emilio Goeldi série Zoologia. 24:1–17.

Selys Longchamps E. 1853. Synopsis des Calopterygines. Bulletim de Academie Belgique. (annexe):1–73.

Trifinopoulos J., Nguyen L.-T., von Haeseler A., Minh B.Q. 2016. W-IQ-TREE: a fast online phylogenetic tool for maximum likelihood analysis. Nucleic Acids Res.

Yu G., Smith D., Zhu H., Guan Y., Lam T.T. 2016. ggtree: an R package for visualization and annotation of phylogenetic tree with different types of meta-data. .

Zessin. 2011. Neue Insekten aus dem Moler (Paläozän/Eozän) von Dänemark Teil 1 (Odonata: Epallagidae, Megapodagrioniidae). Virgo, Mitteilungsblatt des Entomologischen Vereins Mecklenburg 14:64-73

General Conclusion

The Neotropical *Polythore* damselflies are a new model system to study color polymorphisms in nature. I was able to quantify color polymorphisms using three novel methods, and establish and discriminate morphotypes present in *Polythore*. Species discrimination was possible despite intra- and interspecies variation in wing color patterns among species of *Polythore*. However, these morphotypes were not consistent with the genetic species recovered with molecular data, suggesting that color pattern is not a reliable character for the species delimitation of this group as previously thought by taxonomists. Exploring the genetic diversity across seventeen populations of thirteen of the described morphospecies, I detected that geography explains most of the genetic diversity within this genus. The multilocus coalescent species tree reconstruction supported the presence of 15 independent lineages for which coalescent times were extremely short; suggesting a possible recent radiation within this group. The Bayesian species delimitation models supported with high probabilities the nodes estimating a species tree comprising 15 lineages. I discovered five new species which will be described in later papers, four of which are examples of cryptic diversity (e.g. same color pattern divergent mtDNA). Finally, the family level phylogenetic reconstruction supports the idea that *Polythore* has one common ancestor from which these highly polymorphic wing morphologies have originated. Furthermore, the time divergence analyses suggest that the Andes Cordillera and Amazon basin formation played an important role in diversification of these Neotropical taxa. Why so many colors? I still haven't answered this question, however now I know it is not due to common descendant, they might be because of a natural selection or sexual selection forces maintaining them in nature. My

further studies will concentrate in testing both of these possibilities using field experiments coupled to genomic analyses in order to understand how selection is shaping these phenotypes.